Department of Chemical Engineering

Bachelor Thesis

OPTIMAL DESIGN OF A CHP MICROGRID WITH A MILP APPROACH

Author

Petros Papadopoulos

Supervisor

Ioannis K. Kookos

Associate Professor

Patras, February 2018

Acknowledgments

This bachelor thesis was conducted at the laboratory of Plant Design and Process Optimization, Department of Chemical Engineering, University of Patras, during the academic year 2017-2018. There is a number of people, whose advice and support throughout this period have made this effort possible, and to whom I would like to express my deepest gratitude.

First of all, I would like to personally thank my supervisor, Associate Prof. Ioannis Kookos, for giving me the opportunity to conduct this study among his research group. His invaluable advice and guidance have helped at an outmost degree with the completion of this thesis.

I would also like to thank Prof. Michael Zachar for his aid in retrieving and sharing valuable statistical data of his research, upon which this thesis was based.

The two members of my examination committee, Associate Prof. Eleftherios Amanatides and Associate Prof. Alexandros Katsaounis, also deserve my gratitude for agreeing to participate.

Last but not least, I would like to express my most sincere thanks to my family and friends, whose encouragement and support has played a significant role throughout this whole period.

Abstract

Microgrids are complete energy subsystems that contain both distributed energy resources (DER) and the consumer (load) into the same interconnected distribution network. They are integrated into the traditional electrical network (macrogrid) and are located in close proximity to the end-users, enabling them to meet demands in both power and heat (CHP). Although they can communicate and interact with the macrogrid, they appear to it as independent entities, able to control their own loads and resources. While microgrids usually cooperate with the macrogrid to meet the demands of their loads, they can disconnect from it and operate autonomously in an "islanded mode". There are many drivers, including environmental and economic, which make microgrids a promising technology of tomorrow's power industry.

This research focuses on the assessment of the cost-optimal design and operation of a generic microgrid, capable of meeting both heat and power demand of Sarnia, Ontario. The considered microgrid consists of microturbines, wind turbines, solar photovoltaics, electric and natural gas-fired boilers, a lead-acid battery bank and the load. A mixed integer linear program (MILP) is formulated, containing unit design variables, as well as weather and load data from Sarnia, to evaluate both optimal unit selection and each unit's hourly operation throughout the system's lifetime. The program is solved by the CPLEX12 solver in GAMS, considering hourly intervals throughout a years' period, for a system's total lifespan of 20 years. Three case studies are conducted; a reference case, a minimum autonomy scenario and an emissions reduction scenario.

The results from the optimization of the reference case show that the sole purchase of utility power and natural gas will produce the least-cost solution, which raises at 6.51 M$, due to high initial capital investments and installation costs of the equipment. Nevertheless, a 25 percent minimum contribution from the microgrid's resources results to a 0.5 percent increase to the net present value of costs yet achieves a 9 percent reduction in the annual carbon emissions afflicted by all sources.

Optimal technology selection may significantly differ for small changes to the selected constraints of the program. Microturbines are highly favored, since they can be used as CHP, mitigating the equipment's purchase cost, thus making them a more competitive solution. On the other hand, the excessive usage of microturbines for CHP production, sometimes leads to a considerable waste of energy. The results of this study also show that renewable technology suffers from the issue of the asynchronous power production and consumption, which leads to either a NPV increase due to storage costs, or the waste of the excess power that is produced.

Table of Contents

List of Figures

List of Tables

Chapter 1

Introduction

Many emerging environmental concerns, along with certain inadequacies that occur from the traditional power grid, create the necessity of the power sector's transition into a new era. The new power generation and distribution network ought to have minimum environmental impacts, high efficiency, while meeting future, rapidly growing demands. A straightforward, swift and cost-effective transition to the future grid is a challenging engineering subject. A prominent technological concept, able to meet all of the above-mentioned criteria, is the microgrid.

Microgrids are energy subsystems that contain both generation units and the consumer, within a well-defined electrical distribution network, which appears as an autonomous entity to the grid. These systems have the ability to isolate from the traditional distribution network and operate independently, meeting the demands with their own sources, without causing any disturbance to the grid. Currently powering facilities like residencies, hospitals, companies, university campuses, industrial blocks, jails and military bases, either partly or wholly, microgrids can meet a wide range of energy demands (Lasseter, 2007; PNNL, 2016).

Able to employ distributed generation technology, microgrids also create the opportunity to utilize renewable resources. What is more, their close proximity to the end-user enables them to reuse the produced thermal energy, to meet both heat and power demands, significantly raising the system's total efficiency. Due to the variety of the microgrid's distributed resources that can be employed, and the versatility of the demands they can meet, the cost-optimal design of a microgrid is a subject of interest for many researchers.

Microgrid cost-optimal planning is a challenge currently faced by the international engineering and scientific community. There are many approaches that have been proposed for the effective distributed technology selection in energy-related problems. Most of them are solved by either exact methods, such as mixed integer linear programming (MILP), which is quite effective but takes some computation time, or by heuristic methods, which simplify the problem and give a good approximation of the optimal solution (Abdmouleh et al., 2017).

There are many research studies in the international bibliography, that use the MILP method to evaluate optimal designs of microgrids. Mashayekh et al. (2017) create a synergistic microgrid model, able to meet power, heating and cooling (trigeneration) demands of a specific load, which they solved with DER-CAM decision support tool, used for planning and design optimization of energy systems. A combined heat and power microgrid application was presented by Mehleri et al. (2013), in a case study which involved real weather and load data from a neighborhood in Athens, Greece. They managed to construct a MILP which also took into account the design of the heating and power distribution network, which they solved using the CPLEX solver in GAMS. Except from unit sizing and selection, Omu, Choudhary and Boies (2013), also took into account unit location and distribution network structure.

This study aims at the construction of a MILP for a microgrid, which will be solved in GAMS, by using the CPLEX12 solver, to evaluate the cost-optimal distributed technology selection and unit operation, for several policy scenarios. The approach which was followed is similar to Zachar, Trifkovic and Daoutidis (2015) study, which is also focused on the construction of a MILP, to assess the distributed technology variation through a series of policies.

The model solution consists of three separate sections. In the first section, a replication of the reference case results, presented in Zachar, Trifkovic and Daoutidis' (2015) study is attempted, to check the validity of the constructed optimization program. The second and the third section, force a minimum microgrid contribution to the annual power demand and a reduction to the carbon emissions afflicted by all sources, respectively.

The distinction of this study, lies on the technology selection, which may differ in a high degree from that of the corresponding study of the authors mentioned previously, due to differences in the calculation approach of some parameters and the mathematical approach followed in declaring policy constraints. Another feature is that this study considers, presents and discusses the microgrid's wasted power and heat that occur during the optimization of this program. The model that is constructed in this study shall serve as the basis for future research.

The formulation process of the microgrid's mixed integer linear program is extensively described in Chapter 3. It is followed by the optimization solutions for each scenario in Chapter 4, which also includes a detailed discussion of the results. Basic conclusions which derive from the optimal solutions are summed up in Chapter 5, while some recommendations for further research of this study are reviewed in Chapter 6. Chapter 2 offers a comprehensive explanation about energy production, environment-related issues, power transmission and distribution techniques and microgrids. It also provides the basic optimization tools, necessary to understand the formulation and solution process that will follow.

Chapter 2

Background Information

This chapter contains key information and details about the power industry and the environment, required to comprehend the drivers that make microgrids a necessity of the future. The most dominant power production, storage, transmission and distribution technologies are going to be analyzed, to clarify the advantages and challenges faced by each, along with the impacts they may cause. A brief explanation of the terminology and the necessary optimization techniques, is also available in the last section of this chapter.

2.1 Energy and the Environment

There is an ever-increasing global concern about the environmental impacts caused by human kind. The combustion of fossil fuels for power generation leads to the release of pollutant gases in the atmosphere that contribute to the enhancement of several natural phenomena and the disturbance of multiple ecosystems. In this section some of the negative effects caused by human activities, and especially by power production, will be discussed.

The greenhouse effect is a phenomenon naturally occurring in the earth's atmosphere. Briefly, the majority of the solar radiation that manages to penetrate the earth's atmosphere is absorbed by the surface and a smaller portion is deflected back to the atmosphere. Most of the deflected radiation is released into space, yet a smaller part is absorbed by the greenhouse gases (GHGs) in the atmosphere. The process by which this effect is taking place results in the raise of the atmosphere's average temperature. While this phenomenon occurs naturally, human activities enhance it, resulting in a rise in global average temperatures (earthobservatory.nasa.gov, 2018; Department of the Environment and Energy, 2018).

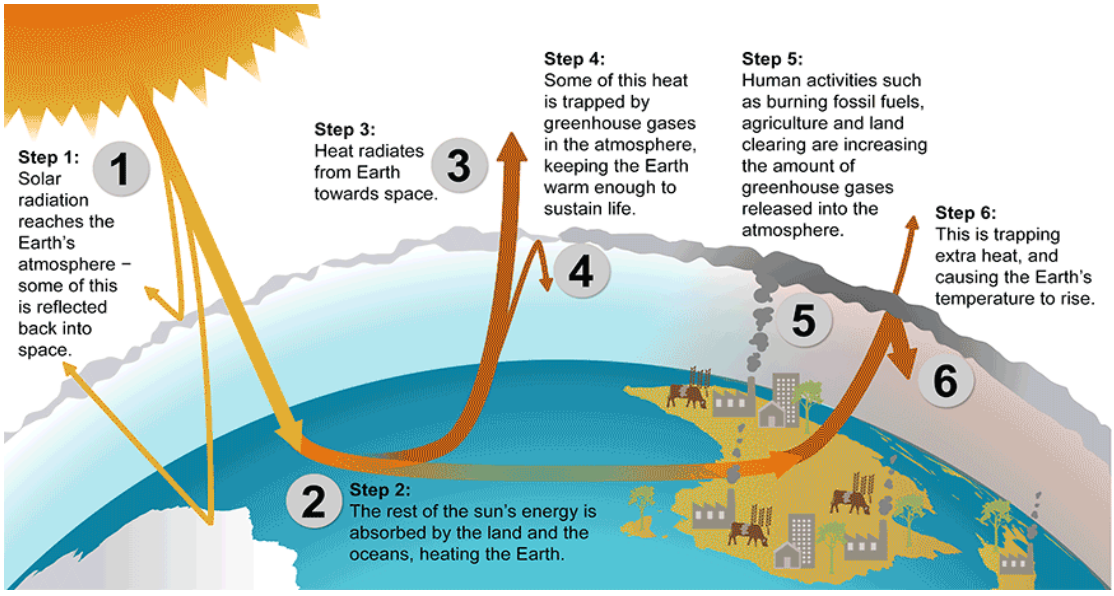

Figure 2.1: The process of the greenhouse effect and average temperature rise (Department of the Environment and Energy, 2018)

The **main GHGs** that contribute to the enhancement of the effect are water vapor, carbon dioxide and methane. While **water vapor** accounts for the most of the effect, it has an average atmospheric residence time of about 9 days due to the water cycle, which is rather small compared to years or centuries for the other two, so it is not treated as a pollutant. Nevertheless, it acts as a positive feedback to the changes of other GHGs in the atmosphere, since its concentration is being governed by the Clausius-Clapeyron relation, making it sensitive to temperature changes. An increase in the concentration of the other GHGs would result in an increase of the average temperature, which would increase water vapor concentration, further amplifying the phenomenon (IPCC, 2014).

Carbon dioxide and methane are components that are also naturally present in the atmosphere. Although methane absorbs much more solar radiation than carbon dioxide, the latter has a much higher concentration, so it contributes about 4 times more to the greenhouse effect (IPCC, 2014).

The main sources of carbon dioxide are **natural emissions** such as ocean release, plant, animal and soil respiration. Naturally emitted carbon dioxide is removed from the atmosphere by a biogeochemical process known as **carbon cycle**, which is depicted in figure 2.2. In that steady state process, the total mass of carbon is exchanged between oceans, large forested areas, the soil and the atmosphere (earthobservatory.nasa.gov, 2018).

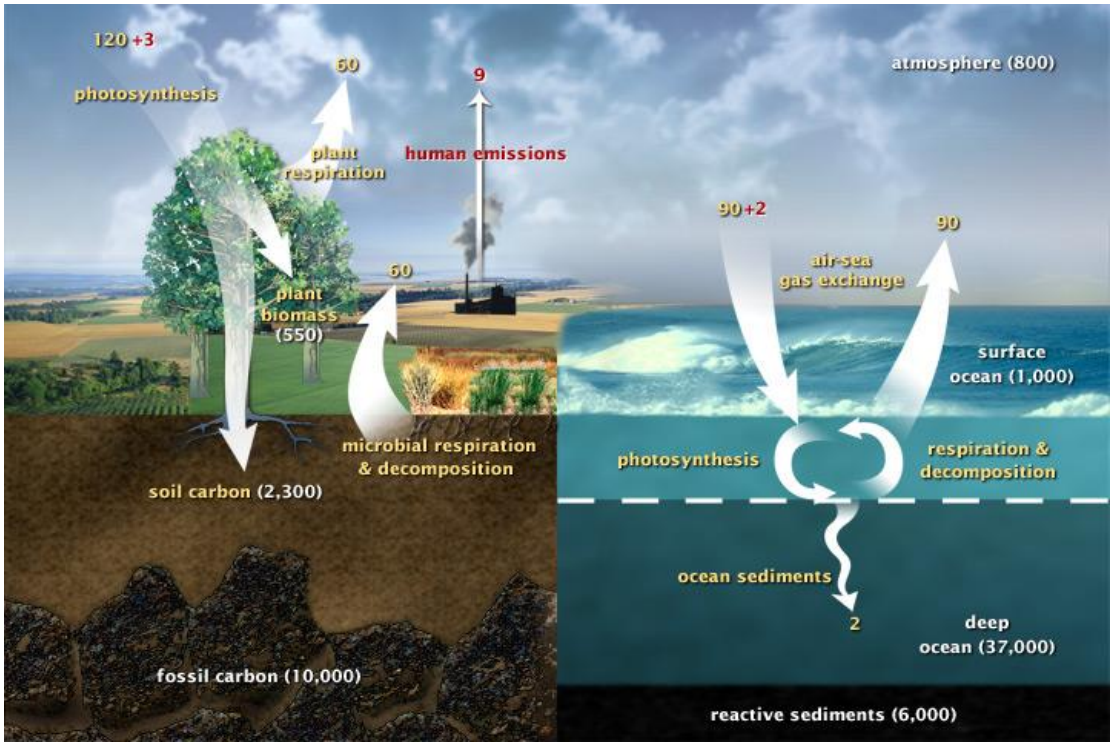

Figure 2.2: Carbon dioxide cycle and its affection by anthropogenic emissions (earthobservatory.nasa.gov, 2018)

Anthropogenic emissions, though lesser, have an enormous impact on this process. The addition of more carbon in the system, in conjunction with deforestation, causes an overall permanent increase to the carbon mass balance. About 40 percent of human emissions are currently being absorbed by the oceans and vegetation, while the rest remains in the atmosphere (IPCC, 2014).

Fossil fuel use is the primary source of anthropogenic carbon dioxide emissions. A strong dependence has been built upon them, year after year, since the industrial revolution. Throughout that period (of about 250 years), a substantial proportion of the hydrocarbon

reserves worldwide, which took millions of years to evolve, has been consumed. EPA and IPCC studies, conducted in 2014, show that power and heat generation sector accounts for 25 percent of all anthropogenic emissions making it the largest single source, as shown in figure 2.3.

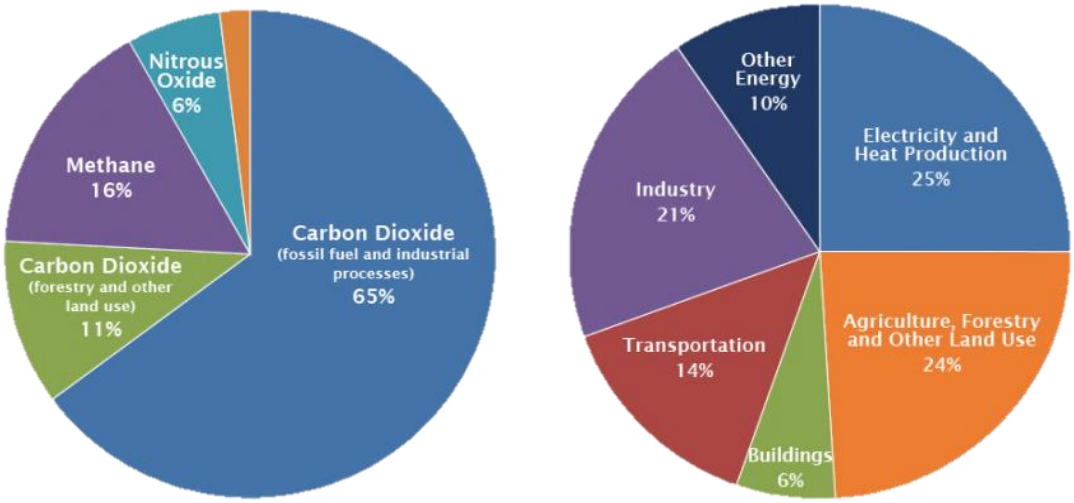

Figure 2.3: Anthropogenic GHGs (left) and anthropogenic carbon dioxide emission by source (right) (IPCC, 2014)

Rain acidification is another phenomenon caused by fossil fuel burning. The combustion of fossil fuels, along with greenhouse gases, leads to the release of components like sulphur dioxide (SO_2) and nitrogen oxides (NO_x). These chemical elements react with oxygen and other components found inside water droplets that are formed into the atmosphere, producing sulphuric and nitric acids (US EPA, 2018).

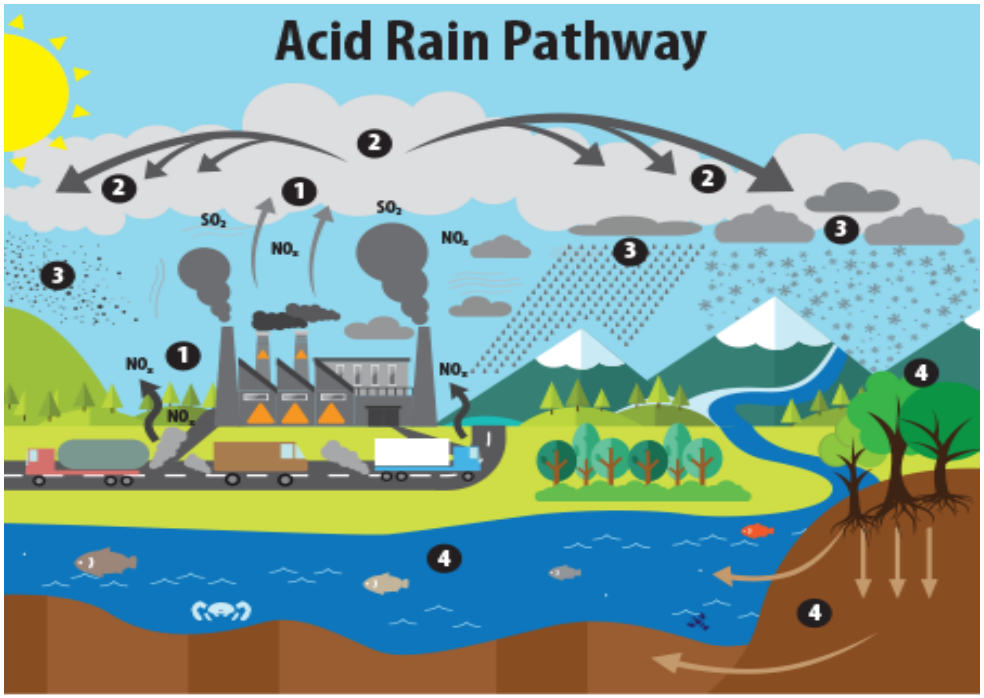

Figure 2.4: Rain acidification process, transfer and affection on ecosystems (US EPA, 2018)

Fossil fuel use for energy production is responsible for about two thirds of sulphur dioxide and a quarter of nitrogen oxides that currently reside in the atmosphere. As shown in figure 2.4,

strong wind currents can transfer these pollutants through very long distances, while due to the water cycle, rain acidification can affect all kinds of ecosystems, from oceans to remote and tropical forests (US EPA, 2018).

Life cycle assessment or analysis (**LCA**) is a way to keep track of all the environmental impacts from human activities, processes and products. It is a method used to evaluate the harm that has been afflicted to the environment from a product system, from raw material acquisition to end use and disposal. This tool is currently under research, since it has great potential to aid in the environmental protection, by being utilized as a guideline in the design of eco-friendlier processes as well as policy and strategies implementation.

2.2 Power Production Technologies

A key factor for a prosperous and growing society is to provide sufficient energy for the people and the industry. Electricity production is the world's largest and fastest growing end-use energy sector, estimated to have a 45 percent increase until 2040. Although carbon intensive fossil fuels provide the majority of the global power demand, long-term prospects for electricity from renewable sources and natural gas are rapidly improving (OECD/IEA, 2015; World Energy Council, 2016).

The transition to less pollutant processes is dependent upon a dilemma between least-cost and environmentally friendly options. As the technology progresses and investments are being made in renewables and ecological sources and the cost of clean power production is gradually declining. Eventually, a time will come where clean power will be much less costly than burning fuel, though this time may not come in the near future, since the energy industry is built upon long-term investments and long lead times.

2.2.1 Generation from Fossil Fuels

Energy production from fossil fuels is the foundation of modern society's economy. Recent studies project fossil fuel reserves depletion time to approximately 37 years for oil and natural gas, and 107 years for coal. Still, fossil fuels meet about 85 percent of the global energy demand today and about 76 percent in the power generation sector. The dependence from coal, oil and natural gas is the result of many factors that make them the dominant energy resource (OECD/IEA, 2013; World Energy Council, 2016).

They can be safely contained and transported throughout the globe, while their high calorific value, leads to the release of great amounts of energy upon combustion. As the first fuels used after the industrial revolution they have undergone extensive research, hence all physical properties are well known and are easily accessible. Techniques of obtaining hydrocarbons have also been thoroughly studied resulting in more affordable and efficient extraction and processing.

Coal meets about 30 percent of global energy demands, making it the second largest energy source worldwide. Along with lignite, it is the leading energy source in power production industry, covering up to 40 percent of global electricity needs. Coal is a key factor of economic growth in developing, as well as developed countries, securing a steady supply of power. Its global consumption was raised to 64 percent from 2000 to 2014, making it the fastest growing fuel during that period (World Energy Council, 2016).

Being the least expensive yet most carbon-intensive source, the growing interest from developing countries has a negative impact on the environment. Although there are technologies that can reduce the amount of carbon dioxide emissions, either by raising the efficiency or by partially capturing and storing them, 75 percent of global coal power plants

utilize simple technologies that require relatively small capital investments (World Energy Council, 2016).

Coal plants generate power by heating water into superheated steam, which drives a steam turbine, in a process known as the **Rankine cycle**. This thermodynamic model is used to predict the performance of steam turbine power generation systems in four simple processes (Andrews and Jelley, 2013).

- The first process (1-2) describes an isentropic **pump**, in which saturated water from the condenser is pressurized and driven into the boiler.
- The second process (2-3) is a **water boiler**, basically a large heat exchanger constantly producing superheated water vapor.
- The superheated steam then enters the **turbine** (3-4) and undergoes an isentropic expansion, producing work by driving the turbine's shaft. During this process steam temperature and pressure drop, and it is converted into a saturated gaseous-liquid water mixture.
- The mixture is then led into the **condenser** (4-1) where the previous mixture is condensing at a constant pressure, becoming a saturated liquid, which is then fed to the pump mentioned in the first process, and the same process is repeated.

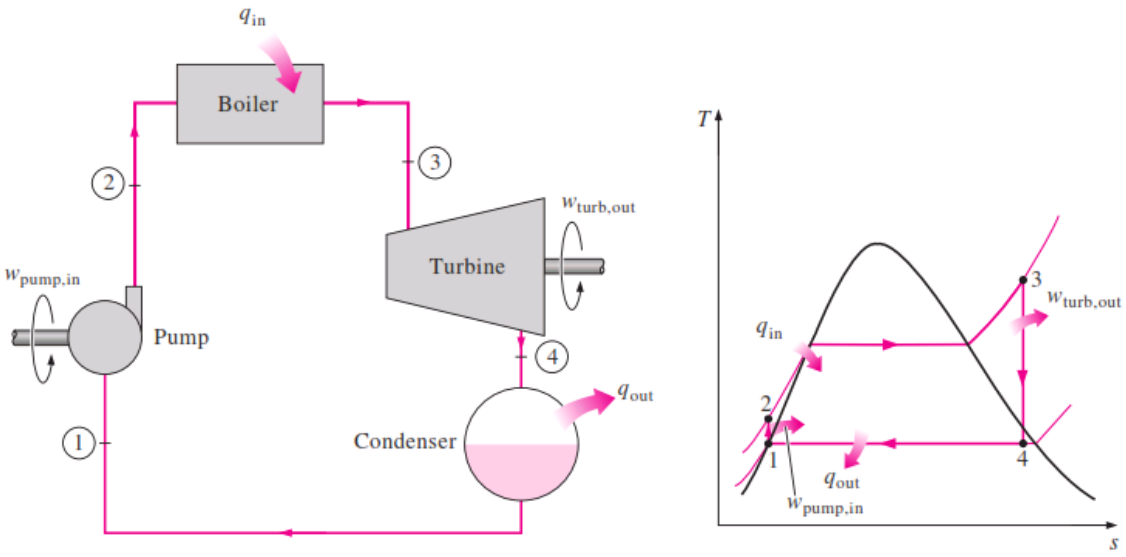

Figure 2.5: Rankine cycle process (left) and its temperature-entropy diagram (right) (Anon, 2018)

The efficiency of the Rankine cycle is proportional to the temperature difference of the steam before and after it enters the turbine and also limited by its specific heat. Due to the Carnot principle, the theoretical maximum efficiency of a system working in a Rankine cycle (considering the temperature differences possible to be achieved with the current technology) is about 65 percent, although in reality this value is much smaller (Andrews and Jelley, 2013).

There are several types of power plants with ranging construction costs currently in use that take advantage of the mechanism described above, in order to generate power at different efficiencies.

- **Subcritical** boiler plants are the fastest to build and the less costly to invest in. A plant of this type offers a relatively small efficiency of about 30 percent and is very popular among fast developing countries, embodying the 75 percent of coal plants worldwide. Due to international mitigations about carbon emissions, this type of technology is

propagated by international energy institutes and is no longer funded by the World Bank, unless necessary (World Energy Council, 2016).

- **Supercritical** plants have efficiencies of about 40 percent and embody the 22 percent of coal fired plants worldwide. The equipment installed requires larger initial capital investments mainly because of the materials used to craft the alloy of the boilers, which are more expensive. A supercritical plant usually emits 20 percent less than a subcritical (World Energy Council, 2016).
- **Ultra-Supercritical (USC)** have an efficiency of up to 45 percent, by working in even higher temperatures and pressures, reducing emissions by a third. The high-quality materials used to build the equipment require large capital investments, hence only 3 percent of coal plants globally utilize this technology. Advanced-USC plants, which will further enhance the efficiency to about 50 percent, are currently in development in wealthy countries. This promising technology works in more extreme conditions than USC but is based on the same principles. It is estimated to further reduce emissions by 20 percent less than a supercritical plant (World Energy Council, 2016).
- **Integrated Gasification Combined Cycle (IGCC)** plants use special equipment in order to produce syngas from coal in a process called gasification. Syngas is a fuel mixture in gaseous form, containing primarily hydrogen and carbon monoxide, and in fewer quantities carbon dioxide, emitting less pollutants upon combustion. This fuel is burned, driving a combined cycle turbine which generates power with an efficiency of about 45 percent. Although these plants have high efficiency and low emissions, they require high capital investments to build. The production of this gaseous fuel can take place either inside a gasifier located above ground, or underground inside the coal seams (World Energy Council, 2016).

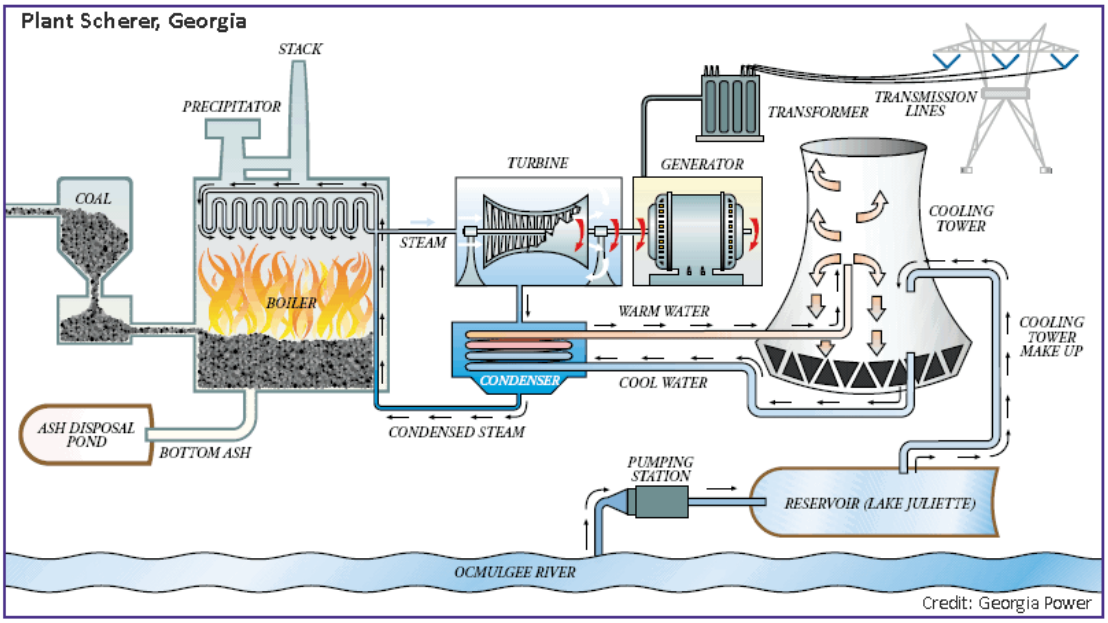

Figure 2.6: Process flow diagram of the subcritical coal thermoelectric plant Sherer in Georgia (georgiapower.com, 2018)

Oil is the world's leading source in regards with global energy demand, covering about 33 percent of its total needs. As one of the most important trading commodities in the world, oil and its products play a very important role in our daily lives and in modern society's economy. Petroleum products are used both as fuels and as raw material from the petrochemical industry (World Energy Council, 2016).

Petroleum-fired power plants cover a very small amount of electricity demand worldwide and are usually fired up during times of peak power demand, due to the high price of oil. Energy generation takes place in a similar way to coal fired plants, boiling water to superheated steam in a Rankine cycle (World Energy Council, 2016).

Natural gas is a very important resource, both for total energy demand and for global power generation, covering 24 and 22 percent of each, respectively. Being the least carbon-intensive fossil fuel, it is proposed as a possible and efficient way of reducing carbon emissions for electricity generation as well as many other processes that require great amounts of energy. That also makes it the only fossil fuel whose demand is expected to grow in the next years, since it has the potential to aid in the transition of the power generation sector into a more ecological era (OECD/IEA, 2013; World Energy Council, 2016).

Electricity production from gas is taking place inside the gas turbines which work by the **Joule-Brayton cycle**, that involves three main sections. The **compressor**, in which a stream of pressurized air is introduced into the system. The **combustion chamber**, where the fuel is introduced via a ring with a steady flow, in order to create a homogeneous mixture, which is then combusted. The combustion raises the temperature and the pressure of the stream. The stream enters the **turbine** in order to expand and produce power. The turbine is made of rotating airfoil blades. The expansion of the hot stream causes the blades to rotate and generate power as well as draw and compress more air (Andrews and Jelley, 2013).

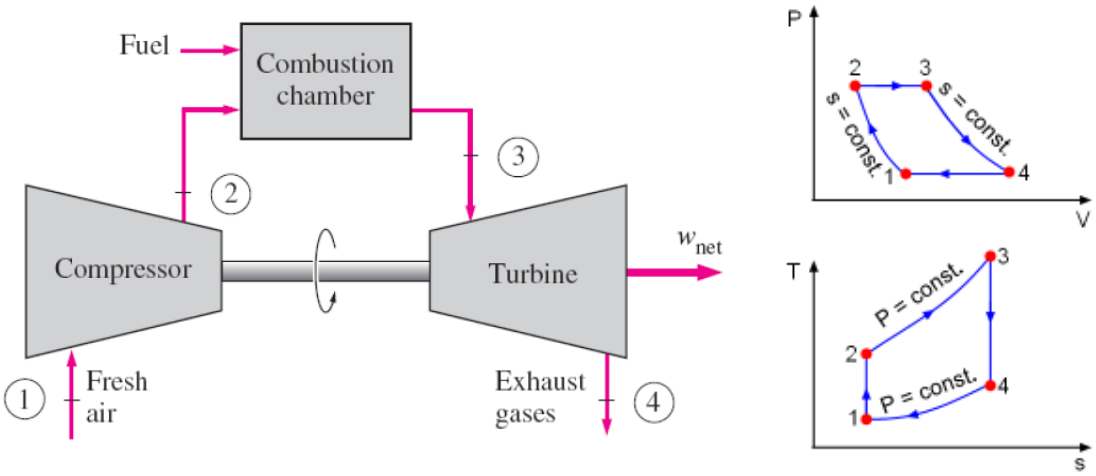

Figure 2.7: An ideal Joule-Brayton cycle process (left) and its pressure-volume and temperature-entropy diagrams (right) (Meirong, H. and Kurt, G., 2017 and ecourses.ou.edu, 2018)

There are two main categories of gas turbines used in gas fired power plants, as shown in figure 2.8. The **heavy frame** engines, that work in low pressure ratios and have relatively large sizes, and the **aeroderivative** engines, which derive from jet engines and work on higher pressure ratios, also being more compact in terms of size. Aeroderivative engines have generally smaller power outputs but their relatively small size makes them ideal for distributed power generation. Heavy frame engines have higher power outputs and are larger in terms of size, hence they are often installed in large scale centralized power production plants (Andrews and Jelley, 2013).

Figure 2.8: Heavy frame engine (left) and aeroderivative engine (right) (gepower.com, 2017)

In terms of efficiency, these turbines alone can achieve from 20 to 35 percent efficiencies when working in a simple Joule-Brayton cycle. It is possible to achieve much higher efficiencies by utilizing the excess energy from the exhaust of the turbine, which still has high amounts of thermal energy. This is mainly achieved by two bottom processes that can be added in the end of the system.

- **Combined cycle gas turbines (CCGT)** take advantage of the excess heat contained in the exhaust stream, by heating water to produce superheated steam. As shown in figure 2.9, the steam drives a steam turbine which performs in a Rankine cycle as described above. The efficiency of the combination of the two cycles is now much higher than of each alone, reaching up to 60 percent (Andrews and Jelley, 2013).

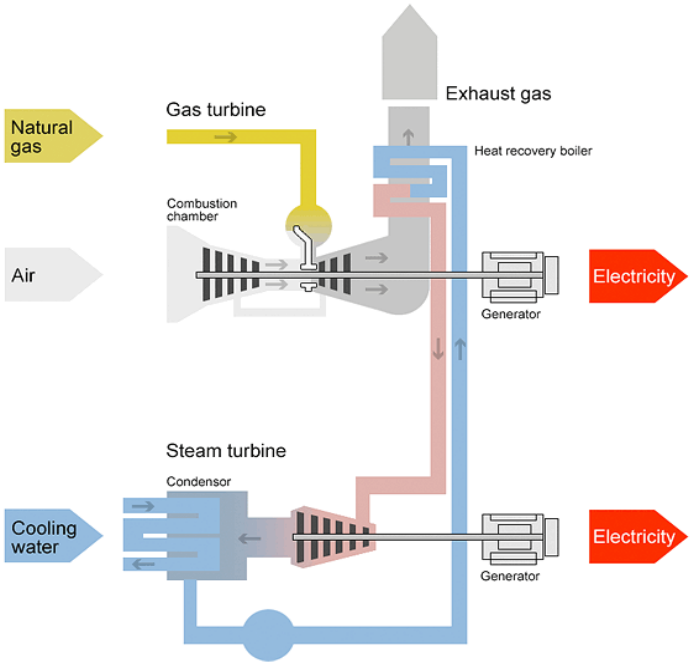

Figure 2.9: A gas turbine with combined thermodynamic cycle (ffden-2.phys.uaf.edu, 2018)

- **Combined heat and power (CHP)** units can achieve even greater efficiencies of about 80 percent, by recovering the excess heat from the condenser of a Rankine cycle. As illustrated in figure 2.10, the heat is used to cover needs in thermal energy in a local community or another industrial plant. Despite the high efficiency that can be achieved by a complete energy system like this, the cost of piping can be excessive, so it is usually preferred by industries for processes that require warm water or utility steam (Andrews and Jelley, 2013).

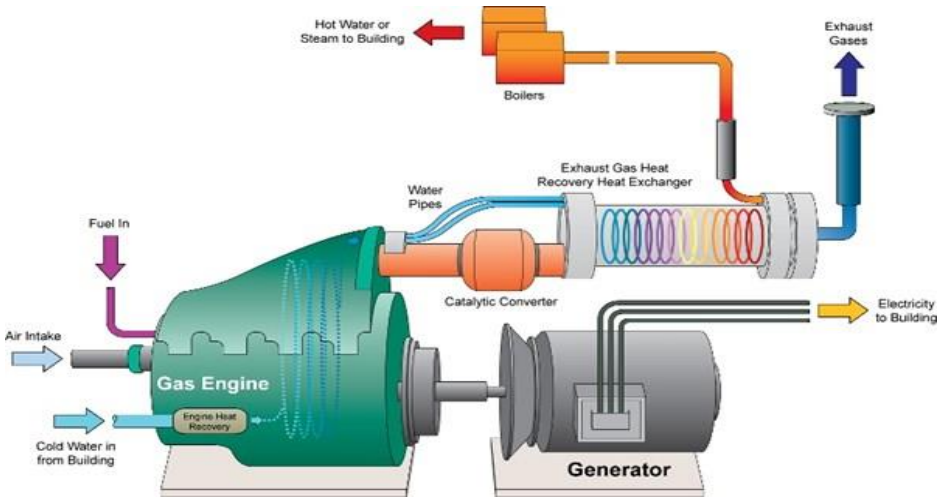

Figure 2.10: Combined heat and power generation by a gas fired engine (energ-group.com, 2018)

2.2.2 Generation from Renewables

As years progress, it becomes ever more obvious that the energy resources that humanity utilizes, need to transit. The environmental impacts from human activities are intensifying, and the effects get more visible over time. Tons of carbon emissions and emission of other byproducts from fossil fuel combustion are unable to be naturally absorbed and stay in the atmosphere for long periods, enhancing phenomena like the greenhouse effect or rain acidification (IPCC, 2014).

What is more, there is a high possibility for current fossil fuel reserves to be depleted in the next century. The extraction of fossils from other reserves may not be economically viable, causing an energy crisis due to humanity's great dependence from them. These are only a few reasons that demand our energy production methods to move forward, into resources that are not harmful for the environment and are not about to be used up (Andrews and Jelley, 2013).

Utilization of renewable resources has the potential to cover all of the issues, since they oppose a much smaller threat to the environment than conventional energy technologies and they are in abundance in nature. Nevertheless, their efficient harvesting and high investment costs are some challenges that scientists and governments still need to overcome (REN21, 2016).

While electric power from renewables is still more costly than that of coal or other fossils, there are many indications that this status will be shifted, since many grand scale renewable power plants are being built at record low prices. In 2015 the installed renewables had a potential to meet 24 percent of the global power demand, with hydropower almost contributing to 17 percent of it (REN21, 2016).

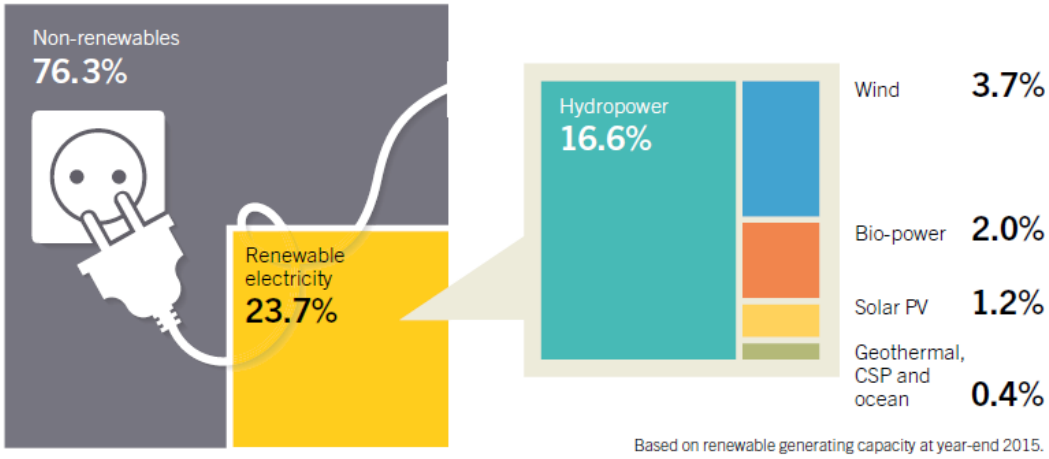

Figure 2.11: Visual representation of the total global demand in electricity met by renewables (REN21, 2016)

Renewables are also the fastest growing technology in the power generation sector, with an average production increase of 2.8% per year from 2015 to 2040, also receiving the two thirds of total global investments in power plants during that period. Wind and solar power plants accounted for almost 77 percent of all new installations in the year 2015, while hydropower installations represented most of the rest (REN21, 2016).

The main renewable resources that are currently utilized mainly consist of hydroelectricity, wind and wave power, solar and geothermal energy and energy from biomass.

Hydropower is one of the most important renewable technologies, covering an important share of the world's global power generation industry with 1064 GW of total installed capacity in 2015. Almost meeting 17 percent of total global power demand, it is the largest source of renewable energy (REN21, 2016).

Figure 2.12: Sayano-Shushenskaya hydropower plant on the Yenisei river, Russia with an installed capacity of 6.4 GW of power (Power Technology, 2013)

Hydro plants take advantage of the natural cycle of the water, and although there have been implications with water dams integrating into this cycle (like the disturbance of several species of fish, etc), progress has been made for the effective resolution of them all (US EIA, 2017).

The main principles used by these plants are rather simple and are based on taking advantage of the contained water's high potential energy, by converting it into kinetic, which converts to mechanical energy, and finally into electricity. Water is let fall from a high altitude to a lower, channeled through a water turbine causing its blades to spin. The mechanical energy is transferred through a shaft to the generator, which produces power (Andrews and Jelley, 2013).

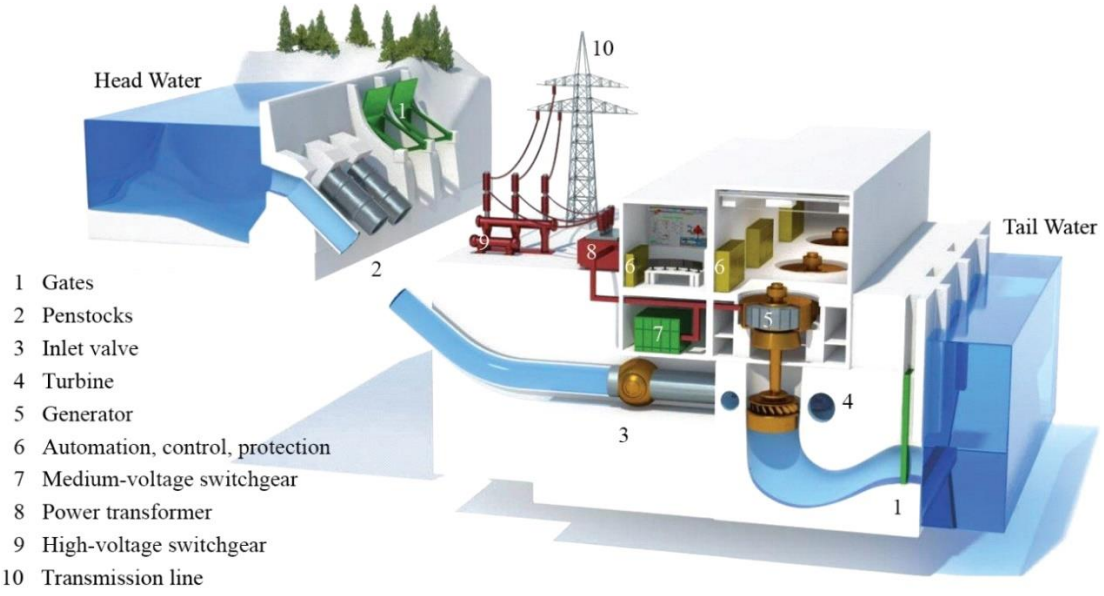

Figure 2.13: A visual representation of a typical hydro plant's main sections (SweetCrudeReports.com, 2018)

Hydroelectric plants vary in sizes and rated power outputs. Ranging from massive facilities like dams, to smaller plants that can take advantage of the water flow in municipal water treatment facilities. Hydropower is one of the least costly energy sources available now, since massive amounts of energy can be produced from hydro plants, while many of them can go from zero to maximum power output in very short time periods (US EIA, 2017).

Bioenergy (or biomass energy) is a term that refers to the utilization of plant or animal-derived products that can be processed in order to produce fuels. The produced fuels are called **biofuels** and are used thoroughly throughout the globe, mainly used as an alternative option to gasoline or mixed with it to reduce its environmental impact (REN21, 2016).

Biofuels are considered a renewable resource since their production is integrated inside the natural cycle of carbon dioxide absorption. Carbon dioxide is absorbed from plantation and converted into carbohydrates and oxygen in a process known as photosynthesis. Combustion of the biomass would result into a null cycle, since the amount of carbon dioxide emitted has already been, and will be absorbed again (World Energy Council, 2016).

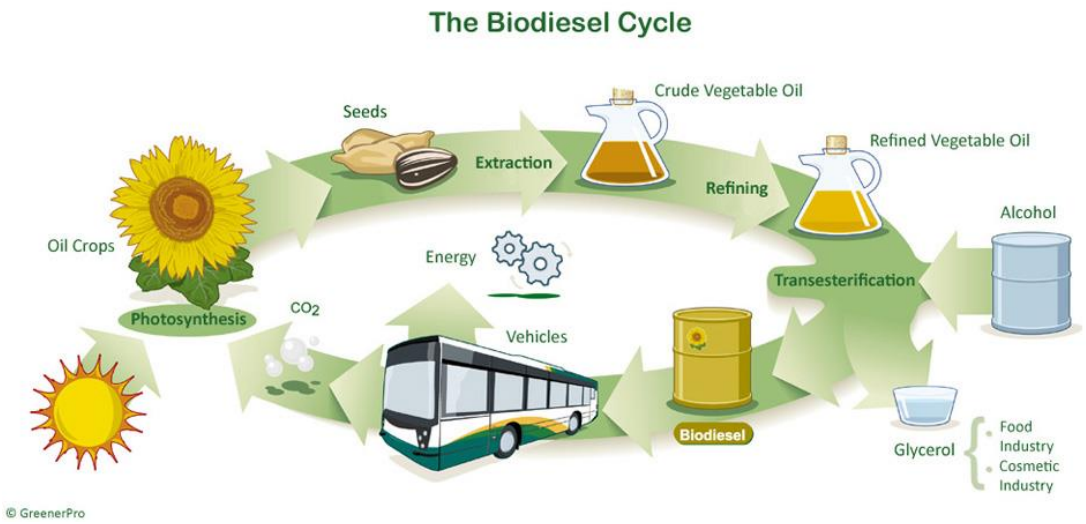

Figure 2.14: Biodiesel use – visual representation of the carbon null cycle (indianbioenergy.com, 2015)

Life cycle assessment (LCA) studies prove very useful in this certain type of renewable, enabling scientists and engineers to monitor and evaluate whether the production process of a biofuel is indeed an eco-friendlier option (World Energy Council, 2016).

Geothermal energy technology takes advantage of the earth's heat in order to cover both heating and power demands. It's a relatively clean and sustainable resource, since no large carbon emissions are released by its extraction and harvesting. While power generated from geothermal energy can be sold in relatively low prices, this resource is scarce. An estimated rated power of 13.2 GW is currently installed globally, while direct geothermal usage installations for heating make for a total capacity of 21.7 GW of thermal energy (REN21, 2016).

Geothermal power plants take advantage of large underground steam reservoirs, in order to drive steam turbines and produce power. They are categorized depending on the quality of the steam inside the cavity, which may require different methods to harvest its energy. There are three main types of technology utilized by geothermal power plants (Andrews and Jelley, 2013; Energy.gov, 2018).

- **Dry steam** plants were the first power plants to utilize geothermal energy, by making direct use of dry steam, located inside underground reservoirs, to drive a steam turbine.

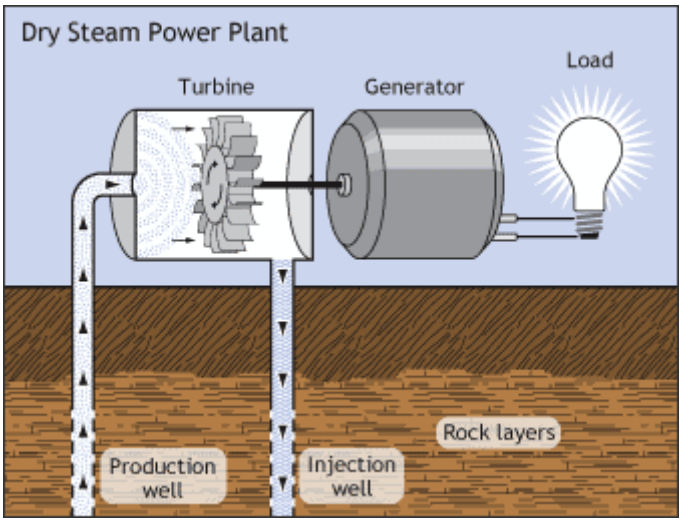

Figure 2.15: Generic process of a dry steam power generation plant (US Department of Energy, 2018)

- **Flash steam** plants are the most commonly used geothermal power plant technology. These plants pump liquid water which has a high temperature (greater than 182 °C) and pressure. The hot liquid water is pumped into a tank of much lower pressure, causing a portion of the liquid water to rapidly vaporize. The steam produced by the rapid vaporization or "flash", is used to drive a steam turbine.

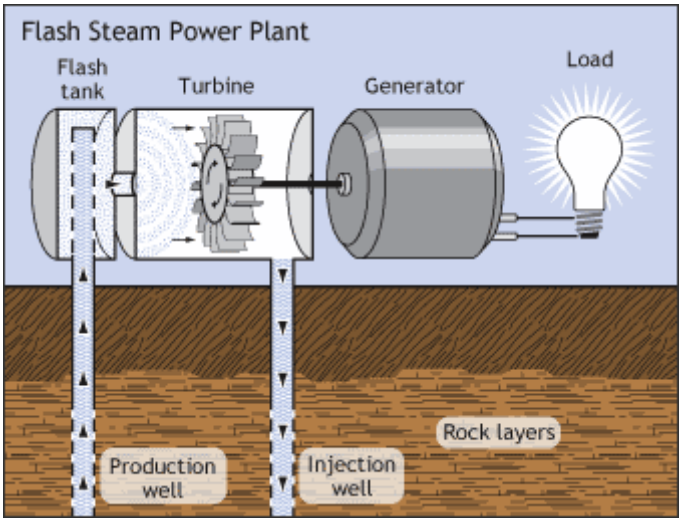

Figure 2.16: Generic process of a flash steam power generation plant (US Department of Energy, 2018)

- **Binary cycle** power plants can utilize water at lower temperature and pressure ranges, yet no hot water from the underground reservoir ever comes in contact with the generator. Liquid water, that has a temperature between 107 °C and 182 °C, is passed through a heat exchanger, in order to heat another liquid with lower boiling point. The liquid evaporates and is used to drive the turbine and produce power.

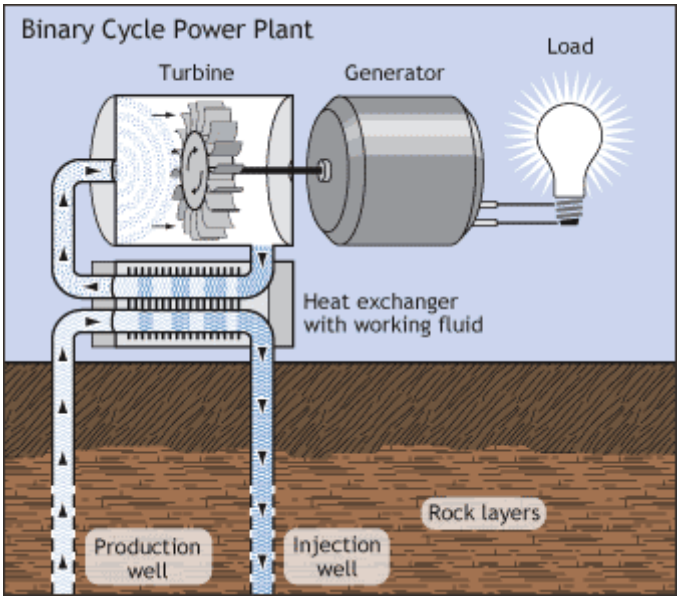

Figure 2.17: Generic process of a binary cycle power generation plant (US Department of Energy, 2018)

Power production from geothermal sources is very versatile in terms of scaling. Small-scale facilities that usually have a low power capacity under 5 MW, have great potential for distributed power generation in rural areas. Their low capital investment costs and CHP capabilities make small scale geothermal power plants a very competitive solution for remote areas (REN21, 2016).

Solar photovoltaics (SPV) is one of the major renewable technologies having a global power capacity of 227 GW, which accounts for almost 1 percent of global power generation in 2015 (World Energy Council, 2016).

Photovoltaic cells work by a direct conversion of the solar irradiance into electric voltage in a process known as the **photoelectric effect**, which is presented in figure 2.18. The photoelectric effect, which occurs naturally in materials called semiconductors, describes the discharge of an electron from a molecule, due to light particles that collide on the surface of the material. The scattered electrons are causing a potential difference between the illuminated and the dark surface, creating an electric current through the material (Knier, 2008; Parida, Iniyan and Goic, 2011).

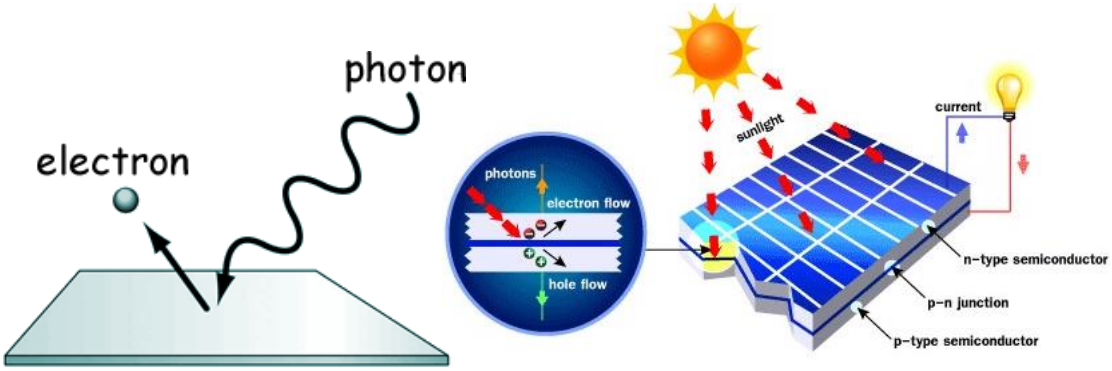

Figure 2.18: The photelectric effect (left) and a solar PV utilizing the solar radiation (right) (Socratic.org. (2016) (left) and thegmcrv.com, 2016 (right))

Although the power that is generated from SPV is mostly clean, it does not achieve high efficiencies and the cost of power output is still not competitive compared to fossil fuels, hence solar investments are heavily dependent on mitigation strategies pledged by governments. The non-continuous availability of solar radiation and the dependence on weather conditions is another issue that needs to be considered while designing a solar farm (World Energy Council, 2016; NREL, 2017).

Nevertheless, a record 25 percent market increase has been achieved in 2014, and manufacturing prices are constantly falling, making it a very promising technology for the future of renewables. As presented in figure 2.19, in the United States, a complete PV system price has dropped by more than two thirds on average, since the beginning of 2010 until the end of 2016 (NREL, 2017).

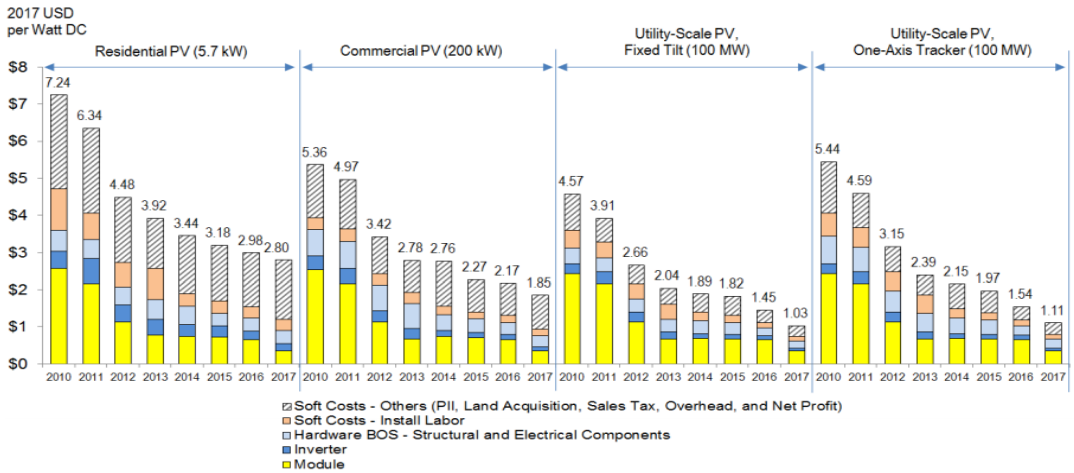

Figure 2.19: Average prices per energy unit for different SPV installation scales in the United States (NREL, 2017)

The efficiency of the produced electricity depends on the light intensity and angle, as well as the material type and manufactured method. While the first two are parameters that are considered later in a solar farm's design, the last two define the rated efficiency and the type of a solar panel.

Solar panels are generally categorized by the cell's crystal purity or alignment. The purer or the more aligned the crystal pledge is, the more efficient is the power generation. Nevertheless, in order to achieve high efficiencies, a higher production cost is required. While new, more efficient types of cells are constantly being researched, the most widespread types of solar panels are three, also presented in figure 2.20 (Andrews and Jelley, 2013; Parida, Iniyan and Goic, 2011).

- **Monocrystalline silicon** solar panels can achieve a relatively high efficiency of about 15 percent. Their high efficiency is the result of a uniform and ordered crystal alignment, which also rises their manufacturing costs. While performing better at low lighting and last longer, they are highly affected by dirt and shades. Their characteristic shape of squares-without-corners is a result of the maximization of their surface, considering that they come from circular silicon wafers.
- **Polycrystalline silicon** solar panels have a smaller efficiency than monocrystalline, reaching 13 percent. They are subjected to fewer processing stages making them much less expensive and a more cost-effective option. They have a square shape, since they can be directly manufactured from a molten liquid mixture.
- **Amorphous thin-film** panels, while cheap, can only achieve efficiencies of about 7 percent. Despite that, their light absorbing layers are about 350 times thinner than that of other silicon panels combined with long gaps between their crystals, makes them very light, flexible and durable.

Figure 2.20: Amorphous thin-film (left) monocrystalline (middle) and polycrystalline (right) solar PV modules (sinetech.co.za, 2018)

Most solar panels are made of semiconductors which are usually silicon based or a silicon alloy, that need to be processed in order to be suitable for electronic usage. In general, the manufacture of such a material is a power intensive process that requires high temperatures to be raised in electric furnaces. With the current global profile in power production industry, this means that a lot of greenhouse gases are emitted for the making of a panel (Parida, Iniyan and Goic, 2011).

However, recent LCA studies show that solar has the potential to be a clean source of energy, since the carbon that is emitted ranges from 1 gCO_2-eq·kWh^{-1} to 218 gCO_2-eq·kWh^{-1} which is a petite value compared to that of fossil fuel emissions. The actual emissions value depends on the country that the panels were manufactured and the insolation that the solar array receives at the location of site (NREL, 2012).

Solar PV arrays use **maximum power point trackers**, electronic voltage converting devices used to reduce the high voltage and match it with the grid's voltage. These devices are essential for the normal operation of a solar plant. On the other hand, **solar trackers** are mechanical devices that are used to rotate each panel, in order to minimize the angle between solar radiation beams and the panels' surface vertical axis, to obtain a maximum efficiency and power output (Andrews and Jelley, 2013).

Wind power generation capacity has increased rapidly over the last decade. As years pass and the technology is constantly optimized, power output efficiency gets higher and the cost of generated wind electric power is constantly dropping.

Wind generation technology has almost achieved a 4 percent of total global electricity generation in 2015, making it the second largest renewable resource after hydropower. The total power capacity in 2015 has reached 435 GW worldwide, while recent policies and mitigations pledged by governments plan to increase the capacity by more than double until 2030 (REN21, 2016).

Wind energy is converted to electricity from the wind turbines. Most wind turbines consist of a few main sections that are common to all generators. The blades act as the turbine, being the part that utilizes the kinetic energy of the moving air streams. The blades are connected to the shaft which transfer the mechanical energy to the generator. The generator is where the electricity is produced. The shaft is usually connected to a gearbox in order to achieve optimal power outputs at several wind speeds (Andrews and Jelley, 2013).

Andrews and Jelley, 2013 as well as the World Energy Council, 2016 describe two main categories of wind turbines, depending on the angle of the axis that the turbine spins, as in figure 2.21.

- **Horizontal axis wind turbines** are the most common type and, as the name suggests, the rotation axis is parallel to the ground. They have the optimal number of three blades in order to take full advantage of the thrust caused by the wind while keeping down manufacturing costs.

  This kind of turbine needs to be pointed in the direction of wind, so that no turbulences (that decrease wind's momentum) are being produced. Smaller wind turbines can achieve that by having a wind vane integrated on top, while large ones use wind direction sensors that connect with a motor to rotate them.

  Large horizontal wind turbines can achieve efficiencies of up to 35 percent, since their tall tower bases allow them to take advantage of faster wind streams.

- **Vertical axis wind turbines** have the shaft that is connected to the generator perpendicular to the ground. Their generator is located at the base, providing a better center of gravity, reducing the structural costs.

  These turbines do not need to be pointed to the direction of the wind so they are simpler. Their special blade design enables them to be closer to the ground, eliminating the cost for building a tall base, as well as maintenance costs.

While they have lower startup speeds, the efficiencies achievable by that technology are relatively small, because of the drag force that is developed by their special design.

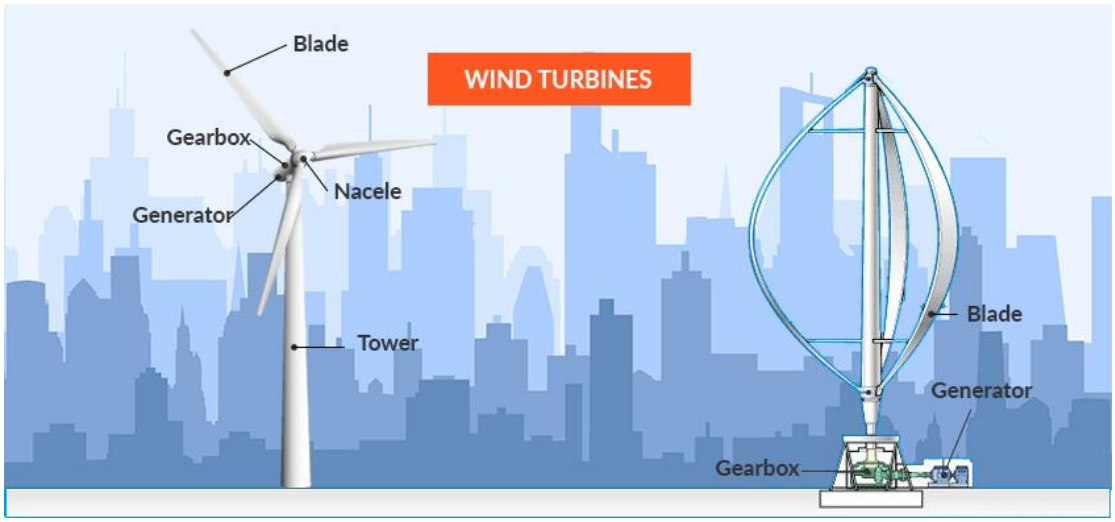

Figure 2.21: A comparison between horizontal axis (left) and vertical axis (right) wind turbines (Lets Go Solar, 2018)

Wind turbines can also be built both **onshore** and **offshore** depending on the region's geographical profile. Offshore windfarms take advantage of the vast open areas of the ocean and are able to deliver high amounts of power very often. As shown in figure 2.22, their special design enables them to float, so they can be installed at all depths. Nevertheless, an offshore windfarm of the same nominal capacity with that of an onshore, generally needs more turbines, since the latter can be built at higher altitudes and take advantage of greater windspeeds (US Department of Energy, 2017).

Figure 2.22: Offshore wind turbines' floating mechanisms (US Department of Energy, 2017)

Although wind farms can produce sufficient amounts of relatively clean and inexpensive energy, with an average price of 0.15 $\$\cdot kWh^{-1}$ in 2015, there are challenges that occur in terms of installation costs, policies and environmental impacts (World Energy Council, 2016).

While the average price of power from wind power has been dramatically reduced the past 10 years, wind power is still a non-competitive option for the most cases and, much like solar power, it is highly dependent on policy decisions of governments. What is more, power generation from wind turbines is dependent on wind speed at the site's location, making it highly variant. The optimal distribution of renewable power during off-peak hours is a challenge that undergoes extensive research in order to be solved (US Department of Energy, 2017).

Another challenge that arises from wind turbines pertains to their aesthetics and the noise they produce due to their blades' rotation. The "not in my back yard" problem, or **NIMBY** for short, is a phenomenon that occurs in many societies, and relates to the public opposition to certain technologies, such as wind turbines, mainly due to aesthetic issues. The NIMBY problem, along with certain environmental impacts (e.g. birds getting occasionally hit by the moving blades, deforestation due to land use, etc.) have led scientists to seek for completely new designs which can meet all the above-mentioned criteria (World Energy Council, 2016).

2.2.3 Generation from Other Non-Renewables

This special category of power production plants produces zero greenhouse emissions, it generates high amounts of power and are able to meet high demands with inexpensive and clean electricity. While some of them play a major role in global power production today (e.g. nuclear fission plants), the most of these technologies are still undergoing extensive research. The research mainly focuses on ways that will enable to harvest the energy of these resources, also making them economically viable and safe to operate at the same time.

Nuclear plants, also referred to as nuclear fission plants, supply a considerable amount of global power production in a surprisingly low cost, making it an important source of energy in both developing and developed countries. More specifically, nuclear power capacity has reached 390 GW in the end of 2015, covering about 11 percent of the global demand in electric power (World Energy Council, 2016).

The rated power output that a single plant can produce is high enough to cover many of a country's needs, both in residential and in industrial sector. That makes nuclear an energy resource that supplies over a third of the electricity needs in 13 countries globally, with France leading the way with a considerable 72 percent of its demand in 2016 (World Energy Council, 2016).

Nuclear electricity production, like coal and oil, is achieved through **steam power generators**. Superheated steam needs to be produced inside **water boilers**, to drive a **steam turbine**. Much like fossil fuels, which release energy upon combustion, energy is released upon a fission reaction of the fuel's nucleus. The basic units of a nuclear power plant and an overall process description is depicted in figure 2.23 (Andrews and Jelley, 2013).

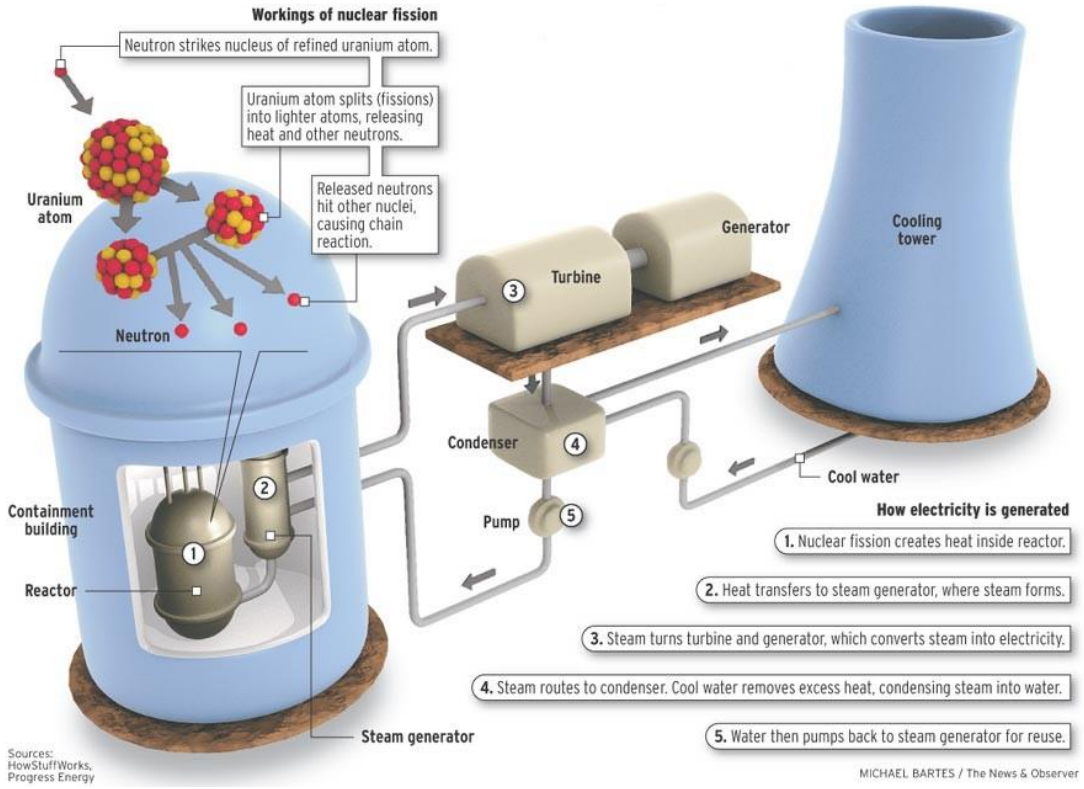

Figure 2.23: Components that constitute a nuclear fission plant (Mechanical Engineering Community, 2017)

Nuclear fission is a reaction that takes place in an atomic level, inside the nucleus of an atom. It describes the process of the subdivision of an atom's nucleus into two lighter nuclei, which also often releases neutrons, radiation and massive amounts of kinetic energy. This can either happen naturally in a rare process known as **spontaneous fission (decay)**, or be caused artificially by deforming the nucleus, to increase its surface area and lose part of its **binding energy**. While all elements' atoms can undergo nuclear fission, very few can sustain it by causing a **chain reaction** (Andrews and Jelley, 2013; Nuclear Power, 2017).

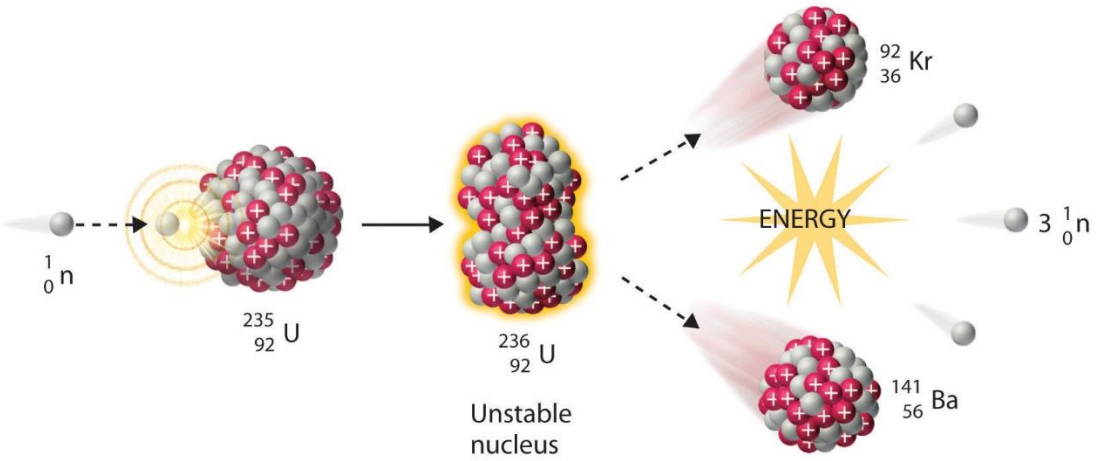

Figure 2.24: The neutron-induced fission reaction process of a Uranium's 235 nucleus (Nuclear Power, 2017)

Uranium-235 and **uranium-238** are elements that are widely used by nuclear power plants, since a chain reaction is feasible and sustainable when one of their atoms is split. The fission of a uranium-235 in figure 2.24, for example, is possible if one of its atoms gets bombarded by a neutron. The atom initially receives the neutron and gets excited, dividing shortly after into

barium-141 and krypton-92 which move at great speeds. During the division, 3 neutrons are emitted on average, each of them bombarding another uranium molecule, constantly reproducing the process, until the fuel is consumed (Nuclear Power, 2017).

The nuclear fission reaction often takes place inside a **pressurized vessel** enclosed in a **radiation shield**. The fissile material, that is usually in the form of **fuel rods**, releases heat upon reaction, which is transferred to an inert gas (typically H_2O or CO_2 or He) that surrounds it. The gas is then led through a **heat exchanger** which uses the thermal energy of the gas to produce utility steam. This whole process is visually represented in figure 2.25. Nuclear power facilities can produce tremendous amounts of electricity, by utilizing this energy intensive process, although there are some issues that need to be addressed (Andrews and Jelley, 2013; Nuclear Power, 2017).

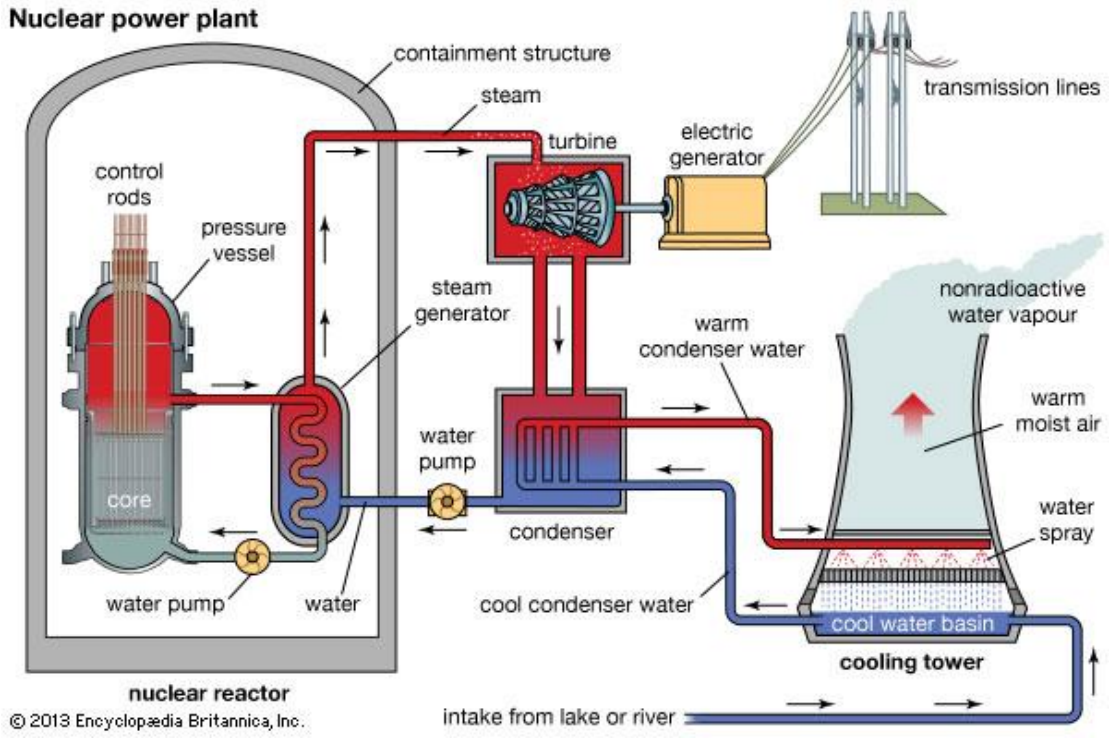

Figure 2.25: Schematic of the working process of a nuclear plant (Encyclopedia Britannica, 2017)

Fission products are being produced by the separation of the fuel's nucleus. They are relatively unstable at the time of their creation and have to go through a series of **beta decays** to regain stability. During that process **gamma radiation** and **fast moving charged particles** are being released (Andrews and Jelley, 2013; Nuclear Power, 2017).

While charged particles generally inflict more damage on humans, it is the gamma radiation that is the main concern when shielding a reactor. The charged particles have very short ranges compared to that of gamma radiation, so it is mainly the latter that needs to be contained, since it can travel through long distances and cause damage (Andrews and Jelley, 2013).

Cost-effective and viable **radioactive waste management** is also a challenge that occurs by this, otherwise clean source of energy. Radioactive waste is a term used to describe both the radioactive products of nuclear fission and any material that has been contaminated by radioactivity (World Energy Council, 2016).

Produced waste can be categorized depending on the level of the radioactivity into **low**, **intermediate** and **high-level waste**. All radioactive materials have the tendency to lose their radioactive nature sooner or later due to decay. The time it takes for half of a material's atoms to decay, is this material's **half-life**. Usually with a short half-life comes an intense energy loss rate (Andrews and Jelley, 2013; World Energy Council, 2016).

In general, it is possible to **treat** the used fuel in order to retrieve any remaining quantities of uranium, as well as plutonium isotopes, formed inside the reactor, also achieving a retrieval of more than 50 percent of the initial energy content. The treatment process of high level radioactive fuel waste is presented on figure 2.26. While some of the fuel wastes can be reprocessed and reused, eventually some will need to be dispatched in ways that protect public health and the environment (World Energy Council, 2016; Nuclear Power, 2017).

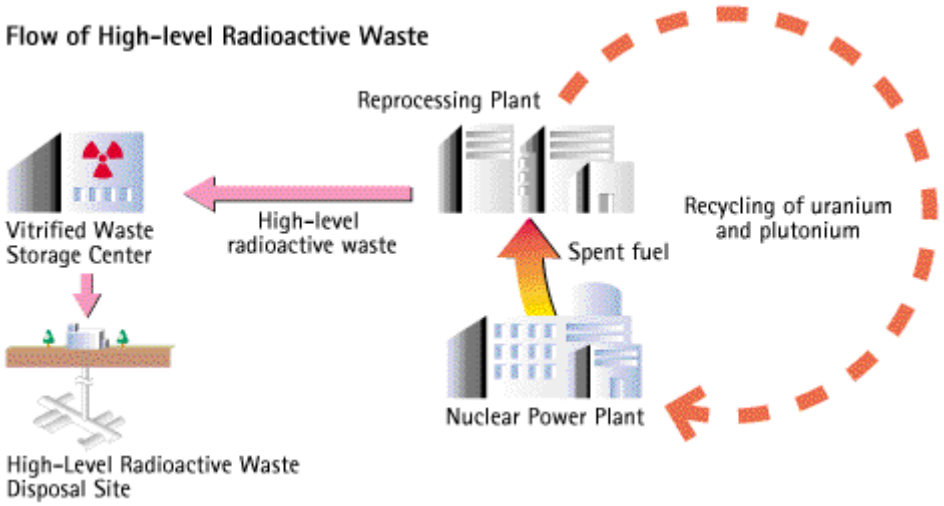

Figure 2.26: High-level radioactive waste disposal process (fepc.or.jp, 1999)

The usual method currently followed for radioactive waste disposal is to first store the waste in facilities that can contain radioactivity. Fuel waste is usually kept into **storage** for several years in order to lose their short-term radioactivity. Storage also takes into account the possible retrieval of the waste to make for an easier management. When the radioactivity of waste drops into safer levels, they are permanently disposed in **underground sealed containers**, the depth of which depends on the radioactivity level of the waste (World Energy Council, 2016).

Despite that nuclear power is a clean, efficient and cost-effective energy resource, it has undergone much criticism throughout the past few years. That is mainly due to accidents that have recently happened, such as the Fukushima disaster in 2011, which has resulted in the evacuation of very large area until now and many years to come (World Energy Council, 2016).

Nevertheless, as stated in the World Energy Council (2016) report: "*the number of safety incidents at nuclear plants recorded by the US Bureau of Labor Statistics for 2012 was 0.4 per 200,000 hours worked, compared with 2.8 for fossil fuel plants, 3.1 for utilities in general and 3.9 for manufacturing industry*".

Nuclear fusion is a promising power generation technology that takes advantage of the high thermal energy that is released by fusion reactions. A fusion reaction, like the one in figure 2.27, is a nuclear reaction that, unlike nuclear fission, describes the permanent conjoint of two nuclei into one heavier element. This process naturally takes place inside the sun, where hydrogen atoms collide and fuse to form helium atoms, also releasing excessive amounts of heat, since they reach a lower and more stable Gibbs energy level (World Nuclear Association, 2017).

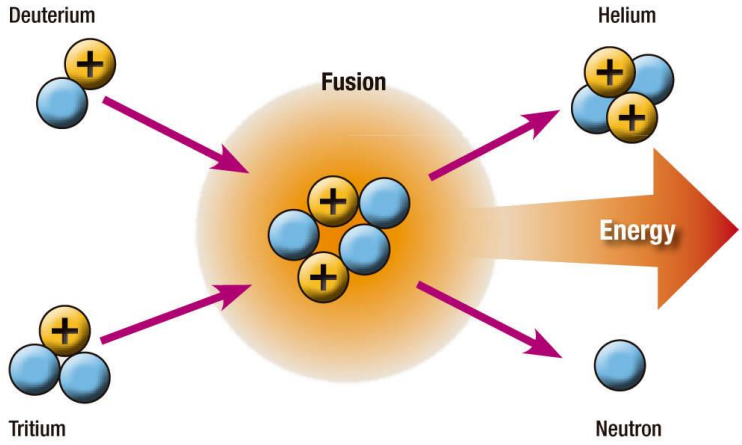

Figure 2.27: A thermonuclear fusion reaction process (nuclear-energy.net, 2017)

A fusion reaction is achieved by producing **hydrogen plasma** where molecules have an average kinetic energy that is high enough to increase the number of collisions, whose force surpasses the repulsive forces between two nuclei, causing them to fuse. This kind of nuclear reaction is called thermonuclear fusion and results in the release of tremendous amounts of energy which can be harnessed. The only known method to control and confine such an energy intensive process is through strong magnetic fields (World Nuclear Association, 2017).

Despite that the theoretical part of the reaction is sufficiently understood and the process artificially reproducible, there are still great lengths that scientists have to go to, in order for fusion power to become a reliable resource. The current research focuses on the optimization of the design of a system that can sustain thermonuclear fusion reactions long enough so that the released energy can be harnessed for power production (World Nuclear Association, 2017).

2.3 Power Storage Technology

Weather-constrained power production inserts randomness as a factor in an already challenging problem, that is to provide a clean and steady supply of electricity both for residential and industrial purposes. The transition to renewable energy sources leads to the need of investing in power storage systems that are capable of storing electricity. Storage of the excess power is a very important aspect of the modern society's energy profile because it enables the use of cleaner energy resources that are not always available in times of need.

Energy storage is a market that has taken off in the last few decades, growing in a similar rate with renewable technology, since these two are somewhat codependent. Storage technology is constantly progressing setting out to cover a variety of applications that may demand either very high or low storage capacities for either long time periods of steady power supply or very short ones, like frequency adjustment (World Energy Council, 2016).

The general idea behind energy storage is to find the most efficient ways to convert electrical energy into other forms that can be conserved for long time periods. Taking that into consideration, most electrical power storage systems can be categorized depending on the conversion that the electrical energy has undergone, into electrochemical and mechanical energy storage systems (Chen et al., 2009).

While there are many more categories and applications, this article will focus only on a few devices are part of these three categories, since they are the most common for stationary applications, like power production.

2.3.1 Electrochemical Potential

Electrochemical potential conversion is a technique which has many application examples worldwide and is very versatile in terms of capacities. The main processes that are of interest are redox reactions that take place inside batteries, as well as the conversion techniques of electricity to a fuel gas, such as hydrogen and methane, and the utilization methods of these fuels. Fuel cells will also be introduced in this chapter, since most authors refer to them as a mean of storing power, rather than a power generation technology (Chen et al., 2009).

Batteries are a very common way of storing electricity by converting it into electrochemical potential. Battery market has seen a rapid growth in the last few years for a wide variety of applications, since they are a compact, reliable and steady power supply, able to have high capacity and efficiency and can change power outputs very fast, depending on the demand (World Energy Council, 2016).

On the other hand, they still have high manufacturing costs, and while they solve the problem of storing clean energy from renewable resources, they may have a high impact on the environment if not properly disposed.

Batteries are comprised of **electrochemical (voltaic) cells** inside of which, electrical energy is stored in the form of chemical potential. When needed, the chemical energy is converted into electrical energy by electrochemical reactions that enable electrons to flow.

While there are many types of batteries, all work by the same principles and contain three main sections. Each cell contains two **terminals**; one anode (negative) and one cathode (positive) made of different materials, usually metallic. The two terminals are separated by an **electrolytic mixture** that enables the flow of electric current though it and between the anode and the cathode. The components that constitute a generic battery can be observed in figure 2.28 (Chen et al., 2009).

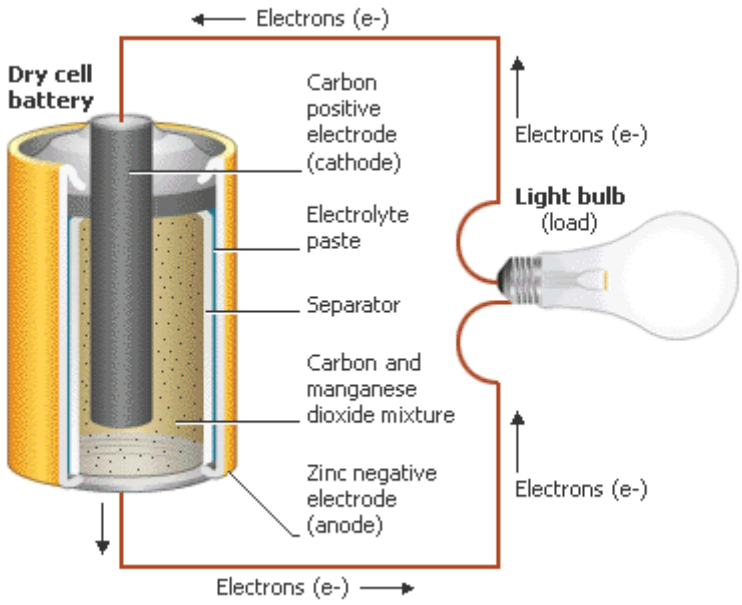

Figure 2.28: Internal components that comprise in a battery (Energymaxout.com, 2018)

The chemical reactions that make batteries work are oxidation and reduction reactions that create the charges needed for an electric potential difference to occur. During discharge, an oxidation reaction takes place inside the cells, and electrons flow from the anode to the cathode

through the circuit, with the electrolyte connecting the two terminals. When charging, reduction reactions take place and the above process is reversed (Chen et al., 2009).

Although not all batteries have the ability to be recharged, rechargeable (secondary) batteries are used in most cases, since the cost in the end of their lifetime is much lower than disposable (primary) ones. Some commonly used rechargeable batteries are briefly discussed below.

- **Lead-acid** batteries, like that in figure 2.29, are the oldest and most commonly used battery type in grand scale applications, since it has a low manufacturing cost, yet have a high durability and storage efficiency ranging from 70 to 90 percent. On the other hand, this battery type is characterized by a small life cycle, reduced performance in lower temperatures and a small power capacity per total mass installed, due to lead's high density. The reactions that take place inside the terminals are: $Pb + SO_4^{-2} \leftrightarrow PbSO_4 + 2e^-$ in the anode, and $PbO_2 + SO_4^{-2} + 4H^+ + 2e^- \leftrightarrow PbSO_4 + 2H_2O$ in the cathode (Chen et al., 2009; Parra et al., 2017).

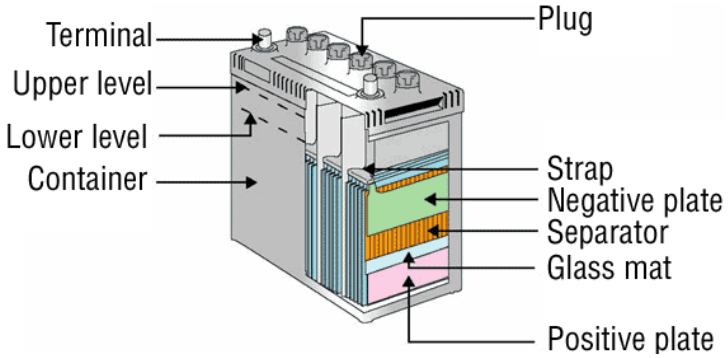

Figure 2.29: The internal components of a lead-acid battery (Baj.or.jp, 2004)

- **Nickel-cadmium** battery is a technology which is quite old as well, finding wide applications like UPS and in telecommunications. Figure 2.30 illustrates the internal components of a Ni-Cd battery. They generally have high energy densities, are sufficiently durable and do not require high maintenance costs. They have an intermediate life cycle which is higher than lead-acid batteries' but still not significant. While they offset in some degree the disadvantages of their counterparts, they have higher manufacturing costs and pose a notable threat to the environment since cadmium is a toxic heavy metal, hence their disposal needs to be done strictly by the existing regulations. The chemical reaction that takes place inside the metallic case is $2NiO(OH) + Cd + 2H_2O \leftrightarrow 2Ni(OH)_2 + Cd(OH)_2$ (Chen et al., 2009).

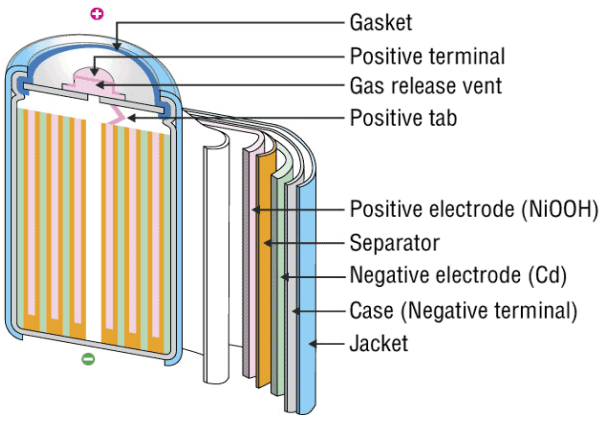

Figure 2.30: Inner parts of a nickel-cadmium battery (Baj.or.jp, 2004)

- **Lithium-ion** batteries are outlined by very high rated lifetimes, power density and efficiencies that can reach an impressive 100 percent, making them specifically suitable for smaller or portable applications. Unfortunately, they are also characterized by very high manufacturing costs, although their production rate has taken off the last decade, which will eventually result in the reduction of their price. The cathode is a metal oxide which has undergone a lithiation process, which results in a material with crystal structure like $LiNiO_2$. The anode is made of a graphitic carbon layer and the electrolytic mixture contains lithium salts like $LiPF_6$. A Li-ion battery schematic is presented in the figure below (Chen et al., 2009; Parra et al., 2017).

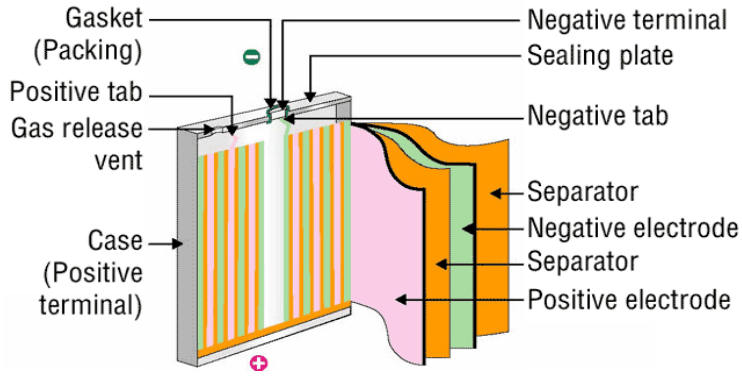

Figure 2.31: Parts that comprise a lithium-ion battery (Baj.or.jp, 2004)

Another battery type is the **flow battery**, whose electrolytic mixture contains at least one electroactive species, which freely flow inside the voltaic cell. The main difference between them and conventional batteries is that the energy is stored in the electrolyte, which is kept outside the battery.

Power-to-gas conversion usually refers to the utilization of voltage for **hydrogen** and oxygen production by water **electrolysis**, a method that is currently undergoing extensive research to become less costly and more efficient. Hydrogen can be stored either as a liquid or in a gaseous form, to be used as a fuel in conventional reciprocating engines, gas turbines or fuel cells to produce power, when needed. (World Energy Council, 2016)

The produced hydrogen can also be used as a reactant in a **Sabatier reaction**, in which hydrogen reacts with carbon dioxide to produce methane and oxygen. This reaction is preferred in many cases, since methane has a higher calorific value, is used for more applications and can be contained and transported more safely and inexpensively. The produced methane could be considered as a renewable resource, if the power that was used for its production was generated by renewables, since it would result in a null cycle (Chen et al., 2009; Parra et al., 2017).

Fuel cells is a technology that has been vigorously researched since the 1960s, when NASA initially used them as a way to meet the demands of Gemini and Apollo missions. Today they are used to power and heat both large public facilities and residencies, converting chemical potential to electricity and heat, efficiently.

All fuel cells consist of an **anode** and a **cathode** separated by an **electrolyte**. Power conversion in this technology is a steady state process, which is also the main difference that separates them from classical solid-state batteries. The fuel, which is constantly replenished and is flowing through the anode, reacts with the oxidant which is flowing through the cathode, releasing electrons that are forced to flow through the circuit creating a current (Chen et al., 2009; Larminie, J. and Dicks, A., 2009).

These systems can be categorized based on the different fuels and electrolytes that are used. A brief discussion of fuel cell types will follow.

- **Hydrogen fuel cell** is a general category of fuel cells that use hydrogen as a fuel. Examples of this technology are Proton Exchange Membrane (**PEMFC**), Alkaline (**AFC**) and Phosphoric Acid fuel cells (**PAFC**). In general, hydrogen moves through the electrolyte to react with oxygen and produces electricity and water, in an exothermal reaction. The whole process is depicted in figure 2.32. They are characterized by high energy densities and good scalability and modularity. Nevertheless, it still is an expensive technology, with quite small rated efficiency ranging from 20 to 50 percent (Chen et al., 2009; Larminie, J. and Dicks, A., 2009).

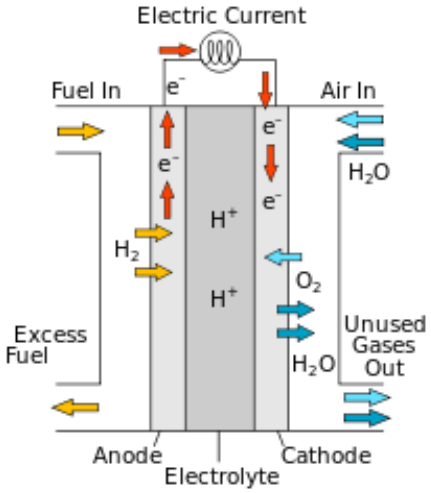

Figure 2.32: Reaction process of a generic hydrogen fuel cell (Dervisoglu, R., 2012)

- **Direct-methanol fuel cell** (**DMFC**) is a proton exchange fuel cell that, as the name suggests, the fuel, which is methanol, is directly fed into the system, eliminating the need of expensive pretreatment of the fuel. The overall reaction is $CH_3OH + 1.5O_2 \rightarrow CO_2 + 2H_2O$, also releasing electrons in the process. Due to osmotic phenomena that take place inside the cells, these systems have a small rated power output and are relatively inefficient, but are able to produce small, yet steady amounts of energy for a long time. A direct methanol fuel cell working process is presented in figure 2.33 (Chen et al., 2009; Larminie, J. and Dicks, A., 2009).

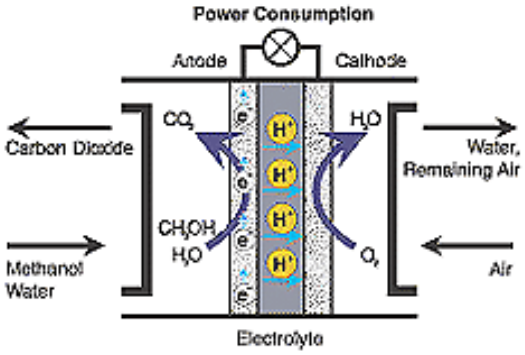

Figure 2.33: Working process of a DMFC (nfcrc.uci.edu, 2017)

- **Molten carbonate fuel cells** (**MCFC**) use an electrolyte that is usually made from lithium potassium or lithium sodium carbonate salts, as shown in figure 2.35. They operate at medium to high temperatures of about 650 °C in which temperature range, the fuel can be reformed inside the cell, eliminating the needs for pretreatment. Nevertheless, the electrolyte which is in liquid state needs to constantly be replenished with carbon dioxide, since carbonate salt ions are being consumed during the reaction that takes place in the anode. While typically, the efficiencies this type can achieve reaches up to 60 percent, it takes quite a long time to reach such a high temperature after a startup, so are only used for stationary applications. The high temperatures also enhance the already corrosive nature of the catalyst, which results in a relatively small equipment lifetime (Chen et al., 2009; Larminie, J. and Dicks, A., 2009).

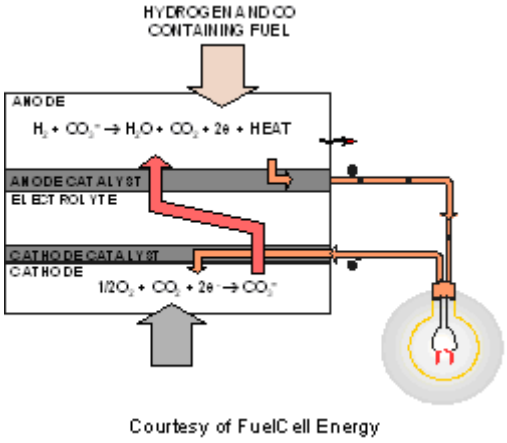

Figure 2.34: Working process of a MCFC (nfcrc.uci.edu, 2017)

- **Solid oxide fuel cells** (**SOFC**)operate at high temperatures ranging from 800 °C to 1000 °C, which enables them to directly utilize fossil fuels that are reformed inside the cell. The electrolyte is a ceramic made of yttrium stabilized zirconium oxide, whose pores enable oxygen molecules to travel though it and react with hydrogen molecules in the anode, to form water and release electrons, as presented in figure 2.34. While SOFCs can achieve efficiencies of at least 60 percent, they need long time periods to reach optimal operation temperatures and, just like MCFCs, are mainly used for stationary power generation (Chen et al., 2009; Larminie, J. and Dicks, A., 2009).

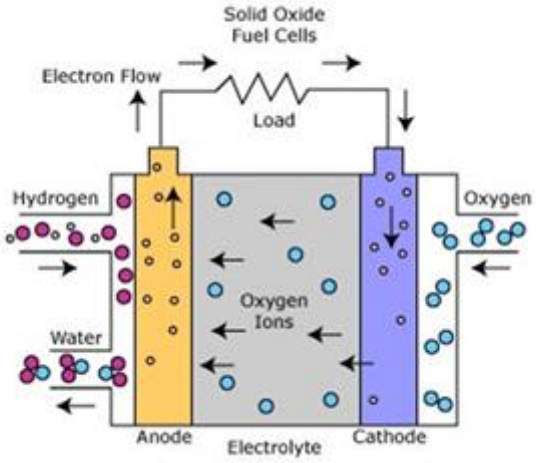

Figure 2.35: Reaction process of a SOFC (protonex.com, 2017)

Fuel cells are usually treated as single parts that are integrated inside a more **complex power generation system**. Much like gas turbines, the hot exhaust stream from the fuel cells that operate in high temperatures can be utilized, by adding a **bottoming cycle**, to further raise the efficiency. The bottoming cycle can either be a combined cycle, to produce more power, or the utilization of the thermal energy to meet heat demands of nearby establishments (Larminie, J. and Dicks, A., 2009).

2.3.2 Mechanical Energy

Mechanical energy storage refers to techniques that store electric energy by converting it to either potential energy, or kinetic energy. When electricity is abundant, it is used to power motors that either propel water to a high altitude or compress air into large tanks, converting electric energy to potential energy.

Kinetic energy can also be a form of storage, by spinning heavy disks, in order to achieve high momentum. These systems have low capacity costs and can be efficient, to an extent. They can either be used to power cities for hours, days, even years, or are simply used to moderate frequency losses during power transmission.

Pumped hydroelectric is the most important power storage system currently in use, in terms of total global capacity. This technology has been vigorously studied the past century and is now well understood, generally finding application in large scale facilities that may need to cover high loads for very long-time periods (World Energy Council, 2016).

They have the highest rated capacities, comparing to other electric storage technologies, that generally range from 100 MW to 3000 MW, and efficiencies that range from about 70 to 85 percent, considering effects such as the evaporation that lead to loss of water mass. High capacity combined with their significantly big lifetime, which ranges from 30 to 60 years, result in a reduction of the cost per unit of power stored, making this storage type relatively inexpensive (Chen et al., 2009).

Its operation principles are quite simple and typically involve three main sections. **Two vessels** that need to be located in different altitudes in order to create hydraulic potential difference. A **pump** is needed to elevate the water mass into the highest vessel during time periods of excessive power production. Finally, a **water turbine** needs to be installed at the bottom in order to harvest the kinetic energy of the falling water's mass and turn it to electricity. It is obvious that the greater the water mass that is released and the altitude difference between the two reservoirs, the higher is the power output (Chen et al., 2009; Andrews and Jelley, 2013).

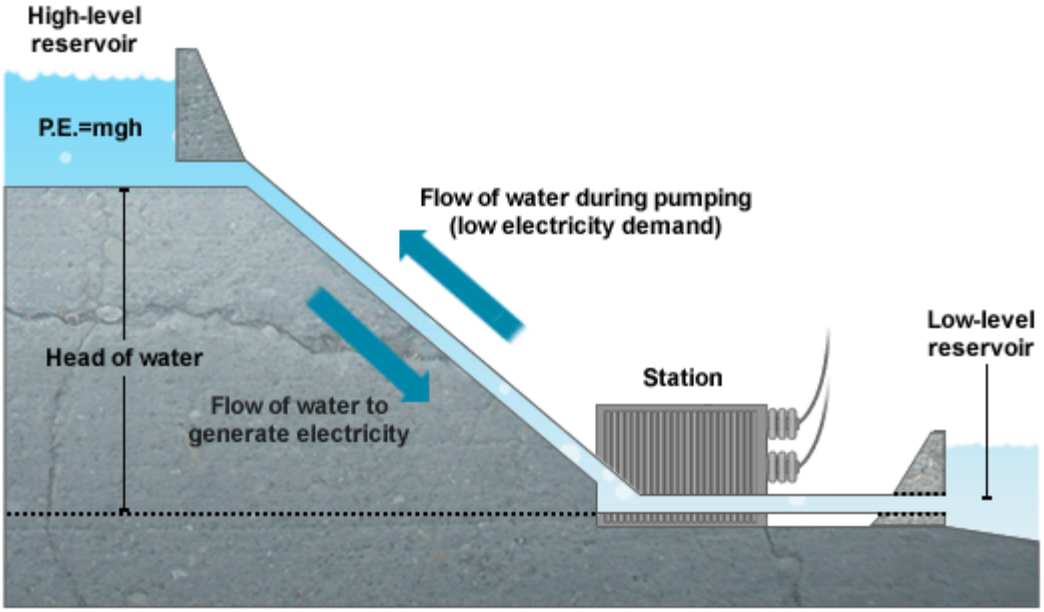

Figure 2.36: Schematic of a typical pumped hydroelectric storage plant (Energy Storage Sense, 2017)

It can be immediately realized that the major disadvantage of this technology is that the site of the facility needs to provide sufficiently large altitude differences and large water masses at the same time, making it a scarce resource, while initial capital investments are also very high (Chen et al., 2009).

Compressed air energy storage is the second and only other technology with almost as high storage capacity and power output as the pumped hydroelectric's. This technology is designed to have a power output that can range between 50 MW and 300 MW that can last for many hours, even days. Many units are installed globally, since energy can be stored and produced at a low cost, and at quite high efficiencies that can range from 70 to 90 percent. Systems that utilize compressed air technology are capable of operating in daily cycles, in order to minimize energy costs and maximize the efficiency (Chen et al., 2009; World Energy Council, 2016).

Units that use this technology store electric energy during off peak periods by powering **compressors** that pressurize air into a large tank. These tanks usually are **underground cavities** from dry salt mines, since they are almost impermeable and can store air mass for even years without having any losses. They can also withstand the high pressures of about 4 MPa to 8 MPa that are required to operate the system, and are inexpensive (Chen et al., 2009).

In peak demand periods, the compressed air is controllably let out, heated by **heat exchangers** and led into a turbine train which contains both **high and low-pressure gas turbines**. The air is then mixed with natural gas and is combusted inside the low-pressure turbine, producing more power. The exhaust stream then is used to heat the pressurized air from the tank, as shown in figure 2.37 (Chen et al., 2009).

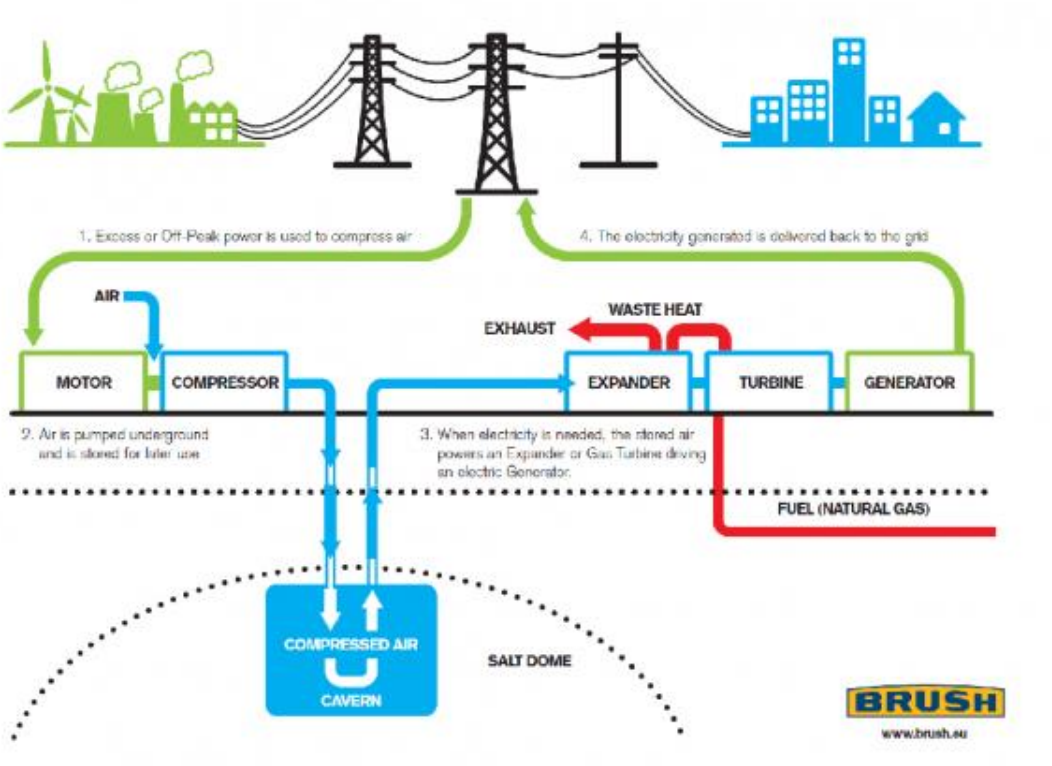

Figure 2.37: Schematic of a compressed air storage system (brush.eu, 2018)

It is an integral part of this system that the air has to be mixed with natural gas in order to be combusted so that the system can be efficient. This reliance on fossil fuels, makes this system less attractive, since pollutant emissions have to be produced every time it is operated. Another major drawback is this system's dependence on an already preexisting underground cavity, since the construction of a pressure tank of such size would make power production from this unit economically infeasible (Chen et al., 2009).

Flywheels are a very old technology and are mainly used to make up for voltage and frequency drops that often occur during power transmission. The way they work is really simple, since they mainly involve a massive disk that revolves at high speeds, as explained in detail in figure 2.38 (World Energy Council, 2016).

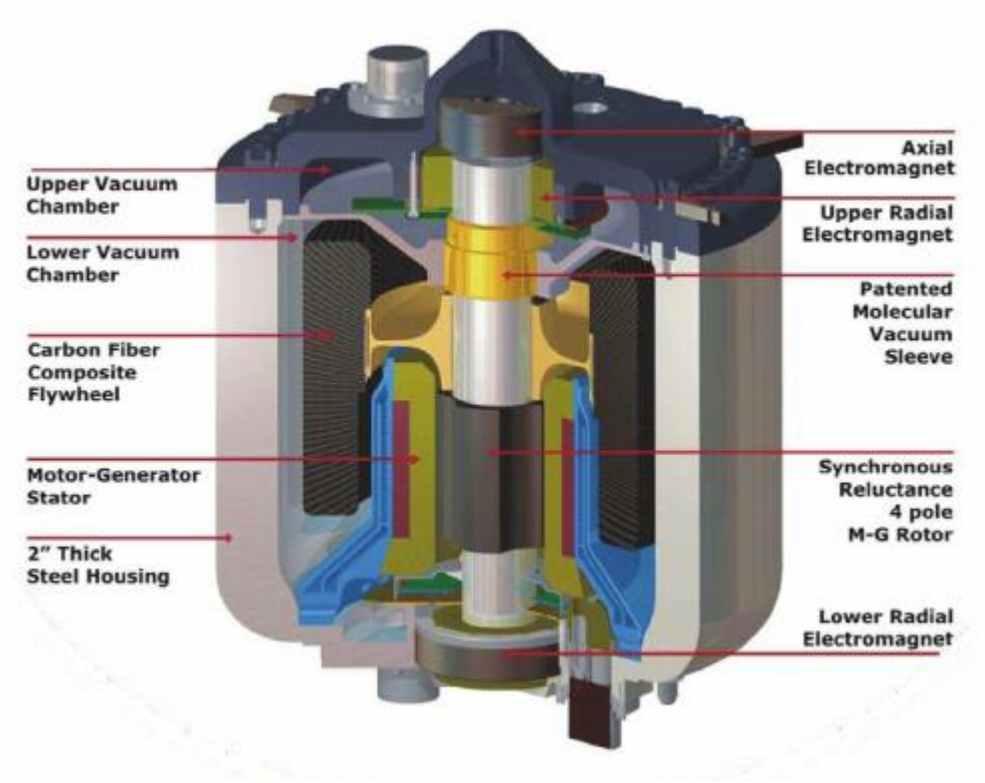

Figure 2.38: Internal components of a flywheel energy storage unit (power-thru.com, 2016)

When charging, the disk is accelerated by a motor, while during discharge, the motor acts as a generator, taking advantage of the disk's angular momentum to spin a turbine and produce power. Design simplicity that leads to long life cycles and high efficiencies that are somewhat between 90 and 95 percent, are some of the main advantages that this system has to offer (Chen et al., 2009).

2.4 Traditional Grid and Microgrids

In the previous chapters, an extensive description of the most important power generation and storage technologies has been carried out. These technologies are currently employed mainly by public or private energy generation companies that produce power in large scale facilities.

While this way of resource harvesting generally works, providing large amounts of good quality energy for both residential and industrial use, there are issues that often arise from the way that the electrical grid is currently set-up.

These topics are going to be evaluated in this chapter, right after a general explanation of the power grid's working process is conducted. A thorough description of distributed energy generation and the microgrid concept will also be managed.

2.4.1 Centralized Generation

Centralized power generation refers to the current way that power is produced, transmitted and distributed to the end users, by large centralized plants. Technically, they are called centralized because they are built away from the load and only a few facilities cover the majority of its demand (US EPA, 2017; McDonald et al., 2012).

These facilities are able to meet all kinds of demands, from heavy industrial to residential, usually providing low cost power originating from a variety of energy sources. The produced electricity is delivered from the production site to the consumer by a large network of cables, pylons and power management and regulation stations, forming an electric network also referred to as **macrogrid**, depicted in figure 2.39 (PNNL, 2016; McDonald et al., 2012).

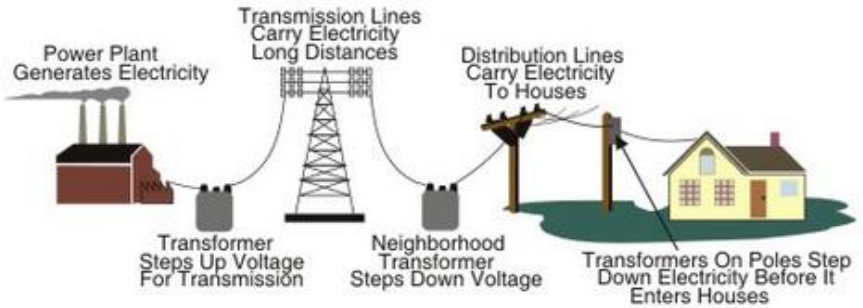

Figure 2.39: Schematic of power delivery to consumer, from generation to transmission and distribution (US EPA, 2017)

Briefly, the electricity that is produced in the plant undergoes a voltage increase by a **step-up transmission substation** and led through **transmission lines**. High voltage is essential for long distance power transmission to minimize energy losses, while it is also utilized by some types of industry. High voltage is then decreased to **medium and low voltage**, by **step-down transmission substations**. It is finally led to the corresponding end-users by the **distribution system**, which is shown in figure 2.40. This complicated system embodies the largest physical machine ever constructed by human kind (PNNL, 2016; McDonald et al., 2012).

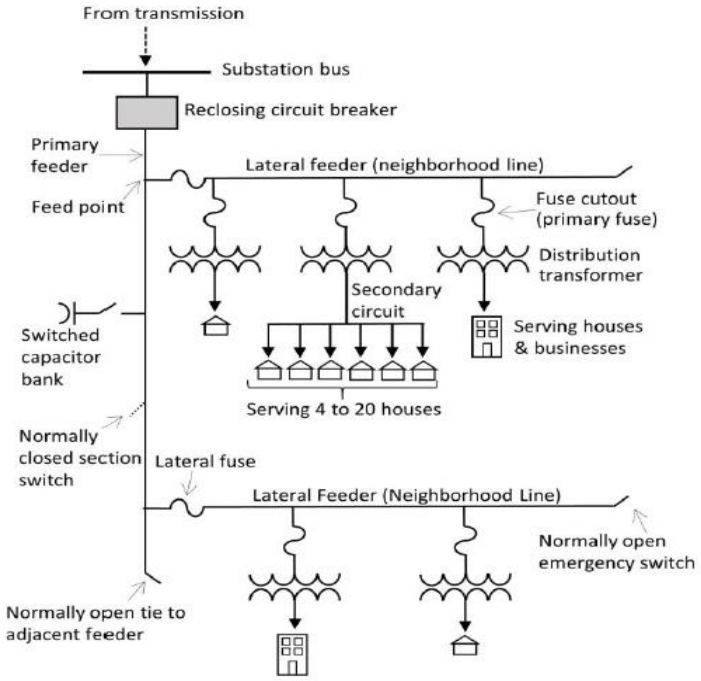

Figure 2.40: A more detailed schematic of the power distribution system (PNNL, 2016)

Power transmission lines are **interconnected**, enabling electricity to travel through various routes of long distances that often cross national borders. When load demands exceed a central power plant's capacity, other power plants can make up for it, to prevent black-outs. Interconnection of transmission lines requires all power sources to operate at exactly the same frequencies, otherwise many complications may occur (PNNL, 2016; McDonald et al., 2012).

Interconnected **smart grids** communicate with each other, sharing load information to readjust distribution routes in case of the occurrence of an unexpectedly high demand. Smart grids are an upgrade to the traditional distribution network that enables a **two-way communication** between the end-user and the utility power provider. A smart grid can also exchange information about demands and production with distributed energy sources, in order to find the optimal route and minimize energy losses (PNNL, 2016).

2.4.2 Distributed Generation and Microgrids

Distributed generation (DG) refer to power production from small-scale resources that are spread through and are integrated to the traditional grid. They are able to utilize a variety of resources, both renewable and non-renewable, as well as energy storage units. The diversification of the technology that can be employed gives the opportunity to reduce the carbon intensity of electricity and heat production (Lasseter, 2007; McDonald et al., 2012).

Microgrids are systems that contain both distributed energy resources and loads at the same interconnected network. While microgrids are interconnected and interact with the traditional grid through a point of common coupling, they are independently controlled and can disconnect via a static switch to operate autonomously in an "islanded mode". The autonomous operation may be used to mitigate grid disturbances to enhance its resilience. Located in a close proximity to the end-user, these systems can cover both electrification and thermal energy needs by cogenerating heat and power, to increase the overall efficiency of the energy production (Lasseter, 2007; PNNL, 2016).

Although there many microgrids that differ in design and power outputs, they generally consist of the **distributed generation units**, the **energy storage units** and the **load**, all connected to a **controller,** as shown in figure 2.41. The load may be any equipment or process that consumes power or heat. The microgrid's controller is its center of command, receiving information about consumption to optimally regulate each equipment's actions, minimizing costs and power losses. The controller is also responsible for decisions related to the microgrid's common point of coupling with the macrogrid. The two-way communication of these systems is crucial for the efficient distribution route management (Lasseter, 2004).

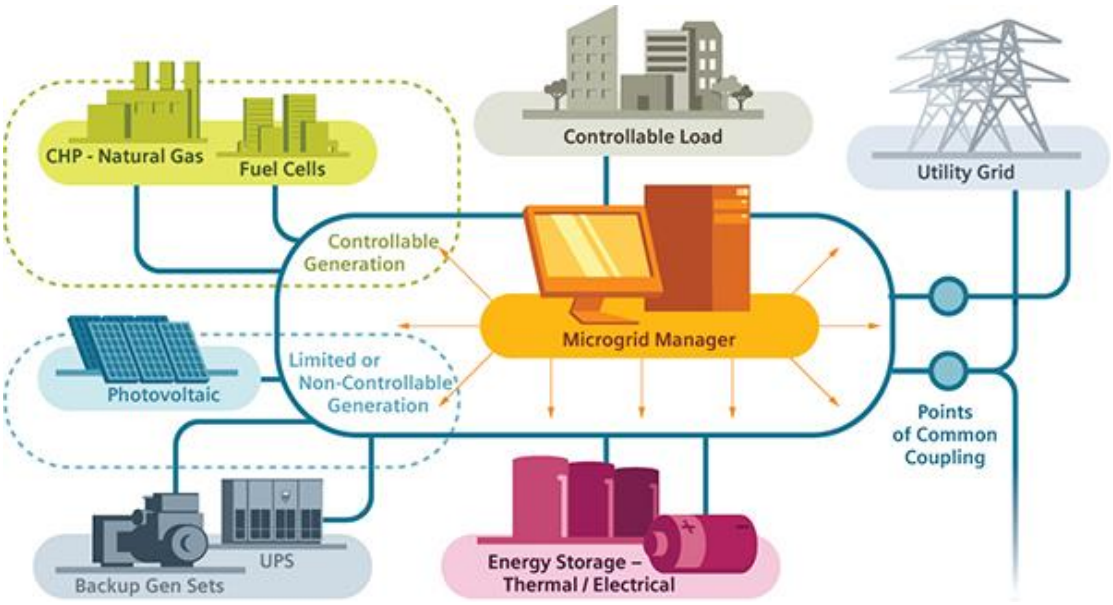

Figure 2.41: General components that a microgrid consists of (w3.usa.siemens.com, 2017)

The following figure depicts a microgrid concept introduced by Lasseter 2007. The microgrid in figure 2.42 consists of several feeders that are normally connected to the macrogrid through the point of common coupling. Each feeder contains micro loads that are either sensitive or unimportant. In case of a blackout, the microgrid's sensitive components can island from the macrogrid, through the static switch, to be protected. The sensitive micro loads in feeders A, B and C can work independently with locally generated power and connect to the microgrid through nodes 8, 11, 16 and 22 which also control their operations.

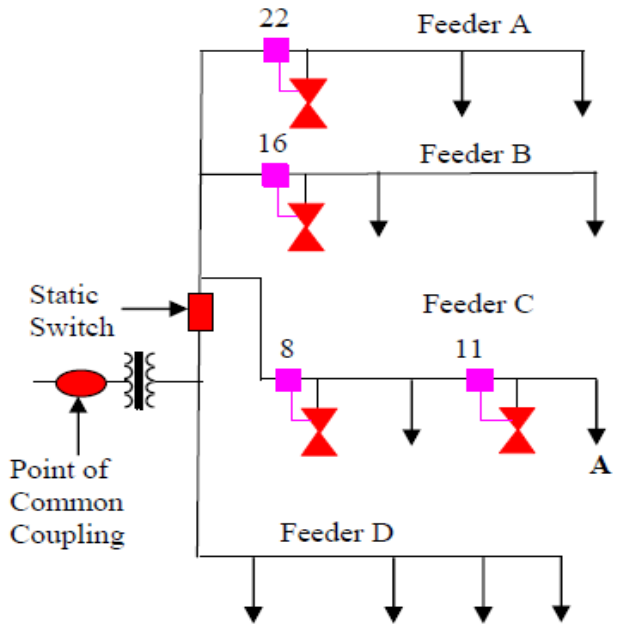

Figure 2.42: Schematic of Lasseter's microgrid concept (Lasseter, 2007)

Microgrids are a smart grid technology, since they enable the autonomous management and monitoring of the load and can exchange information with the utility provider. These systems' categorization can be arbitrary, since they can cover many ranges in demand and can offer a variety of utilities. Nevertheless, PNNL and the US Department of Energy, present four types of microgrids; single customer, partial feeder, full feeder, and full substation, depicted in figure 2.43.

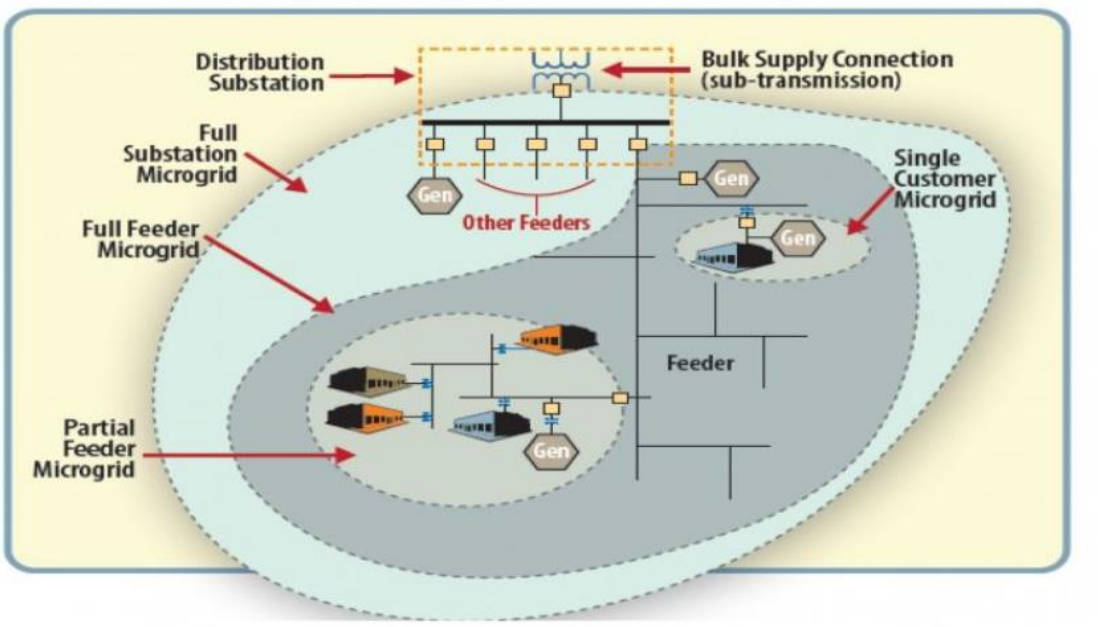

Figure 2.43: Schematic of the four microgrid concepts presented by PNNL (PNNL, 2016)

These microgrid types mainly pertain to the number of micro loads they meet and each load's level of demand.

- **Single customer** microgrids are relatively small-scale energy systems which can be disconnected from the grid and operate almost completely autonomously. A single customer microgrid, as shown in figure 2.44, may partially or wholly meet the demands, both thermal and electrical, of facilities like university campuses, military bases, hospitals and industrial blocks, to either reduce costs, raise energy efficiencies and protect sensitive components (PNNL, 2016).

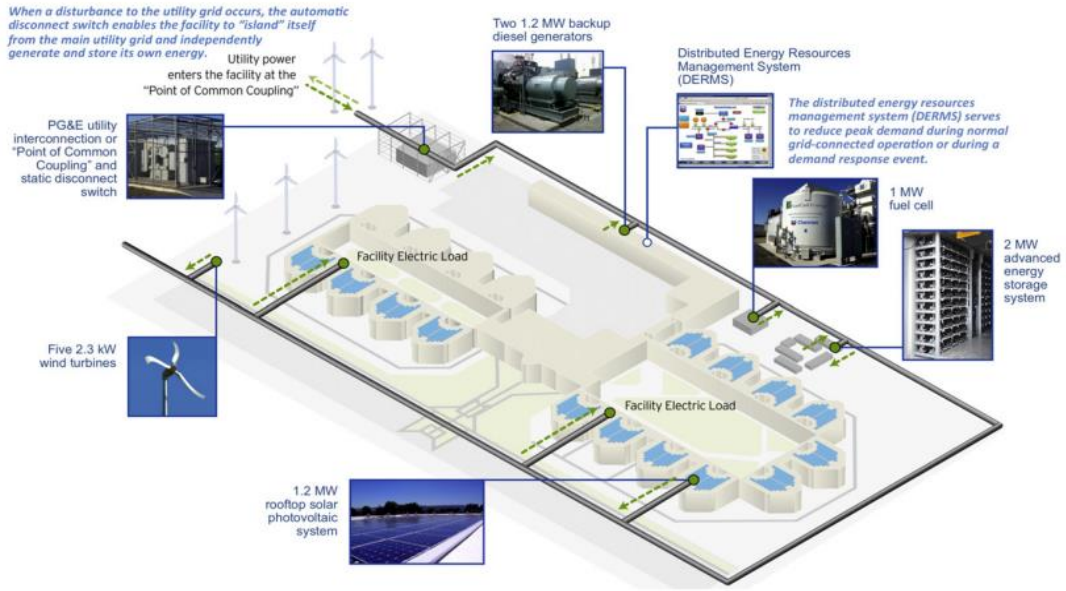

Figure 2.44: Demonstration of the commercial application of a single customer microgrid, Santa Ria Jail, Dublin (Ton and Smith, 2012)

- **Partial and full feeder** microgrids may meet the demands of multiple individual consumers at once. That is, they can utilize already preexisting distribution

infrastructure to deliver power generated by local distributed resources, but still operate independently from the traditional grid (PNNL, 2016).

- **Full substation** microgrids have distributed power generation units separated from the load via a distribution substation. This concept is more than 10 years old and is widely used since it solves many compatibility issues between the power from the macrogrid and the power generated by the distributed resources. This design also helps with location related issues, since the generation units can be located at different sites from the load (but still in close proximity) (PNNL, 2016).

Microgrids have repeatedly been proposed as a possible solution to address some of the traditional grid's drawbacks, by integrating into it and upgrading it. These systems have many positive aspects, that may make them a prospective solution for the energy future.

- One of the most important advantages of microgrid technology is its **reliability** in power generation and transmission, by being able to operate in an islanded mode. Many high-tech industries, companies and even public facilities employ microgrid technology, to assure a steady power supply that will keep sensitive equipment running, even during macrogrid blackouts, saving millions of dollars in repairs (PNNL, 2016; Ton and Smith, 2012; Lasseter, 2004).
- Another fact that favors these systems is the **high-quality power** they may generate, which does not suffer from frequency and voltage drops, a phenomenon that occurs often in large scale energy networks and may damage sensitive electronics (Ton and Smith, 2012; PNNL, 2016).
- Microgrids can be built **resilient**, able to withstand extreme weather conditions that result in prolonged power outages, due to damages in transmission and distribution lines and substations, which may take many days to repair (Ton and Smith, 2012).
- They generally have **high energy efficiencies**, since they can take advantage of both heat and power generation, due to their close proximity to the end-users. Centralized power plants deal with great amounts of energy, but are only capable of utilizing an average range of 33 to 45 percent of it, while the rest of it is being dumped to the environment. Also, a significant average of 8 percent of the globally generated power is being lost during transmission and distribution, while almost 60 percent of the remaining power is used for space and water heating. Microgrids can reach an efficiency of up to 80 percent, by recovering the thermal energy that is generated by distributed resources, to meet heating demands located on site. Figure 2.45 illustrates a rough estimation of the losses per 100 units of energy, both for centralized power generation and for the distributed generation of heat and power (Ton and Smith, 2012; Lasseter, 2007; OECD/IEA, 2015).

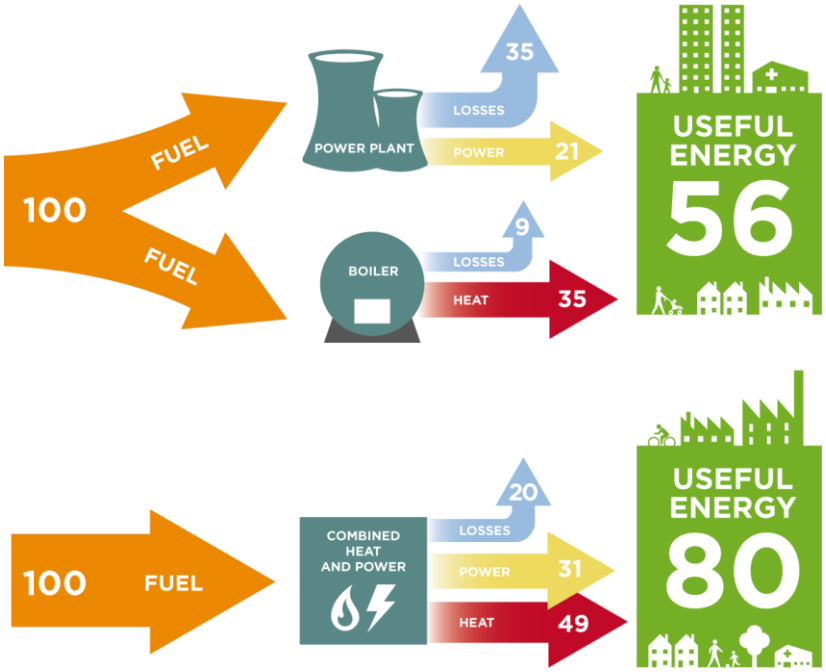

Figure 2.45: Energy losses from centralized power production versus the energy losses by combing heat and power utilization (P3ppartners.com, 2015)

- Microgrids also have many **environmentally friendly prospects**, that arise both from the variety of distributed generation technologies that can be installed and from the high efficiencies they can achieve as CHP systems. If a customer wishes to decrease their environmental footprint, they can choose technologies that can exploit renewable sources or less carbon intensive fossil fuels like natural gas. Furthermore, the efficient utilization of both heat and power leads to an overall minimization of centralized energy generation (Ton and Smith, 2012; Lasseter, 2004).
- There are many **benefits from the small-scale design** of these systems, for both the centralized network and private investors. Microgrids have been recommended as a cost and time efficient upgrade strategy from a traditional electrification network into a modern smart grid, enabling for a smoother transition that should not affect large areas. Their small scale also gives customers the ability to modernize their equipment more frequently and with reduced costs. The small scale also gives the opportunity for private investors to build their energy system in multiple steps, potentially reducing their initial capital investments (Ton and Smith, 2012; PNNL, 2016).

While it may seem that microgrids could be the future of the electrical smart network transition, there are obstacles that this technology needs to overcome, in order to prosper. These difficulties occur due to both legal and technical matters (e.g. costing per energy unit purchased by different distributed generation unit investors, or frequency compatibility with the macrogrid etc.), which need to be resolved. Nevertheless, the integration of this system into the traditional grid is undergoing extensive research, because it may solve many of its fundamental problems. (PNNL, 2016; Abdmouleh et al., 2017).

Due to the versatile nature of the microgrid's distributed resources, the variety of the loads they can meet and the weather uncertainty, the optimal planning of a microgrid for cost elimination is a challenge that has drawn the attention of the scientific community in the recent years. In the next section of this chapter, commonly used optimization techniques for microgrid planning will be analyzed, right after an introduction to the concept of mathematical optimization is performed.

2.5 System Design Optimization

A solid mathematical methodology for finding optimal solutions in many problems has been of great interest for many centuries. There are many practical problems in science, engineering, finance and statistics fields that require the employment of optimization methods, to define the set of actions that need to be taken, in order to achieve the best possible solution (Kookos and Koutinas, 2014; Rao, 2005).

2.5.1 Optimization Basics

Optimization is a mathematical concept that employs common tools used in mathematics, with an ulterior purpose of finding either the minimum or the maximum value of a function, that is usually constrained inside a domain of values, by adjusting all the conditions of the problem (Rao, 2005).

The element of interest is a function that, in mathematical optimization, is called the **objective function**. The objective function is influenced by its variables' values which are usually defined inside a region of feasible values. These can be expressed mathematically by the following statement:

$$\begin{gathered} \min_{x} f(x) \\ subject\ to\ x \in X \end{gathered} \tag{2.1}$$

The objective function f, needs to be minimized with respect to x, whose values are defined inside the **feasible region** X. If $X = \mathbb{R}$, the problem is called **unconstrained**, since the variable *x* can have all real values. On the other hand, if $X = \{x: x^L \leq x \leq x^U\}$, where x^L and x^U are the region's lower and upper bound respectively, the problem is **constrained**, since the variable's values are enclosed inside a region with defined bounds (Kookos and Koutinas, 2014).

Usually, in constrained optimization, the region *X* is described by a set of multiple equations or inequalities and region *X* is often given by the system's feasible solutions. Constraints which are in forms of equations are usually denoted as *h* and inequalities as *g*, so a general constrained minimization problem can be written as:

$$\begin{gathered} \min_{x} f(x) \\ subject\ to \\ h(x) = 0 \\ g(x) \leq 0 \\ x \in X = [x^L, x^U] \end{gathered} \tag{2.2}$$

Generally, one of the most common ways of classifying optimization problems is by the objective function's and its constraints' properties. Taking that into consideration, we call a program linear when all of its components (the objective function and the constraints) are affine. A set of linear equations can have the following form (Kookos and Koutinas, 2014).

$$\begin{bmatrix} a_{11}x_1 + a_{12}x_2 + \cdots + a_{1n}x_n = e_1 \\ a_{21}x_1 + a_{22}x_2 + \cdots + a_{2n}x_n = e_2 \\ \vdots \\ a_{m1}x_1 + a_{m2}x_2 + \cdots + a_{mn}x_n = e_m \end{bmatrix}$$

Its simple form can be written as: $A \cdot x = e$ where A is the matrix of constant coefficients a_{ij}, while x is the vector of variables and e is a vector of constant values e_i. Likewise, inequality constraints can be written as $B \cdot x \leq d$. Hence, in general, a **linear program (LP)** has the following form (Kookos and Koutinas, 2014).

$$\begin{gathered} \min_x c^T \cdot x \\ subject\ to \\ A \cdot x = e \\ B \cdot x \leq d \\ x \in X = [x^L, x^U] \end{gathered} \tag{2.3}$$

Note that the objective function is also linear, since c is again, a horizontal constant vector. If the objective function or at least one of these equations and inequalities was not linear, then the problem would be called a **non-linear program (NLP)** and should be described by the more general form of 2.2 (Kookos and Koutinas, 2014).

Optimization problems aim at the determination of either the minimum or the maximum value of a function that is defined within a feasible region. That said, the point x^* is called the **global minimum** of the optimization problem, if the following expression is true (Kookos and Koutinas, 2014; Rao, 2005).

$$f(x^*) \leq f(x), \forall\, x \in X \tag{2.4}$$

The expression in 2.4 is true for problems that consist of continuous variables and differentiable functions. The points x^* that return a zero gradient in the objective function may be **local minima** or **maxima** which are called **stationary points**. For example, the local minima or maxima of an unconstrained objective function can be calculated by setting to zero its derivatives, with respect to all of its variables (Kookos and Koutinas, 2014).

$$\begin{bmatrix} \frac{\partial f(x_1^*)}{\partial x_1} \\ \frac{\partial f(x_2^*)}{\partial x_2} \\ \vdots \\ \frac{\partial f(x_n^*)}{\partial x_n} \end{bmatrix} = 0 \Leftrightarrow \nabla f(x^*) = 0 \tag{2.5}$$

The expression in 2.5 is also called the optimization's **first-order necessary condition**. An objective function may have multiple stationary points. In order to evaluate whether the stagnant point that was obtained is a local minimum or maximum, we need to know whether the function we are dealing with is **convex** or **concave** (Kookos and Koutinas, 2014).

In a convex function, the stationary point will also be its local minimum, whereas, if the function is concave at the stationary point, it will be a local maximum. To evaluate the convexity of a function, we must first build its Hessian matrix. A **Hessian matrix** returns the second-order derivatives of a function, with respect to all of its variables (Kookos and Koutinas, 2014).

$$H = \begin{bmatrix} \frac{\partial^2 f(x)}{\partial x_1^2} & \frac{\partial^2 f(x)}{\partial x_1 \partial x_2} & \cdots & \frac{\partial^2 f(x)}{\partial x_1 \partial x_n} \\ \frac{\partial^2 f(x)}{\partial x_2 \partial x_1} & \frac{\partial^2 f(x)}{\partial x_2^2} & \cdots & \frac{\partial^2 f(x)}{\partial x_2 \partial x_n} \\ \vdots & \vdots & \ddots & \vdots \\ \frac{\partial^2 f(x)}{\partial x_n \partial x_1} & \frac{\partial^2 f(x)}{\partial x_n \partial x_2} & \cdots & \frac{\partial^2 f(x)}{\partial x_n^2} \end{bmatrix} \quad (2.6)$$

For x^* to be a local minimum, the following expression must be true.

$$d^T \cdot H(x^*) \cdot d \geq 0 \quad (2.7)$$

Where, $d = -\nabla f(x^*)$. The expression 2.7 suggests that the Hessian matrix ought to be **positive semi-definite**, for x^* to be a local minimum. The previous expression is called the **second-order necessary condition** of the optimization. The previous solution process is also known as convex optimization and is the basis for many optimization techniques (Kookos and Koutinas, 2014).

Mixed integer linear programs pertain to linear programs, with the sole difference that they contain at least one integer variable. These variables can either be the number of discrete, undividable objects, or decision-related binary variables as shown below (Kookos and Koutinas, 2014; Rao, 2005).

Integer variable $x \in \{-m, \cdots, -1, 0, +1, \cdots, n\} \; where \; n, m \in \mathbb{Z}$

Binary (decision) variable $x = \begin{cases} 1 & if \; true \\ 0 & if \; false \end{cases}$

In general, an integer program is called an all-integer, when all of its variables are integer. Likewise, when some of its variables are also continuous, it is called a mixed-integer program. If all the program's variables are binary, only able to obtain values of either one or zero, it is called a zero-one program. The same categorization is true for non-linear integer programs. An overview of the integer optimization program categorization, is presented in figure 2.46 (Rao, 2005).

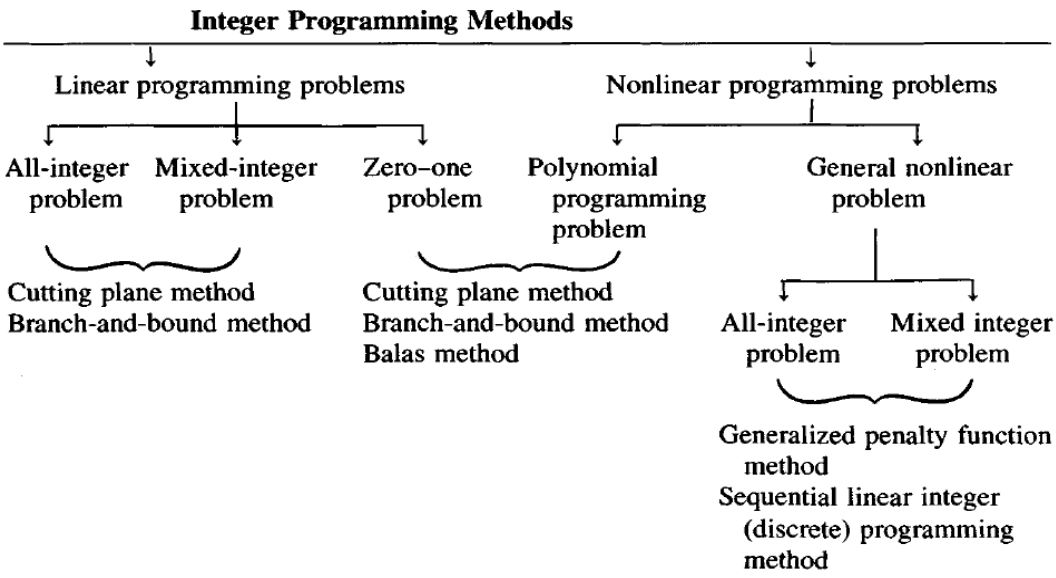

Figure 2.46: Overview of the categorization of the integer programming methods (Rao, 2005)

Many engineering optimization problems, require the employment of integer variables, instead of continuous.

2.5.2 The SIMPLEX Method

The SIMPLEX method was first introduced by G. B. Danzig in 1947 and is currently used to solve linear programs of varying difficulty and sizes. It is a recursive method, based on the sequential and systematical approach of a linear program's optimal solution (Kookos and Koutinas, 2014).

Although this method is used for complex problems, a simplified example can prove trivial for its understanding. Hence, we may consider the following linear optimization program which can be visually represented in figure 2.47.

$$\min_{x1,x2} -x_1 - x_2$$

$$subject\ to$$

$$x_1 + 3x_2 \leq 10$$
$$2x_1 + x_2 \leq 8$$
$$x_1, x_2 \in \mathbb{R}^+$$

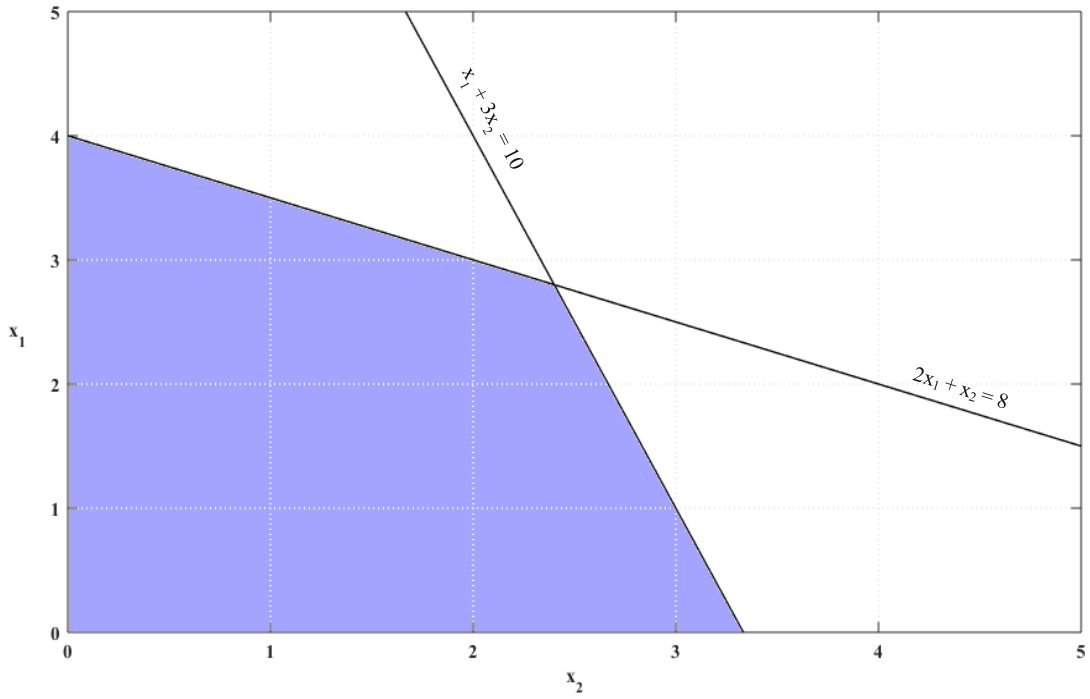

Figure 2.47: Visual representation of a linear program (Author, 2018)

According to a fundamental theorem of linear programming, the optimal solution of such a program, is always an extreme point. What is more, the number of the extreme points will always be finite, whether the feasible region of a solution is either bounded or not (Kookos and Koutinas, 2014).

Taking that into consideration, it could be possible to define all the extreme points of a problem and check whether they satisfy all the constraints of the problem and the objective function's value at each point. While this is possible for a small program, such as the above-mentioned, the computational power a program of multiple variables would need, would produce more problems than it could solve (Kookos and Koutinas, 2014; Rao, 2005).

As mentioned previously, the SIMPLEX method is a recursive process that does not require the location of all the extreme values of a program. The basic process considers an initial extreme point inside the feasible region and a repetitive allocation to a neighboring extreme point only if it reduces the value of the objective function. The iteration of this process will eventually result in the location of the extreme point which will correspond to the minimum value for the objective function. The method may be terminated if the obtained extreme point returns a smaller objective function value than its neighboring extremes (Kookos and Koutinas, 2014; Rao, 2005).

2.5.3 The Branch and Bound Method

While mixed integer linear programs (MILP) have many similarities to linear programs, they actually are problems of different nature, and require different techniques and methods to solve. Figure 2.48 illustrates a comparison between the solutions of the simple linear program of the previous subsection, and its integer counterpart. It is obvious that the solutions of the integer linear program (marked with dots) are much fewer than the number of feasible solutions of the linear program, but pertain to different optimization techniques (Kookos and Koutinas, 2014).

$$\min_{x1,x2} -x_1 - x_2$$

$$subject\ to$$

$$x_1 + 3x_2 \leq 10$$
$$2x_1 + x_2 \leq 8$$
$$x_1, x_2 \in \mathbb{Z}^+$$

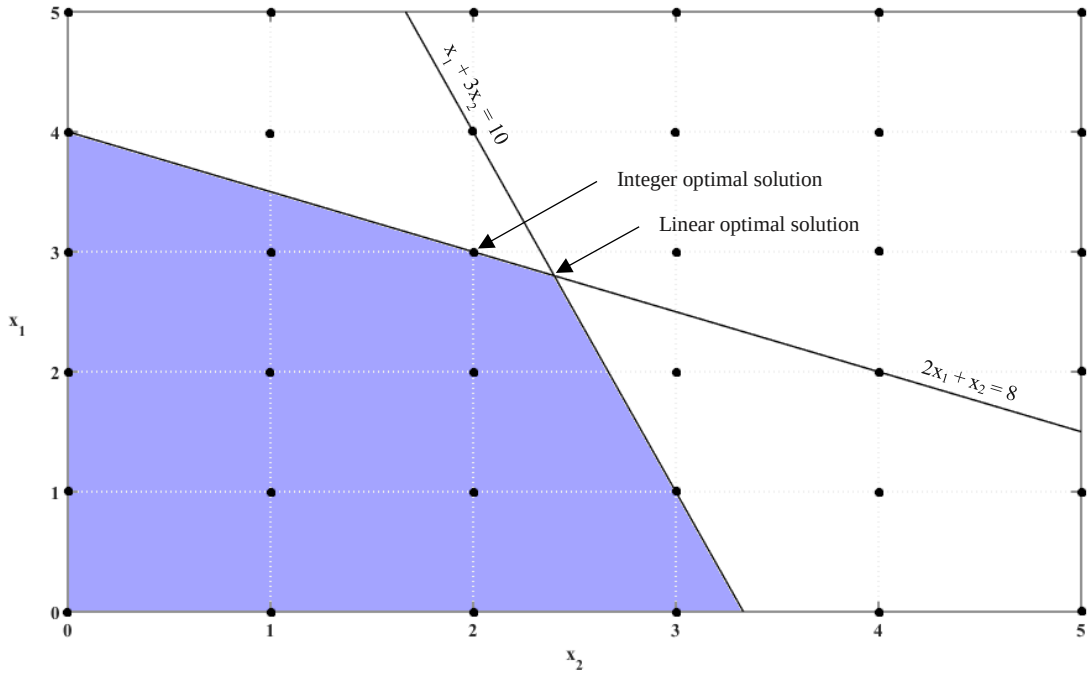

Figure 2.48: Comparison between the solution of a linear program and its integer linear counterpart (Author, 2018)

Although it is possible to calculate an integer solution of a MILP by employing linear programming techniques and rounding the obtained variable values to the nearest integer value (e.g. 1.6 boilers ≈ 2 boilers), it is not always guaranteed that this will not result in the violation of the other constraints of the program. What is more, the rounding may result in a solution which is far from the optimal (Rao, 2005).

The fundamental idea behind the branch and bound method, is the systematical and repetitive reduction of the program's upper bounds and the increase of its lower bounds, until the optimal linear solution occurs which at the same time satisfies the integer restrictions (Kookos and Koutinas, 2014).

Supposing that we have managed to construct a recursive function which enables for a series of upper bound (U) reduction and a lower bound (L) increase, so as:

$$U^0 \geq U^1 \geq \cdots \geq U^k$$

$$L^0 \leq L^1 \leq \cdots \leq L^k$$

Let's also suppose that at the step k, the following statement is true:

$$0 \leq U^k - L^k \leq \varepsilon$$

Where ε, is a small positive number. For the objective function (f^*) the following statement is true by definition:

$$L^k \leq f^* \leq U^k$$

Taking that into consideration, it can be assumed that the optimal solution of the objective function can be evaluated, for a relative error of ε. This implies that in the branch and bound method, the integer program is not directly solved (Rao, 2005).

The reduction of the upper bound is based on the fact that any feasible solution is an upper bound for the optimal solution. This is due to the fact that the value of the objective function calculated at the optimal solution without the integer restriction, is always smaller than any other feasible integer solution (Kookos and Koutinas, 2014).

The lower bound increase is based on the root relaxation of the program's integer restrictions and solving it as a continuous problem. Hence, a relaxed problem is an integer program whose integer restrictions have been temporarily, either partly or wholly, lifted. For example, we can substitute the integer restriction of $x_i \in \{1,2,3,4\}$ with its relaxed counterpart $x_i \in [1,4]$, where $\{1,2,3,4\} \subseteq [1,4]$. This means that the relaxed program is a superset of its integer equivalent, while its optimal solution can be considered as a lower bound, since it will always be optimal (Kookos and Koutinas, 2014; Rao, 2005).

We may consider the following integer problem which can also be illustrated in figure 2.49.

$$\max_{x_1,x_2} 5x_1 + 8x_2$$

$$subject\ to$$

$$x_1 + x_2 \leq 6$$
$$5x_1 + 9x_2 \leq 45$$
$$x_1, x_2 \in \mathbb{Z}^+$$

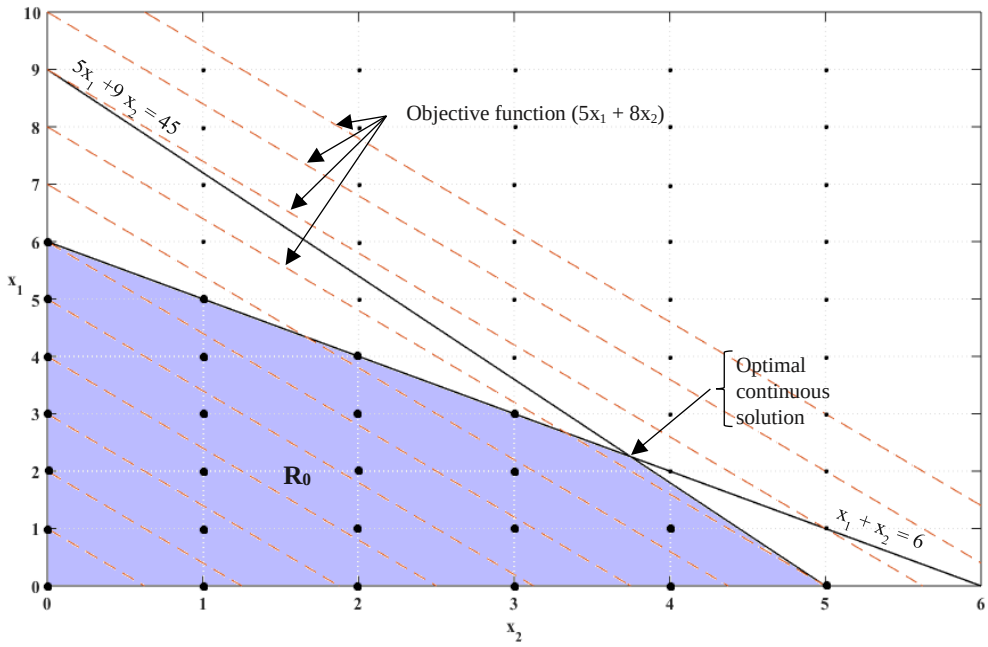

Figure 2.49: Branch and bound method – integer program optimization visual representation part 1 (Author, 2018)

As presented in figure 2.49, the initial problem is secluded inside the feasible region R_0, bounded by its two initial constraints. The integer solutions of the problem are represented by the highlighted dots. The relaxation of the problem would result in a linear program which can be solved by the SIMPLEX method, resulting in a real optimal solution for the objective function (*f*) of 41.25, which is also noted on the figure (Kookos and Koutinas, 2014).

At this moment, it is possible to readjust the lower bound of the problem into $L^1 = 41.25$, but it is not yet possible to decrease the upper bound, since an integer solution has not been found yet. The main problem is now separated into two smaller continuous subproblems, called **nodes**, by rounding the continuous variable which is closer to its integer value, as shown in figure 2.50. If the all the variables of the problem have the same distance from their integer values, then the selection of the integer that is to be rounded occurs randomly (Kookos and Koutinas, 2014; Rao, 2005).

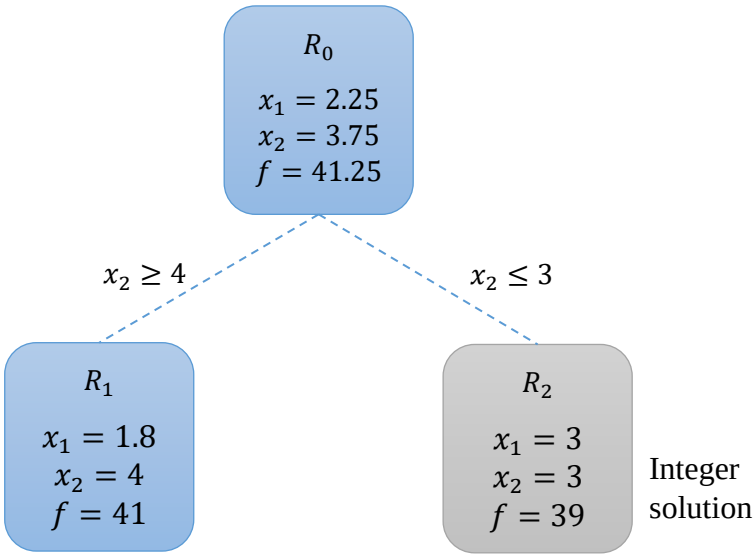

Figure 2.50: Branch and bound method – first split of the main problem into two subproblems (Author, 2018)

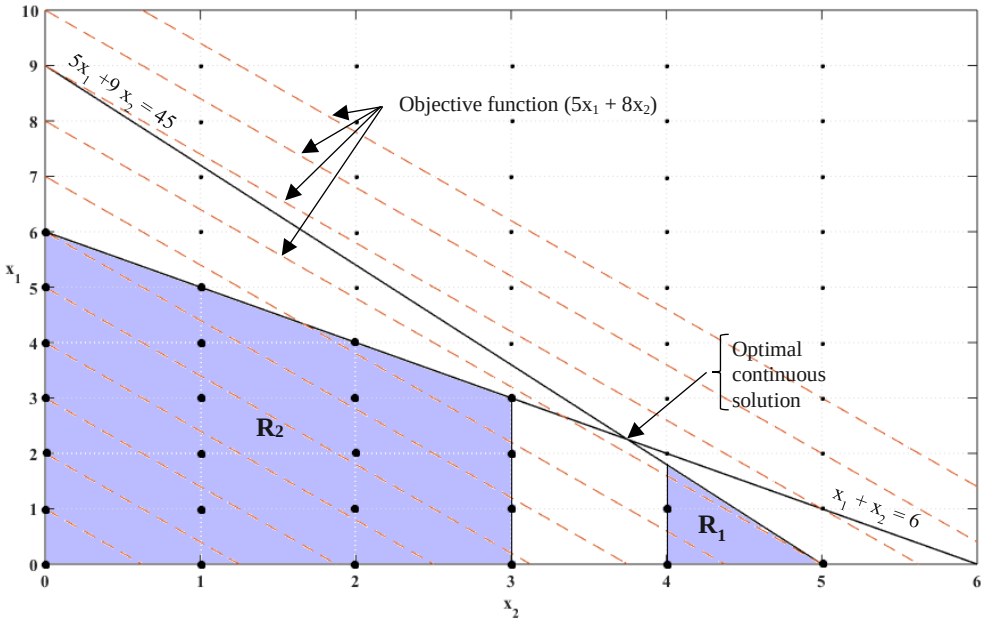

Figure 2.51: Branch and bound method – integer program optimization visual representation part 2 (Author, 2018)

Note that although an integer solution was obtained at region R_2, it may not be the optimal solution and the method cannot be yet terminated. The branching and the adjustment of the bounds should be continued for each region until one of the following conditions is true for each region (Kookos and Koutinas, 2014; Rao, 2005):

1. The relaxed problem reaches an **infeasibility point** (e.g. when a solution that satisfies the initial constraints does not exist)
2. The solution of the relaxed problem is an **integer solution**
3. The continuous solution of the relaxed problem is **inadequate** compared to an integer solution that has already been obtained (to this point of the optimization).

The discontinuation of the subdivision of the nodes (**fathomed nodes**) marks the termination of the branch and bound method process. According to these conditions the final form of the example will be as follows (Kookos and Koutinas, 2014).

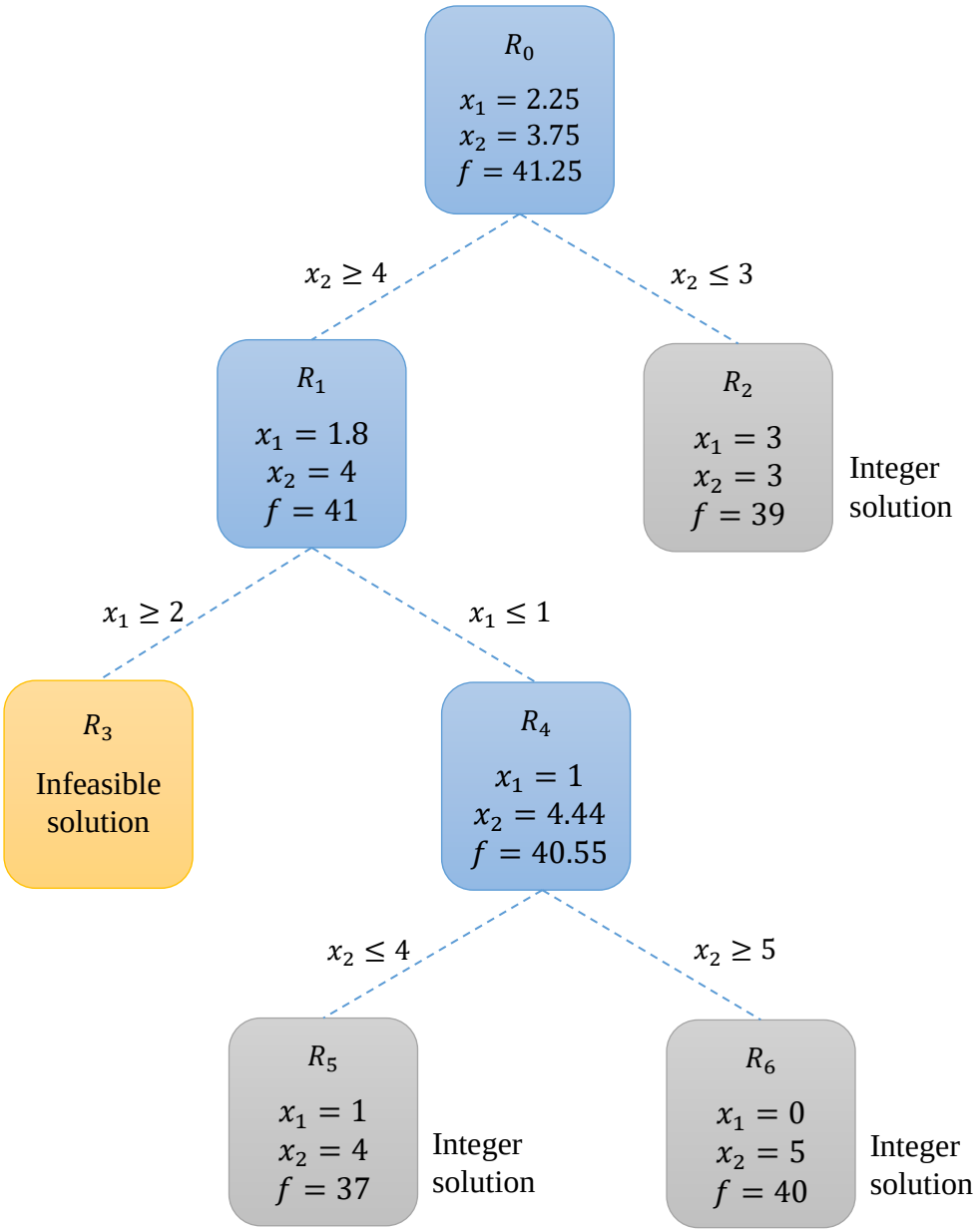

Figure 2.52: Branch and bound method – final form of the program's branches (Author, 2018)

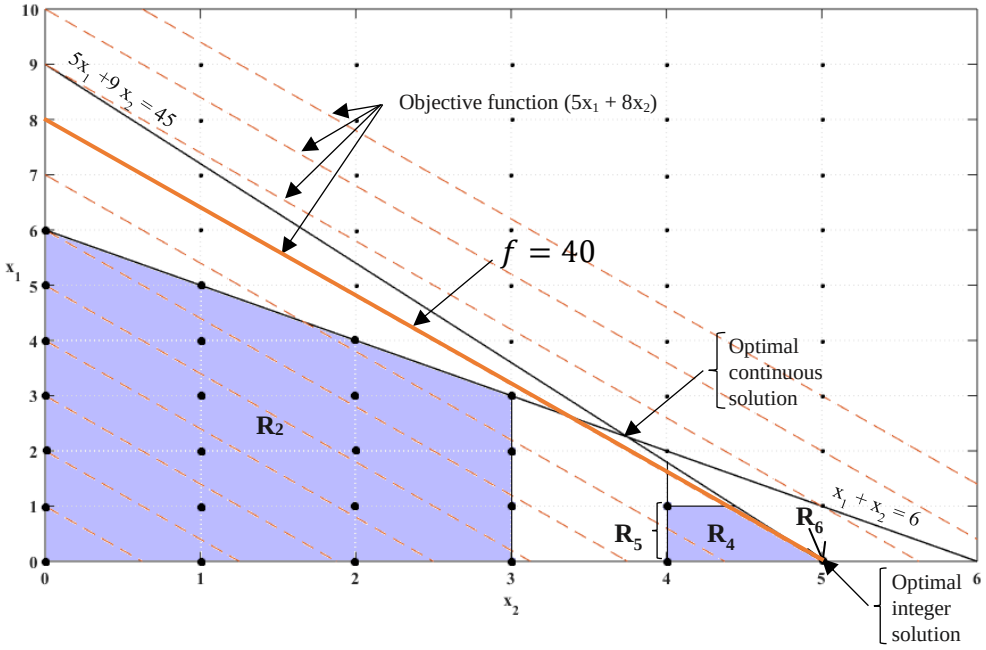

Figure 2.53: Branch and bound method – integer program optimization visual representation part 3 (Author, 2018)

Chapter 3

Mathematical Model Formulation

The scope of this study is to assess the economic viability and the potential environmental benefits from the utilization of distributed resources in a microgrid, designed to meet power and heating demands of a specified load. This chapter focuses on the detailed construction of the optimization program, after a brief explanation of the problem is being made.

Several case studies will be conducted, each having a different additional linear constraint, to observe the variations in technology selection. The mixed integer linear program (MILP) that results, will be solved with the CPLEX solver which is available in GAMS. A nomenclature of all the symbols used in the program is presented in table 3.1.

Table 3.1: Nomenclature of the symbols that will be used for the formulation of the optimization program

Continuous Variables	
Capex	Capital expenditures (NPV of capital costs)
E	CO_2 emissions
G	Natural gas consumption
L	Energy storage level
NPC	Net present value of costs
Opex	Operational expenditures (NPV of annual costs)
P	Power output
Q	Heat output
Binary Variables	
x	is on
y	is installed
z	is started up
Subscripts	
b	Battery bank
dump	Dump load
grid	Macrogrid
j	Electric boiler
l	Load demand
m	Microturbines
n	Gas-fired boiler
NG	Natural gas
s	PV array
w	Wind turbines
ref	Reference
U	Upper bound
L	Lower bound
p	Purchase
e	Electricity
h	Heat
Superscripts	
+	Discharging
–	Charging
l	Linear
Parameters	

α	Scaling coefficient
η	Energy conversion efficiency
γ	Heat-to-power ratio
χ	Sizing variable
d	Discount rate
i	Inflation rate
φ	Present value interest factor for annuity
θ	Present value interest factor
A	Commodity cost
C	Capital cost coefficient
f	Fractional availability
h	Altitude
H	Insolation
k	Proportionality constant
O	Maintenance cost coefficient
t	Hour of the year
F	Carbon emissions coefficient
T	Temperature
v	Wind speed

3.1 Problem Description

As explained in chapter 2 in detail, microgrids are energy systems that contain both distributed generation and storage units, as well as the load at the same location. In order to quantify and evaluate the economics of a microgrid, a case study needs to be conducted with real weather, power and heat consumption data from a specified load location.

The load of interest is set to be Sarnia, Ontario, a city with an annual demand of about 3.65 GWh in power and 3.45 GWh in heat. The microgrid must be designed to fully meet the demand in thermal energy, while electricity may either be generated from the microgrid's distributed resources or be directly purchased from the macrogrid.

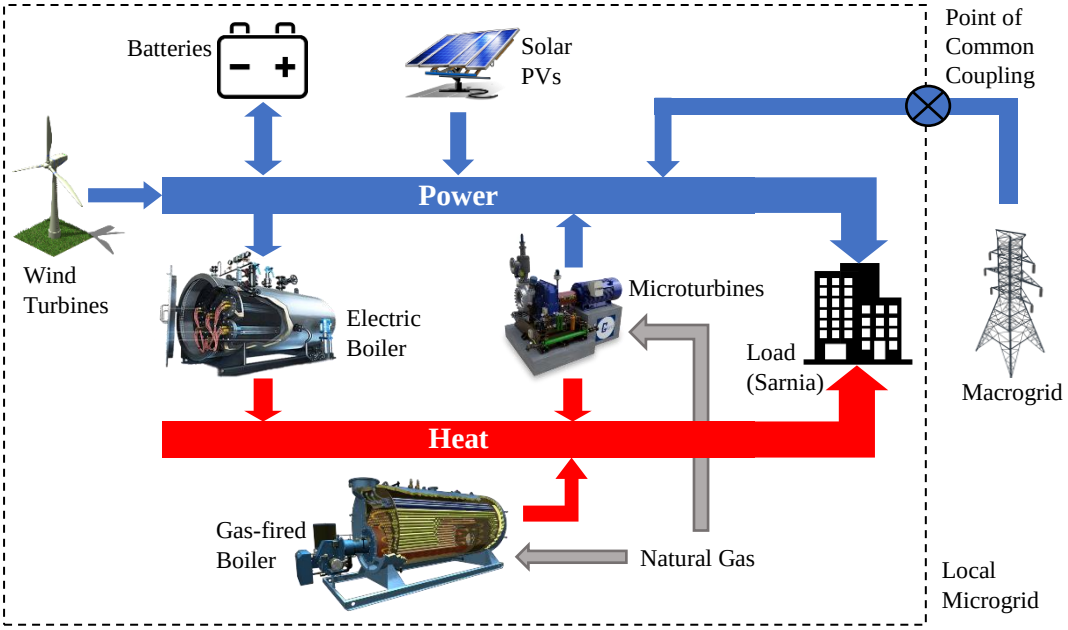

Figure 3.1: Simplified schematic of the microgrid's components and their contribution to the system (Author, 2017)

As illustrated in figure 3.1, the components that constitute the microgrid are distributed generation and storage units, as well as the load. The distributed energy resources that are considered in the system consist of wind turbines, solar photovoltaics, gas microturbines, a battery bank, electric and natural gas boilers. The microgrid is connected to the macrogrid via the point of common coupling, enabling the purchase of utility power to meet load demands.

The total lifetime of the system is set to reach 20 years of daily operation. Weather and load data is being collected in hourly intervals for one year. To simplify the model, it is assumed that the same weather and power consumption profile is being annually repeated throughout the 20 years of the system's operation.

In the mathematical program, the obtained data will be considered as hourly set points, during the optimization. That is, for every hour of the year, the program will create corresponding single equations and variables, using the obtained data of each time interval as constant values. Hence, it is of great importance that all the constraints of the program have a linear form, since a non-linear integer program of the same size may be very hard to solve.

This chapter is focused on the construction of the mathematical model of the microgrid, which considers all design parameters and aspects of the components of interest. The microgrid's design variables result from its distributed technologies' rated outputs and capacities, the number of microturbines to be installed and the hourly outputs. The aim of the model's optimization is to evaluate the least-cost scenario option, by finding the optimal combination, sizes and operation of the available equipment.

Since the sizing variables used to calculate the costs are the rated power outputs, the equipment design equations will be simplified linear relations that only take power and heat outputs into account. While these relations may provide a good approximation to each equipment's real behavior, they do not consider specific technical properties, such as the total number of solar PV modules that need to be installed, voltage adjustments, wind turbine blade sizes, etc. What is more, this generic microgrid model focuses on distributed resource technology selection and does not consider optimal distribution routes and network design.

3.2 Linearization of Capital Costs

There is a significant variation in the costs of the energy production units, mainly because of the high quantity of the available data and the rapid technological advancement. In general, a unit's capital cost of purchase is proportional to a characteristic sizing variable, though this relationship may not always be linear (Kookos, 2009).

A non-linear relationship which can accurately describe the capital cost of many industrial units, has been recommended by M. Guthrie (Kookos, 2009):

$$C_p = \left(\frac{\chi}{\chi_{ref}}\right)^a \cdot C_{p,ref} \tag{3.1}$$

Where, χ is the equipment's sizing variable, C_p is the corresponding cost of purchase, while the subscript "ref" denotes the values obtained by a reference source. The exponent a is scaling coefficient, which usually receives values ranging from 0.3 to 0.9, depending on the equipment type (Kookos, 2009).

A linearization of costs needs to be performed in order to simplify the final model, since the computation of a non-linear version of the program may prove trivial.

The linear approximation aims at the extraction of a new linear relationship that adequately describes the equipment's cost of purchase, with respect to its sizing variable. To maintain the simplicity of the model, the new affine function must have the form of $C_p^l = C \cdot \chi$, where C_p^l is the linear cost of purchase and C is the linear cost coefficient.

In order to calculate C, the square error between the non-linear and linear cost of purchase, has to be minimized, as shown in figure 3.2. The minimization of the square error takes place between a range of interest for the sizing variables: $\chi \in [\chi_L, \chi_U]$.

$$\min_C \int_{\chi_L}^{\chi_U} \left(C_p - C_p^l\right)^2 d\chi \tag{3.2}$$

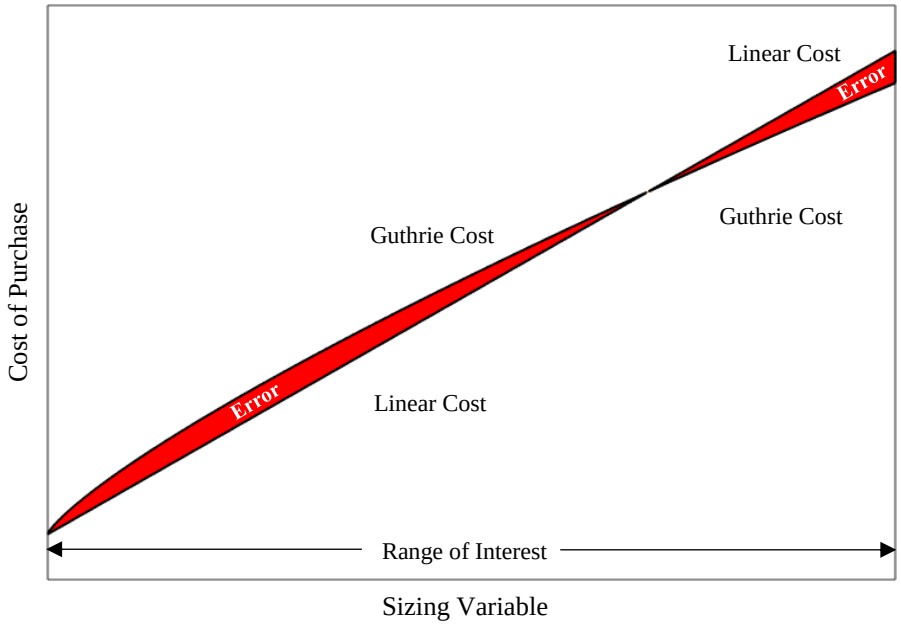

Figure 3.2: Visual representation of the linearization performed at the Guthrie cost equation (Author, 2017)

A substitution of the two costs results in the following expression:

$$\min_C \int_{\chi_L}^{\chi_U} \left[\left(\frac{\chi}{\chi_{ref}} \right)^a \cdot C_{p,ref} - C \cdot \chi \right]^2 d\chi \tag{3.2.a}$$

The minimization of equation (3.2) is done by setting its derivative over C, equal to zero and solving it with respect to the cost coefficient.

$$\frac{d}{dC} \left\{ \int_{\chi_L}^{\chi_U} \left[\left(\frac{\chi}{\chi_{ref}} \right)^a \cdot C_{p,ref} - C \cdot \chi \right]^2 d\chi \right\} = 0 \tag{3.2.b}$$

The result is a relationship that is used to calculate values of C for each equipment.

$$C = \frac{3C_{p,ref}}{\chi_{ref}^a \, (2+a)} \frac{\chi_U^{2+a} - \chi_L^{2+a}}{\chi_U^3 - \chi_L^3} \tag{3.2.a}$$

The linear capital cost coefficient is calculated for all the equipment, except for microturbines, since they are installed as individual units with a predetermined capacity and cost. The values of the calculated costs, along with the values of the parameters used, are presented in table 3.2.

Table 3.2: Parameters used for the calculation of linear costs and the solution of each equipment

Unit class	Capital cost coef. (C)	Reference size (χ_{ref})	Reference cost ($C_{p,ref}$)	Scaling coef. (α)	Size range ($\chi_L - \chi_U$)
Solar PVs	5.0 k$/rated kW_e	300 kW_e	1.62 M$	0.94	0 – 2000 kW_e
Wind turbine	3.4 k$/rated kW_e	300 kW_e	1.38 M$	0.80	0 – 2000 kW_e
Electric boiler	60 $/rated kW_h	180 kW_h	21.6 k$	0.60	0 – 1500 kW_h
Gas-fired boiler	60 $/rated kW_h	180 kW_h	21.6 k$	0.60	0 – 1500 kW_h
Battery bank	132 $/rated kWh_e	150 kWh_e	45.0 k$	0.95	0 – 5000 kW_e

The capital cost of purchase for every installed microturbine is calculated to be 594 k$ per turbine, each with a rated power output of 165 kW_e. The capital cost of purchase for the other units is estimated after the completion of the optimization. This is possible by multiplying the capital cost coefficient by their sizing variable, which is the rated output, or the rated capacity in the case of the battery bank.

3.3 NPV Factors Calculation

The **NPV factor of capital expenditures** is used in equipment purchase costs. It occurs due to the fact that some units will need to be repurchased at some point in the future, since they have lower lifespan compared to the lifetime of the whole system, which is 20 years (Kookos, 2009).

Since the currency changes at the rate of inflation, the future value of purchase will not be the same. Hence, the future value needs to be converted into a present value.

In general, the future value FV, of a certain initial capital value PV, which has been invested with an annual interest ε, depends on the compound interest relationship (Kookos, 2009):

$$FV = PV \cdot (1 + \varepsilon)^n \tag{3.3.a}$$

Where, n is the time period of the investment (years). The coefficient $(1 + \varepsilon)^n$ is called compound value interest factor (CVIF). To calculate the present value, equation 3.40.a simply needs to be solved with respect to PV (Kookos, 2009).

$$PV = FV \cdot (1 + \varepsilon)^{-n} \tag{3.3.b}$$

In that case, the parameter ε is called discount rate (d), instead of annual interest, while the coefficient $(1 + \varepsilon)^{-n}$ is called present value interest factor (PVIF) and is the inverse value of CVIF (Kookos, 2009).

The PVIF (θ) of each equipment can be computed by the relationship above, by adding them for each year of purchase, considering a discount rate of 8.3 percent. A table which sums up all equipment lifespan is presented below to aid in calculations.

Table 3.3: A summary of each equipment's lifetime used in the calculations of the NPV factor of capital expenditures

	MT	WT	SPV	GB	EB	BB	System
Lifetime (years)	20	20	20	16	16	5	20

$$\theta_b = (1+0.083)^0 + (1+0.083)^{-5} + (1+0.083)^{-10} + (1+0.083)^{-15} = 2.4241$$

$$\theta_n = \theta_j = (1+0.083)^0 + (1+0.083)^{-16} = 1.2792$$

$$\theta_m = \theta_w = \theta_s = (1+0.083)^0 = 1$$

The **NPV factor of operational expenditures** also takes into account the inflation which occurs in an annual rate. Annuity is a series of evenly distributed payments, which take place annually. The present value (PV) of an annuity (A), can be calculated by summing equation 3.40.b for each year (Kookos, 2009).

$$PV = A \cdot (1+\varepsilon)^{-1} + A \cdot (1+\varepsilon)^{-2} + \cdots + A \cdot (1+\varepsilon)^{-n} \quad (3.4.a)$$

Which is equivalent to:

$$PV = A \cdot \frac{(1+\varepsilon)^n - 1}{\varepsilon \cdot (1+\varepsilon)^n} \quad (3.4.b)$$

The parameter that multiplies the annuity is the present value interest factor for an annuity (PVIFA), in which n denotes the future periods of an annuity, whose payment occurs after the end of the first period, and ε is the interest rate (Kookos, 2009).

In this case, the interest rate should be described by the Fischer equation, which calculates the real interest rate under inflation (i) (Kookos, 2009). Inflation is assumed to be constant and equal to 2.3 percent.

$$\varepsilon = \frac{1+d}{1+i} - 1 \quad (3.5.a)$$

The previous equation can also be written as:

$$\varepsilon = \frac{d-i}{1+i} \quad (3.5.b)$$

The PVIFA (φ) is common for all equipment maintenance costs as well as for utility purchase prices. It is possible to be calculated since it is assumed that data regarding weather and load demand will be the same over the next 20 years (Kookos, 2009).

$$\varphi = \frac{(1+0.0566)^{20} - 1}{0.0566 \cdot (1+0.0566)^{20}} = 11.7948$$

Table 3.4: Summary of the calculated NPV factors

NPV factor	θ_b	θ_n	θ_j	θ_m	θ_w	θ_s	φ
Value	2.4241	1.2792	1.2792	1.0000	1.0000	1.0000	11.7948

3.4 Equipment Description and Design

The units that have been preselected to compose the microgrid, are commonly used among similar establishes, making the designed microgrid generic. Furthermore, these distributed energy generation units have the potential to decrease the carbon intensity of the produced electricity, and make the microgrid eco-friendly.

However, not all units may be selected, due to their high costs of purchase, which makes them non-competitive comparing to the inexpensive, yet carbon-intensive power purchased by the macrogrid. The equations for the capital and operational expenditures for each unit are extensively analyzed in the later subsections. The following table sums up the parameters needed for the calculation of the capital and operational costs for each unit.

Table 3.5: Summary of the capital and maintenance cost coefficients used to calculate the system's NPV of costs

Unit type	Capital cost coefficient	Maintenance cost coefficient	Lifespan
Microturbines	594 k$/turbine (3.6 k$/rated kW_e)	0.02 $/$kWh_e$ + 10 $/startup	20 years
Solar PV	5 k$/rated kW_e	52 $/rated kW_e	20 years
Wind turbine	3.4 k$/rated kW_e	0.008 $/$kWh_e$	20 years
Electric boiler	60 $/rated kW_h	0.0075 $/$kWh_h$	16 years
Gas-fired boiler	60 $/rated kW_h	0.0075 $/$kWh_h$	16 years
Battery bank	132 $/$kW_{e,capacity}$	0.00143 $/$kWh_e$	5 years

In general, the equipment capital costs (Capex) are calculated by multiplying the capital cost coefficient of each equipment, with its corresponding sizing variable and the NPV factor of capital expenditures, which was calculated in the previous section.

The operational costs (Opex) comprise of the maintenance costs of the equipment and the purchase costs of natural gas and power from the grid. In general, the maintenance cost of each equipment is calculated by multiplying their coefficient with the sum of the annual output that they have contributed to the system, with the exception of the solar array whose maintenance cost is directly proportional to its rated power output.

Much like Capex, operational expenses for 20 years are also calculated in advance, since the assumption of weather and consumption profile repetition has been made. Hence, all of the maintenance costs, as well as the costs of utility purchase, are multiplied by the NPV factor of operational expenses.

3.4.1 Microturbines

Distributed power applications, such as microgrids, often favor the power production units that make use of natural gas, mainly due to potentially low carbon emissions combined with relatively high efficiencies.

Microturbines are small aeroderivative gas generators that maintain a simple mechanical profile, using only a few moving parts which reduces their maintenance costs. What is more, they create the opportunity to utilize the thermal energy they produce, to meet heat demands, which can raise the fuel efficiency by more than 80 percent. Their rated power output may range from 50 kW to 500kW of electricity.

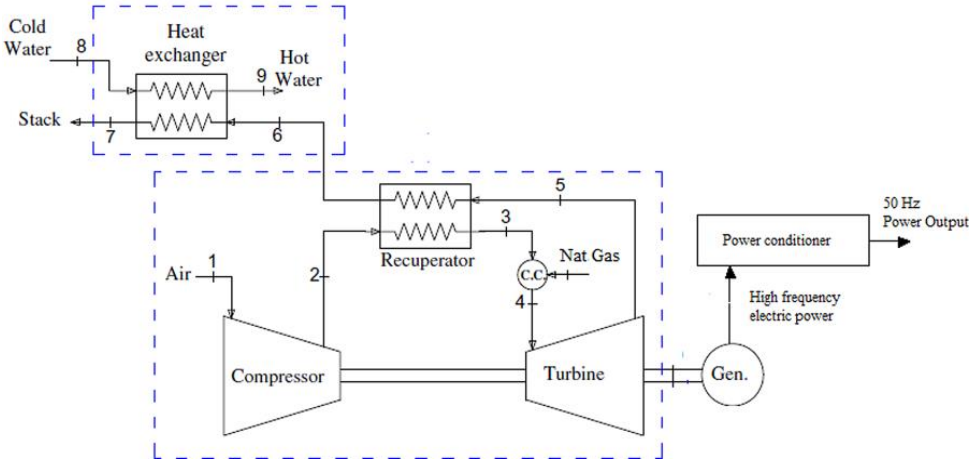

Figure 3.3: Process diagram of a microturbine which combines heat and power generation (Sanaye and Ardali, 2009, edited)

In this case study each microturbine has a fixed rated power output of 165 kW_e and capital cost of $594,000 per turbine installed. Therefore, the total capital expenditures of the installed microturbines are:

$$Capex_m = \sum_m y(m)\, C_m\, \theta_m \tag{3.6}$$

Where, θ_m is the NPV factor for the capital cost of the microturbines and $y(m)$ is a binary variable which is equal to 1 if the microturbine "m" is installed and 0 if it is not installed, disabling the corresponding equation.

The operational expenditures that are considered include the maintenance costs, the cost per startup and the cost of the purchased natural gas which is used as a fuel. All the costs are multiplied by the NPV factor for annual costs φ, which takes into account the inflation rate of every parameter, as well as the discount rate of the future monetary value.

$$Opex_m = \sum_t \left[\sum_m \left(\left(P_m(m,t) \cdot O_m + z(m,t) \cdot O_{startup} \right) \cdot \varphi_m + G_m(m,t) \cdot A_{NG} \cdot \varphi_{NG} \right) \right] \tag{3.7}$$

Where, $z(m,t)$ is a binary variable which is used to track the startups of each microturbine per hour, since they have additional maintenance costs.

Note that the expenses of maintenance and purchased gas are summed over time, since they are hourly set points. Time is declared as a set of 8760 elements (24 hours multiplied by 365 days), in order to consider all the data that has been collected. On account of that, every variable that is dependent on time is actually a set of variables

Likewise, the number "*m*" of microturbines that are considered in the mathematical model is also a set, and every variable that depends on in is a set of variables of the same size. Hence, the number of the elements of that set must be carefully selected, to minimize the number of variables.

By dividing of the average power demand of 417 kW with the rated power output of a single microturbine of 165 kW, the maximum number of microturbines considered in the model, is calculated to be 3 (~2.5).

While its elements are subjected to time and microturbine sets, Opex is a single variable, due to the summation that takes place on the right side of the equation.

Further constraints need to be selected for the complete modeling of the microturbines. The first constraint pertains to each microturbine's power output, which must not exceed the rated power.

$$P_m(m,t) \leq x(m,t) \cdot P_{m,rated} \tag{3.8.a}$$

At the same time, the microturbine needs to operate above 50% of its maximum capability, due to efficiency drops at low set points.

$$0.5 \cdot x(m,t) \cdot P_{m,rated} \leq P_m(m,t) \tag{3.8.b}$$

The equations above are disabled when the microturbine of interest is off ($x(m,t) = 0$), but when the microturbine is on ($x(m,t) = 1$), the hourly power output ($P_m(m,t)$) is constrained to take values which are lower than the rated power and higher than half of it.

For that range, the electrical efficiency (γ_m) and heat recovery ratio (η_m) are assumed to be constant in order to achieve computational simplicity. With this assumption made, the generated heat that is recoverable as well as the fuel consumption are directly proportional to the power output.

$$Q_m(m,t) = P_m(m,t) \cdot \gamma_m \tag{3.9}$$

$$G_m(m,t) = \frac{P_m(m,t)}{\eta_m} \tag{3.10}$$

Table 3.6 summarizes the values of all technical properties needed for the calculation of the generated heat and consumed gas variables.

Table 3.6: Microturbine design parameters for heat output and gas consumption

Parameter	**Value**
$P_{m,rated}$	165 kW_e
γ_m	1.5 $kW_h \cdot kW_e^{-1}$
η_m	0.27

The number of active microturbines, at any given moment, has to be limited by the number of installed microturbines. This can be described by the following:

$$x_m(m,t) \leq y(m) \tag{3.11}$$

The equation above enables the microturbine "m" to operate, only if it is already installed. When installed, the binary variable $y(m)$, takes the value of 1 and $x_m(m,t)$ is free to take values both of one and zero, since it must be less or equal to one.

Startups result in a maintenance cost increase mainly due to surplus fuel usage and equipment wear that takes place in these events. Hence, a track of the times a microturbine has been started up, after a period of inactivity, needs to be kept.

$$z(m,t) \geq x(m,t) - x(m,t-1) \tag{3.12}$$

When a microturbine operates during a period "t" while it was inactive during the previous period "$t-1$", the right side of the previous equation takes the value of one, also forcing the binary variable $z(m,t)$ to have the same value.

On the other hand, when the microturbine was also working during the previous period, or during time periods of continuous inactivity, the right side of the equation reaches zero. Since

the optimization of the program requires the minimization of total costs and startups add to them due to maintenance, the binary variable which tracks them is pushed to zero.

The same is also true when a microturbine turns off after a period of operation, which makes the right side of the equation above to receive the value of minus one, and the variable $z(m,t)$ to receive the value of zero.

3.4.2 Solar Photovoltaics

Solar PVs play a major role in the renewable energy industry, currently producing the cleanest form of energy achievable, by generating power directly from solar radiation. While expensive, PV installation prices are constantly reducing, mainly due to industrial scale up and technological improvements.

In the model, a single PV array is used to utilize solar radiation, using a solar tracker in order to rotate the solar panels and achieve a maximum efficiency. The power production from the solar PVs is directly proportional to the insolation received.

The rated power is the power output achieved for the rated solar radiation, at 1 kW·m^{-2} and a temperature of 25 °C, though temperature dependence is not taken into account. The equation of the hourly power output is given by the following equation:

$$P_s(t) = P_{s,rated} \cdot \frac{H(t)}{H_{rated}} \tag{3.13}$$

The hourly power output of the PV system comes by a fractional availability of the rated output of the array. The availability is the insolation at a certain time, divided by the rated solar radiation, at which the system returns its maximum output. The hourly insolation profile throughout an annum, is depicted in figure 3.4, which was created in Matlab.

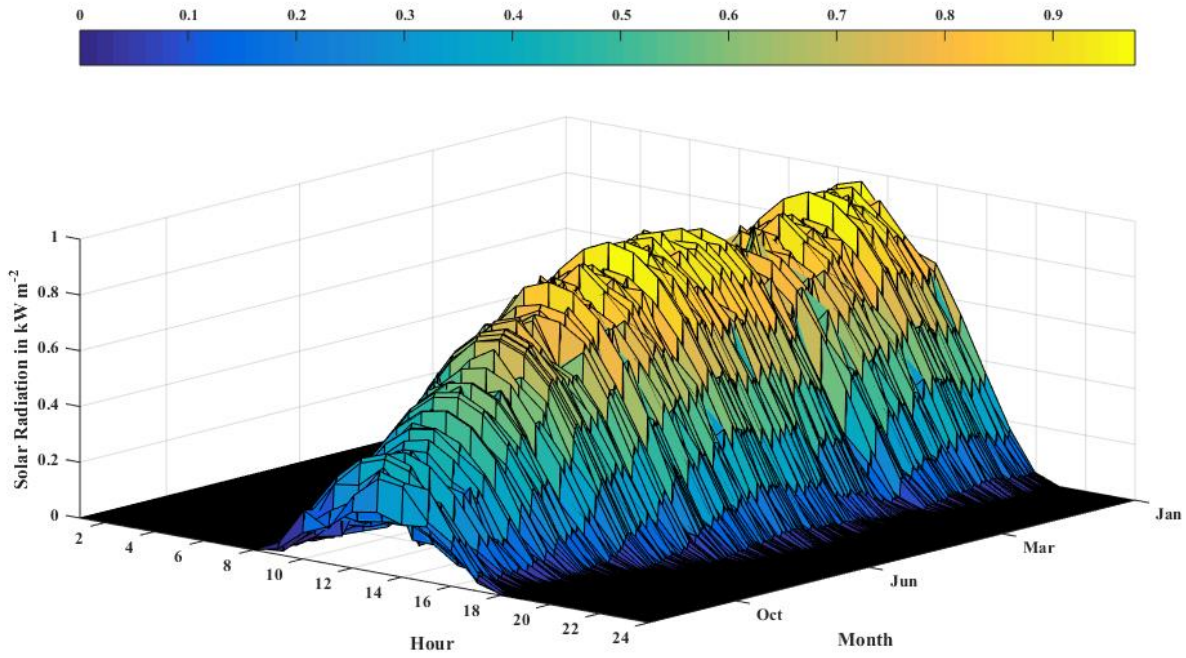

Figure 3.4: Hourly solar radiation profile throughout a year (Author, 2017)

Contrary to the case of microturbines, if the solar PV option is economically infeasible, the rated power will take the value of zero during the optimization, and this technology will not

contribute to power generation. It will later become obvious that the same technique is also employed for other technologies.

The capital expenditures of the installed PVs are computed by utilizing the linear equation obtained, multiplied by the unit's NPV factor for capital cost.

$$Capex_s = P_{s,rated} \cdot C_s \cdot \theta_s \tag{3.14}$$

The operational expenditures for the PVs are directly proportional to the rated output unlike the other equipment of the model, which have a maintenance cost depending on the hourly set points of the variables.

$$Opex_s = P_{s,rated} \cdot O_s \cdot \varphi_s \tag{3.15}$$

3.4.3 Wind Turbines

Wind turbines can be manufactured in a variety of sizes and rated power outputs. Therefore, they can be used in a variety of applications that require clean energy sources. Nevertheless, they have certain challenges to address, such as high manufacturing costs, the randomness of power supply, as well as environmental and aesthetic issues.

However, wind turbine prices are being in a downfall for the past 10 years, although the initial investments they require are still significantly higher compared to fuel-based generation technology. Despite that, they are able to generate large amounts of clean power, since they are a renewable technology which achieves relatively high efficiencies.

The power output of a wind turbine, just like solar PVs, is given in a fractional availability (f_w) of the rated power output, for computational simplicity.

$$P_w(t) = f_w(t) \cdot P_{w,rated} \tag{3.16}$$

Unlike solar PV, the fractional availability of wind power which depends on the wind speed at each time period, is calculated before the optimization by the following relationship.

$$f_w(t) = \begin{cases} 0\,, & v(t) < v_{ci} \; or \; v(t) > v_{co} \\ \dfrac{v(t)^3 - v_{ci}^3}{v_r^3 - v_{ci}^3}\,, & v_{ci} \le v(t) \le v_r \\ 1\,, & v_r < v(t) \le v_{co} \end{cases} \tag{3.17}$$

Wind turbines require the wind to have a minimum velocity, called cut-in speed (v_{ci}), in order for the blades to rotate. A maximum wind speed or cut-out speed (v_{co}) is also considered to prevent turbines from damaging. For high wind velocities, the generated power from the wind turbines corresponds to its rated power. Between the cut-in speed and the rated speed (v_r) the power output is a cubic function of the current velocity.

Wind speed data can be collected for several locations globally, since there has been put a lot of effort to classify many regions depending on their wind power intensity. Nevertheless, wind speeds may differ from one place to another, even if they are in close proximity. Additionally, there are also great variations in wind power due to altitude differences between the location of measurement and the location of site.

In order to overcome this obstacle, many statistical studies have been conducted, aiming to extract a relationship which can be widely used. One general expression which can meet all the previously-mentioned criteria is the power-law relationship presented below.

$$v(t) = v_{ref}(t) \cdot \left(\frac{h}{h_{ref}}\right)^{a} \tag{3.18}$$

Where, h is the altitude of the site of interest and the subscript "ref" concerns the measurements at the reference's location. The scaling coefficient a depends on the geographical features of the site of interest. The wind turbines are considered to be in an open and flat are. All values necessary for the calculation of the fractional availability can be summed up in the table below.

Table 3.7: Parameters used to calculate the fractional availability of wind rated power

Parameter	Value	Parameter	Value
$\boldsymbol{h}$	30 m	$\boldsymbol{v_{ci}}$	3 $m \cdot s^{-1}$
$\boldsymbol{h_{ref}}$	10 m	$\boldsymbol{v_{co}}$	25 $m \cdot s^{-1}$
$\boldsymbol{v_r}$	12 $m \cdot s^{-1}$	$\boldsymbol{a}$	1/7

Reference wind speed data, which has been collected from the location of measurement, is presented in figure 3.5.

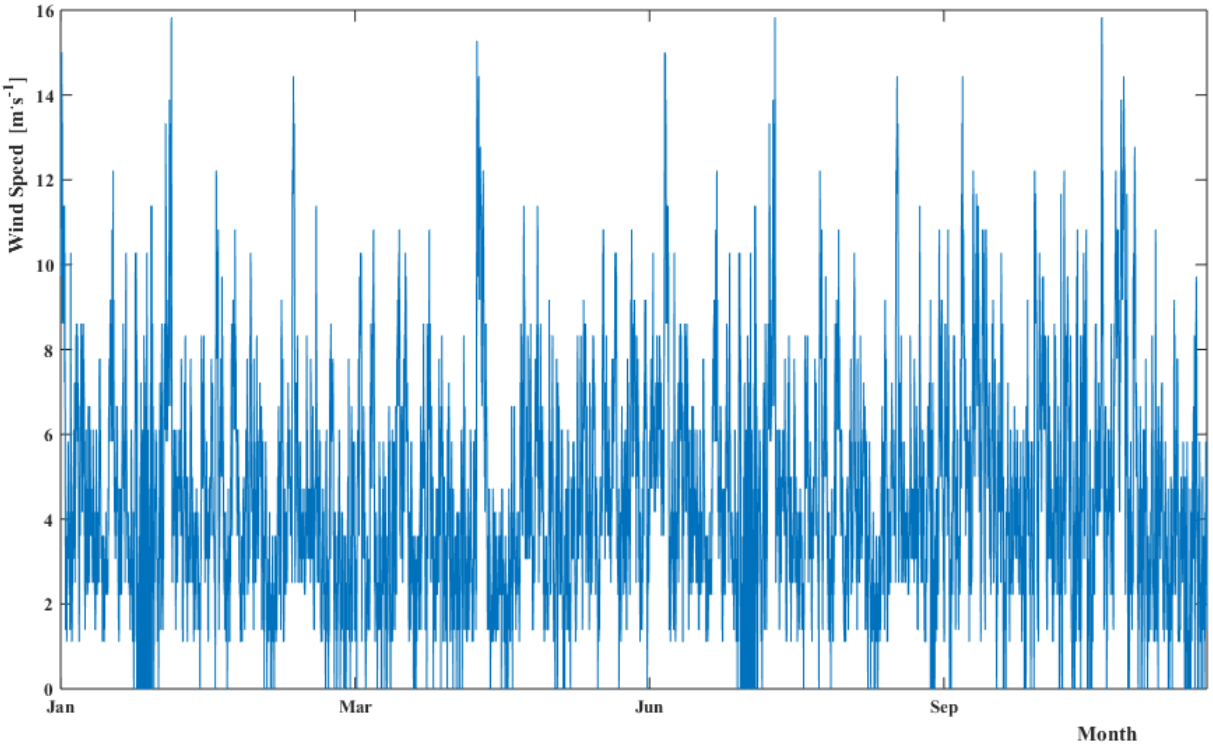

Figure 3.5: Hourly wind speed profile, measured at the site of reference, throughout a year (Author, 2017)

The capital expenditures of the wind turbines are calculated by multiplying the linear capital cost with the equipment's NPV cost factor.

$$Capex_w = C_w \cdot P_{w,rated} \cdot \theta_w \tag{3.19}$$

The operational expenditures are time dependent and must be summed up for a year's period.

$$Opex_w = \sum_t O_w \cdot P_w(t) \cdot \varphi_w \tag{3.20}$$

3.4.4 Water Boilers

Electric and gas-fired water boilers are being considered in order to meet heat demands, both being modeled as plain energy conversion units. The first constraints pertain to the units' heat outputs, which cannot exceed their rated outputs.

$$Q_j(t) \leq Q_{j,rated} \tag{3.21}$$

$$Q_n(t) \leq Q_{n,rated} \tag{3.22}$$

The heat-to-power conversion takes place at nominal efficiencies for both technologies, and have constant values of 0.9 $kW_h \cdot kW_e^{-1}$ and 0.85 $kW_h \cdot m^{-3}$ for the electric and the gas-fired boilers, respectively.

$$P_j(t) = \frac{Q_j(t)}{\eta_j} \tag{3.23}$$

$$G_n(t) = \frac{Q_n(t)}{\eta_n} \tag{3.24}$$

Where, η_j and η_n are the conversion efficiencies, $P_j(t)$ is the hourly power consumption and $G_n(t)$ is the hourly natural gas consumption in kWh.

While the values of energy conversion efficiencies have been considered constant, they are highly reduced when they operate below their maximum heat outputs. However, it is safe to assume that these units can cyclically operate in a sub-hour scale, by either having a maximum heat output or ceasing activity, enabling them to always run in optimal efficiency. For example, if a 30 percent of the rated heat output must be achieved in an hour, the boiler can operate on a maximum output for a third of the time and switch off for the rest.

The capital expenditures of the boilers are calculated from the linearized equation of capital costs.

$$Capex_j = C_j \cdot Q_{j,rated} \cdot \theta_j \tag{3.25}$$

$$Capex_n = C_n \cdot Q_{n,rated} \cdot \theta_n \tag{3.26}$$

The operational expenditures comprise of the maintenance cost for each boiler and an additional expense for the natural gas purchased, used by the gas-fired boiler.

$$Opex_j = \sum_t O_j \cdot Q_j(t) \cdot \varphi_j \tag{3.27}$$

$$Opex_n = \sum_t (O_n \cdot Q_n(t) \cdot \varphi_n + G_n(t) \cdot A_{NG} \cdot \varphi_{NG}) \tag{3.28}$$

3.4.5 Battery Bank

The storage unit that is selected for the microgrid is a lead-acid battery bank. This type of battery is ideal for microgrid establishes, since it has reduced purchase costs, is reliable and can deliver large amounts of power in a very short time.

Other types of batteries such as lithium-based or nickel-cadmium batteries, shall not be considered in this model, due to their high costs and performance inadequacy with respect to the specified operating conditions, which would add more maintenance costs.

The energy storage level of the battery bank can be calculated using a simple energy balance.

$$\frac{dL_b(t)}{dt} = P_b^-(t) \cdot n_b^- - \frac{P_b^+(t)}{n_b^+} \tag{3.29}$$

Where, L_b is the current level of the battery's storage, P_b^- is the power used to charge the battery and P_b^+ is the power that discharges the battery. The charging (n_b^-) and discharging (n_b^+) efficiencies are 90 and 95 percent, respectively.

The energy balance in equation 3.29 calculates the rate at which the energy storage level of the battery changes by time, due to electrical charge and discharge, also considering their respective efficiencies. In the formulated mathematical model, a set of discrete hourly time intervals is considered. Hence, the derivative at the left side of the equation 3.29 can take a linear from and the latter energy balance can be expressed by the equation that follows.

$$L_b(t) = L_b(t-1) + P_b^-(t) \cdot n_b^- - \frac{P_b^+(t)}{n_b^+} \tag{3.30}$$

Equation 3.30 is simply the discrete form of the continuous equation 3.29. The battery's charge level of any given time period $L_b(t)$, results from the changes of its level at the previous period due to charge or discharge.

It is also worth noting that while the charging efficiency is multiplied by the power charge, the discharge is divided by its efficiency. The reason is purely mathematical and occurs from the way the efficiencies were stated in the problem. If the discharge was multiplied by its efficiency, which is less than one, the storage level of the battery would reduce less than the actual power that it contributed to the system. That is, the battery would seem to produce more power its actual storage level.

The storage level should also be limited by the battery's rated capacity and maximum discharge level permitted by the manufacturer. The battery bank should not be allowed to discharge below 20 percent of its maximum capacity due to the possible occurrence of unwanted effects, such as lifespan reduction and potentially permanent damage.

$$0.2 \cdot L_{b,max} \leq L_b(t) \tag{3.31.a}$$

$$L_b(t) \leq L_{b,max} \tag{3.31.b}$$

Unlike microturbines, cycling effects are not tracked in the case of the battery bank, in order to reduce the number of binary variables of the problem. Nonetheless, a small lifetime has been selected for the battery bank, assuming that a full cycle will be taking place in a daily basis.

The capital and operational expenditures of the battery bank are calculated by the two following linear equations.

$$Capex_b = L_{b,max} \cdot C_b \cdot \theta_b \tag{3.32}$$

$$Opex_b = \sum_t (P_b^+(t) \cdot O_b \cdot \varphi_b) \tag{3.33}$$

The maintenance cost of the battery bank occurs from the sum of power that was discharged by it and not by its hourly storage level.

3.5 Heat and Power Balance

Hourly electricity (P_l) and thermal energy (Q_l) demands, which can be seen in figures 3.10 and 3.9, respectively, are fixed values that are extracted from a data sheet obtained from Zachar,

Trifkovic and Daoutidis, 2015, and processed in order to be able to be used in the model. To satisfy load demands, a linear energy balance for power and heat needs to be constructed.

In the power balance, power generated from all the distributed resources, as well as power purchased from the microgrid must be taken into account. Additionally, distributed units that consume power should also be included in the energy balance, along with a variable which is used to track excess power that went to waste (P_d).

$$\sum_m P_m(m,t) + P_s(t) + P_w(t) + P_b^+(t) + P_{grid}(t) = P_l(t) + P_b^-(t) + P_j(t) + P_{dump}(t) \qquad (3.34)$$

Likewise, distributed heat generation units must meet the heat demand of the load (Q_l) at each point throughout a year. The load's heat demand includes hot water both for personal use ($Q_{l,water}$) and for space heating ($Q_{l,space}$). A variable (P_d) is also used to track the thermal energy that was not put to use.

$$\sum_m Q_m(m,t) + Q_j(t) + Q_n(t) = Q_l(t) + Q_d(t) \qquad (3.35)$$

Thermal energy data was synthetically generated by Zachar, Trifkovic and Daoutidis, 2015 since immediate data extraction was not possible. Using weather temperature data ($T_{external}$), interior temperature data ($T_{internal}$), which are presented in figures 3.7 and 3.6, respectively, along with an average building thermal efficiency (k), they managed to calculate the demand used for space heating.

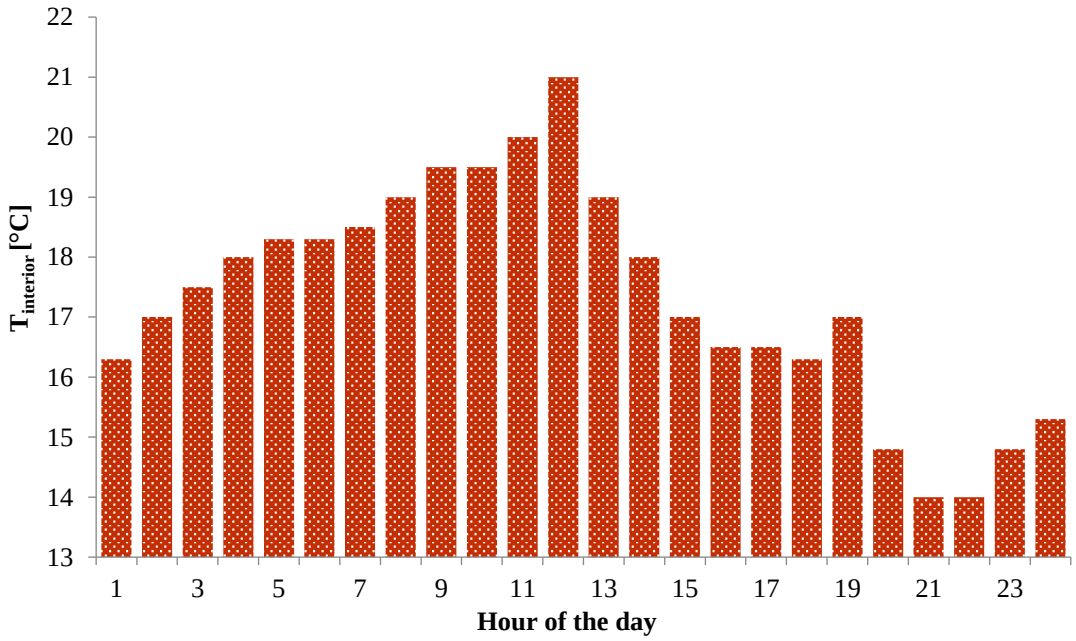

Figure 3.6: Building internal temperature hourly profile throughout a day (Author, 2017)

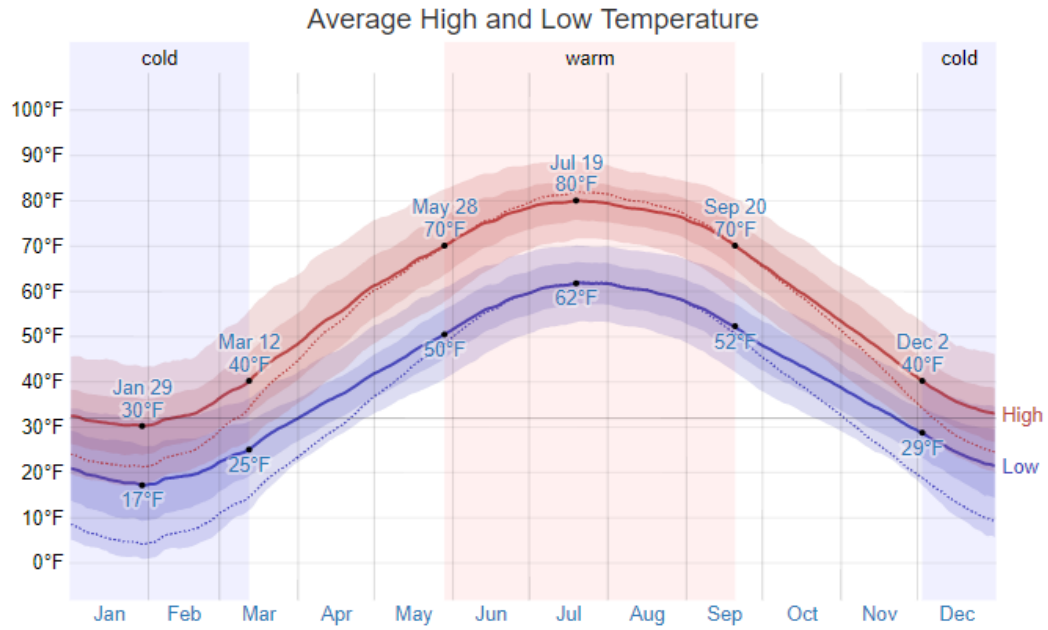

Figure 3.7: Sarnia's average high and low temperature profile throughout a year (weatherspark.com, 2018)

$$Q_{l,space}(t) = \max\left(0, k \cdot \Delta T(t)\right) \tag{3.36}$$

Where, $\Delta T(t) = T_{interior}(t) - T_{exterior}(t)$ and $k = 32.6$ kWh $\cdot$ °C^{-1} is the building's thermal efficiency used as a proportionality constant. The space heating demand in equation 3.36 receives the highest value between 0 and $k \cdot \Delta T(t)$.

If during the time period "t" the required internal temperature is lower than the external, then the temperature difference has a negative value and the space heating demand obtains the value of zero. On the contrary, if during the time period "t" the required internal temperature exceeds the external, then the temperature difference is positive, and so is $Q_{l,space}(t)$.

A daily average pattern of hot water for personal use ($Q_{l,water}(t)$) was able to be obtained and is presented on figure 3.8.

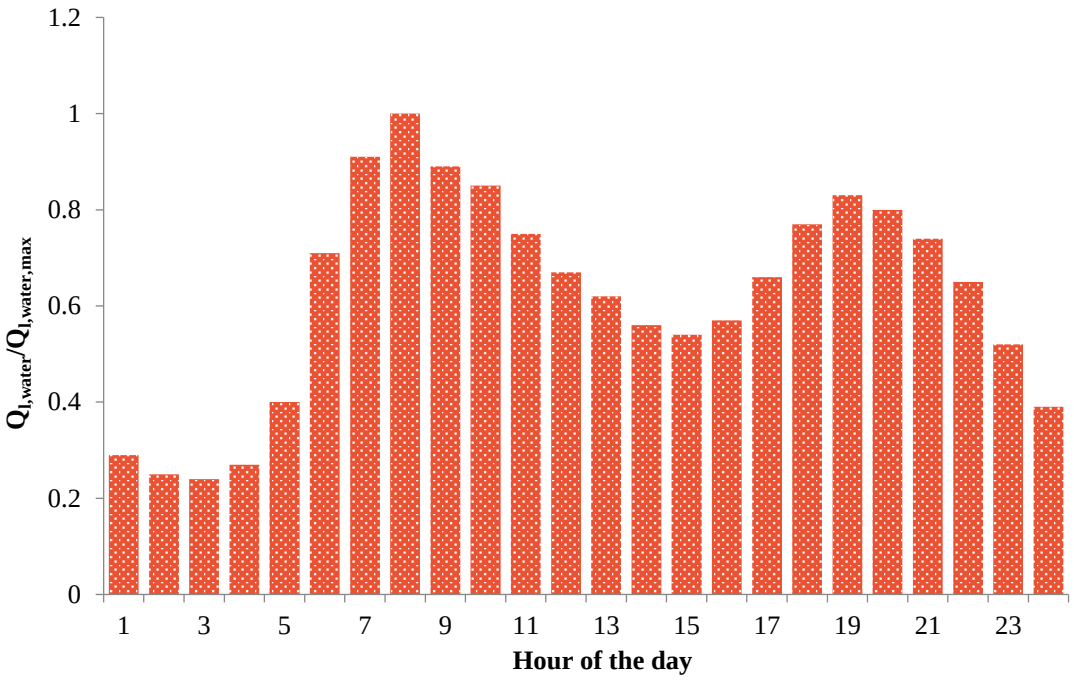

Figure 3.8: Hourly profile of hot water for personal use, normalized by its maximum value, throughout a day (Author, 2017)

The total heat demand of the load results from the sum of the demand for space heating and the demand in hot water for personal use.

$$Q_l(t) = Q_{l,space}(t) + Q_{l,water}(t) \tag{3.37}$$

The overall hourly heat and power demand profile throughout an annum is illustrated in figures 3.9 and 3.10, respectively, which were created with Matlab.

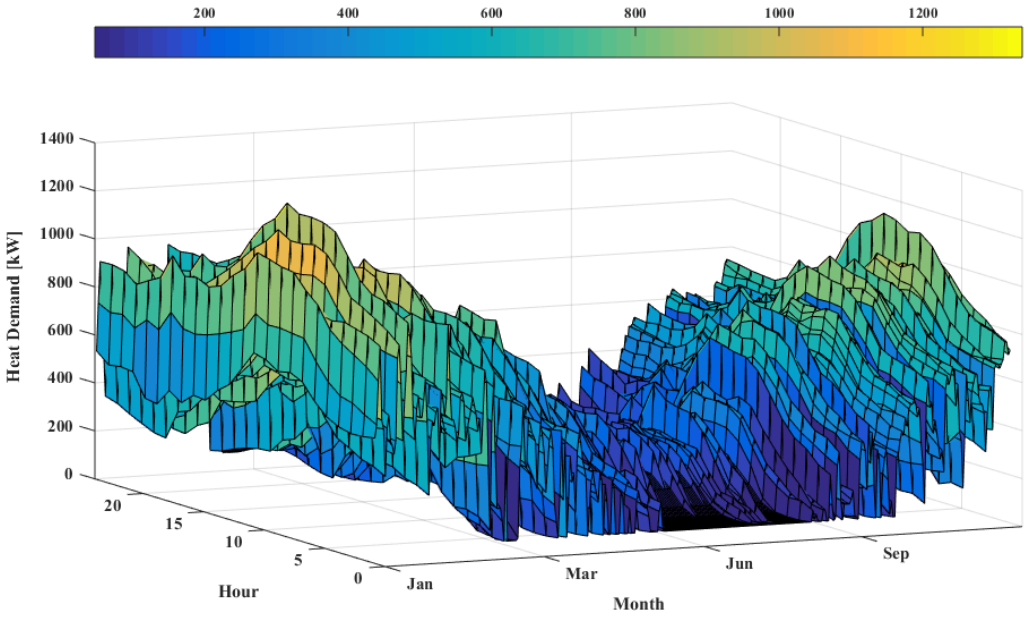

Figure 3.9: Visual representation of the daily demand in heat, throughout a year (Author, 2017)

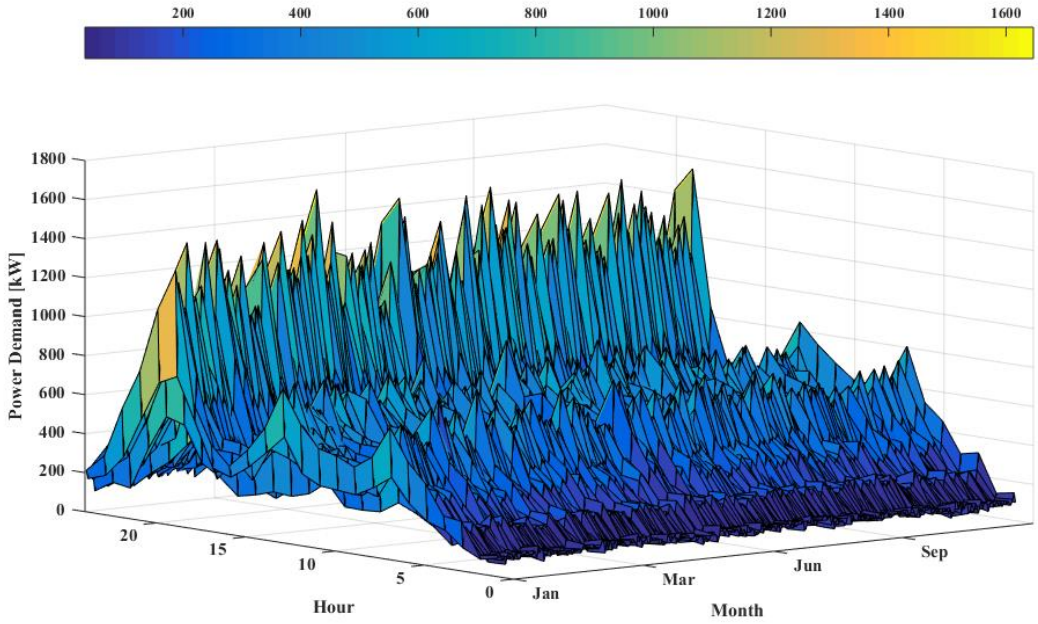

Figure 3.10: Visual representation of the daily demand in electrical power, throughout a year (Author, 2017)

The sum of the hourly power and heat demand data results in the calculation of the total load which is 3.65 GWh and 3.45 GWh respectively.

3.6 Other Considerations and Calculations

This section focuses on parameters that are needed to evaluate environmental impacts and utility costs. Variables that track carbon dioxide emitted from both the microgrid and the macrogrid, as well as the purchase costs of natural gas and power from the macrogrid will be introduced.

3.6.1 Carbon Emissions

The units that produce energy by natural gas combustion are the microturbines and the gas-fired boilers. Natural gas consumption is a variable that is calculated for both technologies in equations 3.7 and 3.20 in m^3.

According to EIA, 117 pounds of carbon dioxide per million BTUs of energy are released upon natural gas combustion. The SI unit equivalent of that value is $0.181 \cdot 10^{-3}$ ton$(CO_2)\cdot kWh^{-1}$ (or $50.3 \cdot 10^{-6}$ ton$(CO_2)\cdot MJ^{-1}$). This number is the natural gas carbon emission coefficient (F_{NG}), which will be used to calculate the total carbon dioxide emitted by the units that consume gas.

$$E_m = \sum_m \sum_t G_m(m,t) \cdot F_{NG} \tag{3.38}$$

$$E_n = \sum_t G_n(t) \cdot F_{NG} \tag{3.39}$$

The total pollutant emissions from the microgrid result from the sum of the previous two.

$$E_{microgrid} = E_n + E_m \tag{3.40.a}$$

Which can also be written as:

$$E_{microgrid} = \sum_{t} G_n(t) \cdot F_{NG} + \sum_{m} \sum_{t} G_m(m,t) \cdot F_{NG} \quad (3.40.b)$$

A similar approach should be conducted for the power that was purchased from the macrogrid. A carbon emission coefficient (F_{grid}) of $0.575 \cdot 10^{-3}$ ton(CO_2)·kWh^{-1} was successfully obtained for a centralized power generation system, assumingly comprising of 37 percent coal and 30 percent natural gas. Macrogrid emissions are calculated by the following relationship.

$$E_{grid} = \sum_{t} P_{grid}(t) \cdot F_{grid} \quad (3.41)$$

3.6.2 Utility Costing

The purchase costs of the utilities are treated as an operational expenditure. An expected annual increase to their prices is also assumed, leading to the following relationships.

$$Opex_{NG} = \sum_{t} \left[\sum_{m} G_m(m,t) + G_n(t) \right] \cdot A_{NG} \cdot \varphi_{NG} \quad (3.42)$$

$$Opex_{grid} = \sum_{t} P_{grid}(t) \cdot A_{grid} \cdot \varphi_{grid} \quad (3.43)$$

Purchase cost for electricity (A_{grid}) rises at 0.108 \$·kWh^{-1} and for natural gas (A_{NG}) at 0.2968 \$·m^{-3}. These values were obtained from Zachar, Trifkovic and Daoutidis, 2015. The cost of natural gas has to be converted to be used in the model, by using its average calorific value of 35.4 MJ·m^{-3}. The converted natural gas cost is 0.0302 \$·kWh^{-1}.

3.7 Objective Function

The primary purpose of the optimization of this microgrid model is to evaluate a least cost solution, which may either include distributed generation units or purchase power from the macrogrid. Hence, the objective function of the optimization must include purchase costs both for equipment and for utilities, as well as maintenance costs.

The total capital expenditures ($Capex$) will result from the sum of the purchase costs of all the distributed resources that were considered.

$$Capex = Capex_m + Capex_w + Capex_s + Capex_j + Capex_n + Capex_b \quad (3.44.a)$$

Substitution of each individual capital expense, will result in the equation below.

$$Capex = \sum_{m} y_m(m) \cdot C_m \cdot \theta_m + P_{s,rated} \cdot C_s \cdot \theta_s + P_{w,rated} \cdot C_w \cdot \theta_w + Q_{j,rated} \cdot C_j \cdot \theta_j + L_{b,max} \cdot C_b \cdot \theta_b \quad (3.44.b)$$

Maintenance and utility costs, summed over the time period of a year, consist in the operational expenditures of the microgrid.

$$Opex = Opex_m + Opex_w + Opex_s + Opex_j + Opex_n + Opex_b + Opex_{grid} + Opex_{NG} \quad (3.45.a)$$

Which, by substitution of its elements can also be written as:

$$\begin{aligned} Opex = {} & O_s \cdot P_{s,rated} \cdot \varphi_s + \sum_t \left[\left(\sum_m \left(P_m(m,t) \cdot O_m + z_m(m,t) \cdot O_{startup} \right) \right) \cdot \varphi_m \right] \\ & + \sum_t (O_w \cdot P_w(t) \cdot \varphi_w) + \sum_t \left(O_j \cdot Q_j(t) \cdot \varphi_j \right) + \sum_t (O_n \cdot Q_n(t) \cdot \varphi_n) \\ & + \sum_t (P_b^+(t) \cdot O_b \cdot \varphi_b) + \sum_t \left(P_{grid}(t) \cdot A_{grid} \cdot \varphi_{grid} \right) \\ & + \sum_t \left[\left(\sum_m \left(G_m(m,t) \right) + G_n \right) \cdot A_{NG} \cdot \varphi_{NG} \right] \end{aligned} \quad (3.45.b)$$

Where, $\varphi_s = \varphi_m = \varphi_w = \varphi_j = \varphi_n = \varphi_b = \varphi_{grid} = \varphi_{NG} = \varphi$. Notice that while its variables are time dependent, $Opex$ is a single variable, since they are all summed with respect to time.

The objective function is the net present value of all costs (NPC) and is the sum of capital and operational expenses that occur.

$$NPC = Capex + Opex \quad (3.46)$$

3.8 Final Model

The final model is a MILP requiring the minimization of the objective function (NPC), which is constrained to a set of equations. The whole model can be summed up below.

$$\min Capex + Opex$$

$$subject\ to$$

$$Capex = \sum_m y_m(m) \cdot C_m \cdot \theta_m + P_{s,rated} \cdot C_s \cdot \theta_s + P_{w,rated} \cdot C_w \cdot \theta_w + Q_{j,rated} \cdot C_j \cdot \theta_j + L_{b,max} \cdot C_b \cdot \theta_b$$

$$\begin{aligned} Opex = {} & O_s \cdot P_{s,rated} \cdot \varphi_s + \sum_t \left[\left(\sum_m \left(P_m(m,t) \cdot O_m + z_m(m,t) \cdot O_{startup} \right) \right) \cdot \varphi_m \right] \\ & + \sum_t (O_w \cdot P_w(t) \cdot \varphi_w) + \sum_t \left(O_j \cdot Q_j(t) \cdot \varphi_j \right) + \sum_t (O_n \cdot Q_n(t) \cdot \varphi_n) \\ & + \sum_t (P_b^+(t) \cdot O_b \cdot \varphi_b) + \sum_t \left(P_{grid}(t) \cdot A_{grid} \cdot \varphi_{grid} \right) \\ & + \sum_t \left[\left(\sum_m \left(G_m(m,t) \right) + G_n \right) \cdot A_{NG} \cdot \varphi_{NG} \right] \end{aligned}$$

$$\sum_m P_m(m,t) + P_s(t) + P_w(t) + P_b^+(t) + P_{grid}(t) = P_l(t) + P_b^-(t) + P_j(t) + P_{dump}(t)$$

$$\sum_{m} Q_m(m,t) + Q_j(t) + Q_n(t) = Q_l(t) + Q_d(t)$$

$$P_m(m,t) \leq x(m,t) \cdot P_{m,rated}$$

$$0.5 \cdot x(m,t) \cdot P_{m,rated} \leq P_m(m,t)$$

$$Q_m(m,t) = P_m(m,t) \cdot \gamma_m$$

$$G_m(m,t) = \frac{P_m(m,t)}{\eta_m}$$

$$x_m(m,t) \leq y(m)$$

$$z(m,t) \geq x(m,t) - x(m,t-1)$$

$$P_s(t) = P_{s,rated} \cdot \frac{H(t)}{H_{rated}}$$

$$P_w(t) = f_w(t) \cdot P_{w,rated}$$

$$Q_j(t) \leq Q_{j,rated}$$

$$P_j(t) = \frac{Q_j(t)}{\eta_j}$$

$$Q_n(t) \leq Q_{n,rated}$$

$$G_n(t) = \frac{Q_n(t)}{\eta_n}$$

$$L_b(t) = L_b(t-1) + P_b^-(t) \cdot n_b^- - \frac{P_b^+(t)}{n_b^+}$$

$$0.2 \cdot L_{b,max} \leq L_b(t)$$

$$L_b(t) \leq L_{b,max}$$

$$E_{microgrid} = \sum_{t} G_n(t) \cdot F_{NG} + \sum_{m} \sum_{t} G_m(m,t) \cdot F_{NG}$$

$$E_{grid} = \sum_{t} P_{grid}(t) \cdot F_{grid}$$

All the model's variables are positive, while the binary variables are constrained to only receive values of one and zero.

Chapter 4

Solutions and Discussion

The mixed integer linear mathematical program, is solved using the General Algebraic Modelling System (GAMS). GAMS is an optimization software able to efficiently handle multidimensional mathematical programs, which may have very large and sparse structures. In this model this feature proves to be very useful, due to the sizeable number of variables and equations that need to be simultaneously considered.

4.1 Listing the Model's Elements

As mentioned in subsection 3.4.1 of the previous chapter, each variable that is set-dependent, is a block of the same size as the set. During the compilation of the program, the block of variables is extracted, resulting in 8760 single variables. The same principle applies for the set of microturbines, this time producing 3 single variables, while a variable that depends on both sets produces 26,280 (3·8760) single variables. Hence, it is possible to calculate the total number of single variables of the model.

Table 4.1: A summary of the variables as declared in GAMS, with the number of single variables that they produce

Variable	Description	Type	Units	Single Variables
y(m)	MT "m" is installed	binary variable	-	3
z(m,t)	MT 'm' is started up	binary variable	-	26,280
x(m,t)	MT 'm' is on	binary variable	-	26,280
NPC	Net present value of costs	variable	$	1
Capex	Capital expenditures	positive variable	$	1
Opex	Operational expenditures	positive variable	$	1
Pwr	Rated power output of WTs	positive variable	kW	1
Psr	Rated power output of PVs	positive variable	kW	1
Qjr	Rated heat output of EBs	positive variable	kW	1
Qnr	Rated heat output of NGBs	positive variable	kW	1
Lbmax	Rated power storage of BB	positive variable	kW	1
Pm(m,t)	MT power output	positive variable	kWh	26,280
Pw(t)	WT power output	positive variable	kWh	8,760
Qn(t)	NGB heat output	positive variable	kWh	8,760
Qj(t)	EB heat output	positive variable	kWh	8,760
Pbplus(t)	BB discharge	positive variable	kWh	8,760
Gm(m,t)	NG consumed by the MTs	positive variable	m3	26,280
Gn(t)	NG consumed by the NGBs	positive variable	m3	8,760
Pgrid(t)	Macrogrid purchased power	positive variable	kWh	8,760
Ps(t)	Power produced by SPVs	positive variable	kWh	8,760
Pbminus(t)	BB charging	positive variable	kWh	8,760
Pj(t)	Power consumed by the EB	positive variable	kWh	8,760
Pdump(t)	Dumped power load	positive variable	kWh	8,760
Qm(m,t)	Heat produced by the MTs	positive variable	kWh	26,280

Qdump(t)	Dumped heat load	positive variable	kWh	8,760
Lb(t)	Energy storage level	positive variable	kWh	8,760
Em	MT CO_2 emissions	positive variable	ton·kWh^{-1}	1
En	NGB CO_2 emissions	positive variable	ton·kWh^{-1}	1
Egrid	Macrogrid CO_2 emissions	positive variable	ton·kWh^{-1}	1

A sum over the single variables of the table would give their total number which is 236,534 single variables.

The same is true for equation blocks, which also extract into single equations upon compilation. The following table will aid in the calculation of the total number of single equations that are considered in the model.

Table 4.2: A summary of the equations declared in GAMS, along with the number of single equations they produce

Equation	Description	Single Equations
eq1	Sum of the capital costs	1
eq2	Sum of the operational costs	1
eq3(t)	Electricity power balance	8,760
eq4(t)	Heat balance	8,760
eq5a(t,m)	Lower bound from MT efficiency constraint	26,280
eq5b(t,m)	Upper bound from MT efficiency constraint	26,280
eq6(t,m)	Useful heat generated from MTs	26,280
eq7(t,m)	MT fuel consumption	26,280
eq8(t,m)	Activated MTs limitation by number of installed	26,280
eq9(t,m)	Track of startups of MTs	26,280
eq10(t)	Solar PVs power balance	8,760
eq11(t)	Wind turbine power balance	8,760
eq12b(t)	Upper bound of EB hourly consumption	8,760
eq13b(t)	Upper bound of NGB hourly consumption	8,760
eq14(t)	Heat to power conversion of EB	8,760
eq15(t)	Natural gas to heat conversion of NGB	8,760
eq16(t)	Battery bank power balance	8,760
eq17a(t)	Lower bound in BB storage level	8,760
eq17b(t)	Upper bound in BB storage level	8,760
mtCO2	MT CO_2 emissions	1
ngbCO2	NGB CO_2 emissions	1
gridCO2	Macrogrid CO_2 emissions	1
obj	Sum of capex and opex (objective function)	1

The total number of single equations that constitute the model is 254,046.

4.2 Reference Case

The MILP model that was presented in subsection 3.6 is solved, using the CPLEX method with a maximum relative gap of 1 percent. In this stage, the aim is to reproduce the results that were

obtained by M. Zachar et al. No other constraints are added to the program and the optimal solution may or may not include any distributed generation units.

The results of the optimization show that power demand is solely met by electricity purchased from the macrogrid, whereas demands in heat are met by gas-fired boilers. That, along with a net present value of about 6.5 M$, adequately describes the results of the reference paper. The solution's parameters are briefly presented in the following table.

Table 4.3: Variable values after the optimization of the Reference Case

Variable	Description	Value
NPC	Net present value of costs	6.51 M$
Capex	Capital expenses	0.10 M$
Opex	Operational expenses	6.40 M$
Σy	Total number of installed microturbines	0
$P_{s,rated}$	Rated output of solar PVs	0 kW
$P_{w,rated}$	Rated output of wind turbines	0 kW
$Q_{j,rated}$	Rated output of electric boilers	0 kW
$Q_{n,rated}$	Rated output of gas fired boilers	1,340 kW
$L_{b,max}$	Rated storage of battery bank	0 kWh
E_m	Emissions afflicted by the microturbines	0 ton(CO_2)·y^{-1}
E_n	Emissions afflicted by the gas fired boilers	744 ton(CO_2)·y^{-1}
E_{grid}	Emissions afflicted by the macrogrid	2,100 ton(CO_2)·y^{-1}

Although natural gas is less expensive than electricity's price per unit of energy, the high installation costs of the distributed generation units, resulted in their rejection. Purchasing power from the macrogrid does not come with any additional equipment installation costs, making it a more competitive solution.

The optimization of this program produces the least cost scenario option, of a microgrid model with no further constraints added. The values of the variables from this solution will be used as a reference (Ref Case) for comparison purposes with the following models.

4.3 Minimum Autonomy Scenario

In this case, a constraint that requires a minimum contribution to the total power demand from the microgrid, is added to the mathematical program. The microgrid should be able to meet a certain fraction of the annual power demand, obtaining a minimum degree of autonomy. An equation that can adequately describe the autonomy level, with respect to power generation, can be seen below.

$$\sum_t P_{grid}(t) \leq (1 - Auto) \cdot \sum_t \left[P_l(t) + P_j(t)\right]$$

Where, $Auto$ is a new parameter which is used to give a certain level of autonomy to the system. The equation above suggests that the total utility power that is purchased throughout an annum, should not exceed a certain fraction of the total demand in electricity, that occurs from the load and the electric boilers. This constraint forces the program to involve the distributed generation technologies in order to cover the demands.

The MILP model is solved with the GAMS software, using the CPLEX method, for a minimum contribution of 25, 50, 75 and 100 percent, from the distributed resources of the microgrid. The next table summarizes the solution parameters for each case.

Table 4.4: Variable values after the optimization of minimum autonomy scenario, for several autonomy levels

Variables	Units	Microgrid Autonomy Level (%)				
		0 (Ref Case)	**25**	**50**	**75**	**100**
NPC	M$(@2017)	6.51	6.54	6.91	7.36	13.89
Capex	M$(@2017)	0.10	0.68	1.25	1.53	9.41
Opex	M$(@2017)	6.40	5.87	5.65	5.84	4.48
Σy		0	1	2	2	3
$P_{s,rated}$	kW	0	0	0	0	0
$P_{w,rated}$	kW	0	0	0	0	1685
$Q_{j,rated}$	kW	0	29	86	0	356
$Q_{n,rated}$	kW	1,340	1062	757	1023	565
$L_{b,max}$	kWh	0	0	5	851	5722
E_m	ton$(CO_2)\cdot y^{-1}$	0	802	1247	1885	1700
E_n	ton$(CO_2)\cdot y^{-1}$	744	373	183	148	169
E_{grid}	ton$(CO_2)\cdot y^{-1}$	2,100	1420	1060	525	0

Figures 4.1 and 4.2 show the contribution to power and heat generation by source, respectively. It is obvious that microturbines are highly favored, since they can meet both power and heating demands, in conjunction with their relatively small installation costs that makes them competitive. One microturbine is installed for 25 percent autonomy, two for 50 percent and three for full autonomy.

When it comes to full autonomy (100%), power from the macrogrid is not allowed to be purchased, so in order to cover the demands in power, wind turbines are also selected, meeting more than 35 percent of the total energy production. As expected, the involvement of wind turbines will significantly raise the net present value of the system.

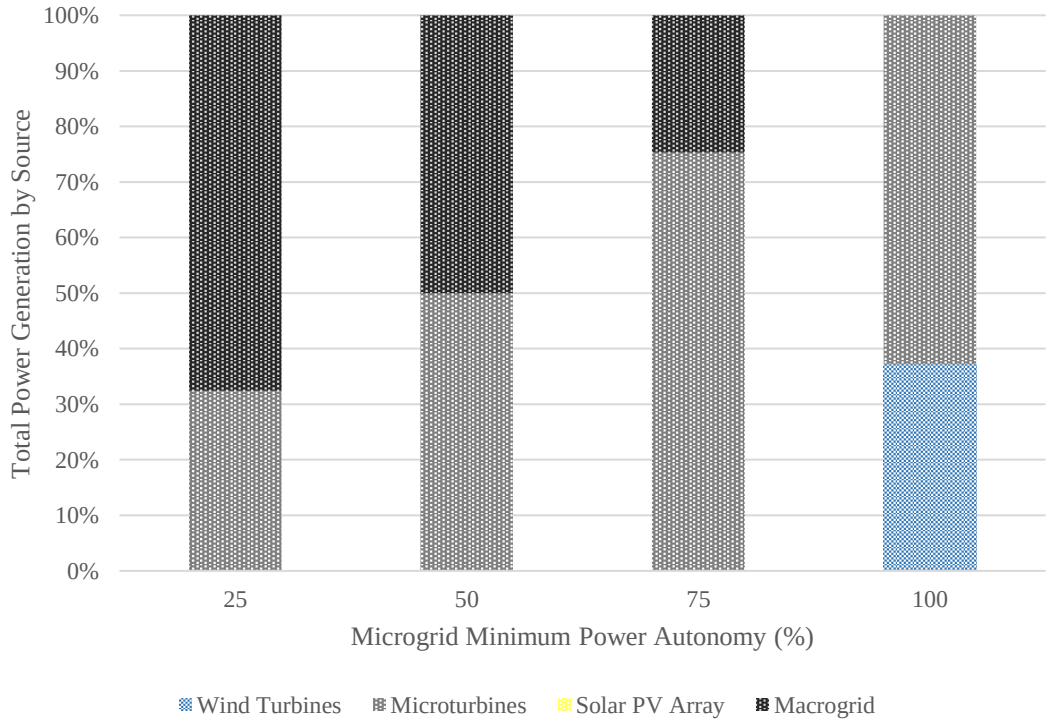

Figure 4.1: Percentage of contribution to power generation by source, for all autonomy levels (Author, 2017)

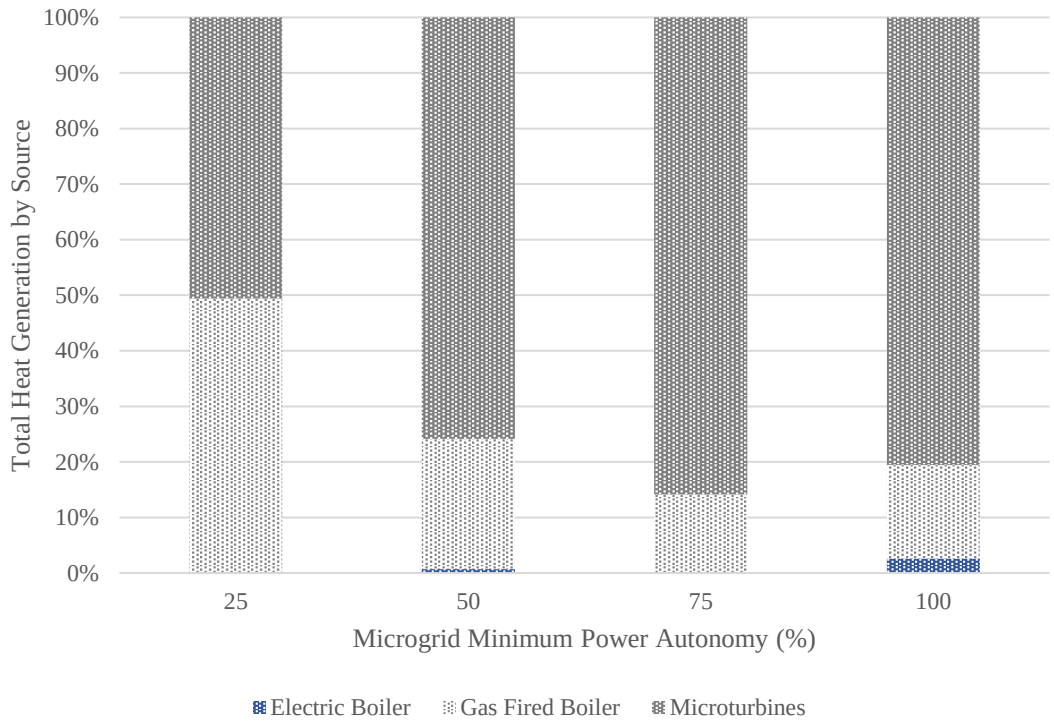

Figure 4.2: Percentage of contribution to heat generation by source, for all autonomy levels (Author, 2017)

Figure 4.3 shows the contribution to the net present value of costs ($NPC = Opex + Capex$), that result from the optimization of each autonomy case scenario for a 20 year period.

Generally, the net present values obtained by the optimization, are of similar magnitude until full autonomy is reached. In full autonomy, the involvement of wind turbines significantly raises the total cost, due to their high installation costs.

The net present value of the reference case is almost equal to that of the 25 percent autonomy case, with the latter option being only about 30,000 $ more expensive, despite that the microturbine installation cost raises to 594,000 $.

This is possible due to the use of natural gas by these units, that is less costly than electricity per energy unit (0.1080 $\$\cdot kWh^{-1}$ for electricity, compared to 0.0302 $\$\cdot kWh^{-1}$ for natural gas), and the units' ability to meet both power and heat demands, also minimizing the need of boilers.

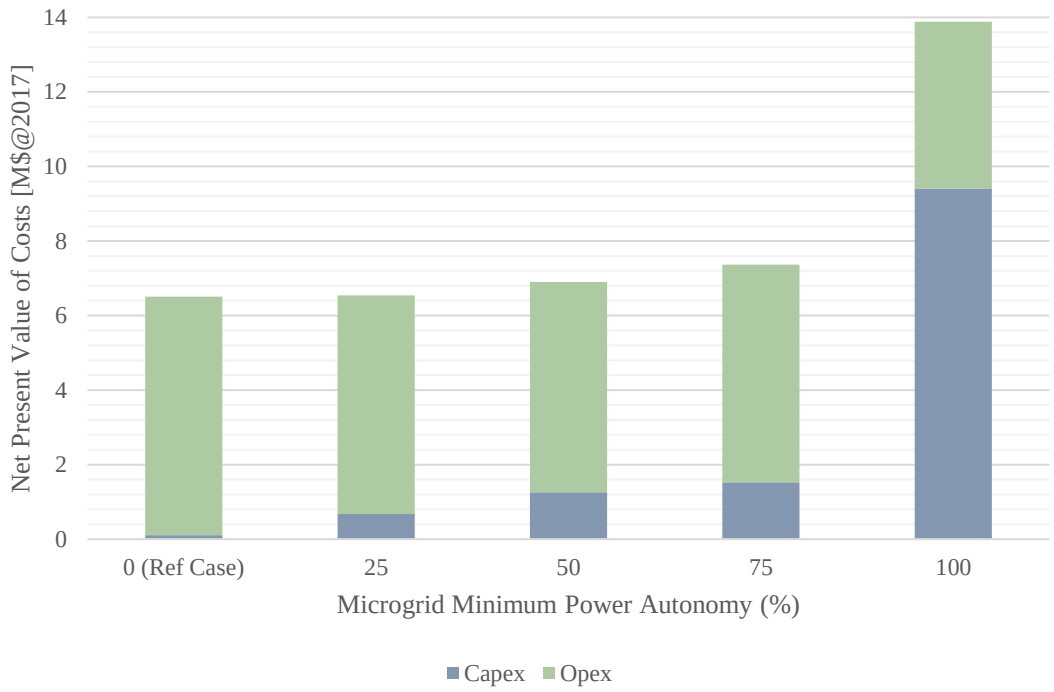

Figure 4.3: Net present value of costs for each autonomy level (Author, 2017)

The total carbon emissions that are produced in an annual base, are presented for each case (including the reference) in diagram 4.4. The annual carbon emissions are reduced by about 10 percent from the reference case for autonomies up to 75 percent. A drastic 34 percent reduction of carbon emissions is achieved in the full autonomy case, due to the selection of wind turbines which cover about 37 percent of the total power production.

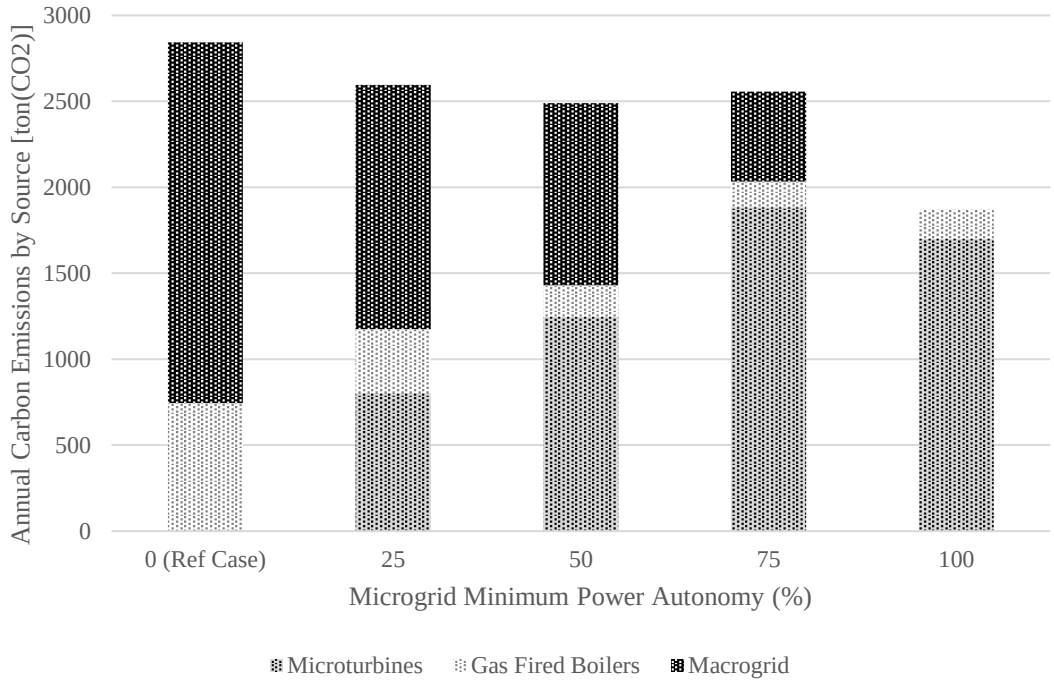

Figure 4.4: Total annual carbon emissions produced per each autonomy case (Author, 2017)

Despite the overall efficiency of the microgrids, some of the electrical and thermal energy that is produced, sometimes needs to be dumped if it is excessive. Figures 4.5 and 4.6 that follow, show the useful and the wasted power and heat that is produced annually, respectively. In the power diagram, the electricity that is consumed by the electric boilers is also considered as useful power.

It is obvious that for autonomies of 75 and 100 percent, there are significant energy losses from the system. This is mainly due to the additional maintenance costs that occur per startup of the microturbines. The program selects as an optimal choice to keep the microturbines running even in periods of low demand in power and heat, rather than shutting them down. What is more, in the full autonomy case, the introduction of wind turbines leads to the generation of even more power during off-peak hours.

On the contrary, the energy production of up to 50 percent autonomy, results in very few losses, since a great portion of the demand is covered by the macrogrid and the gas fired boilers. This enables unusually high demands to be met with the aid of these two, minimizing the losses.

Another fact worth mentioning is that although the thermal energy from the microturbines is enough to meet the demands in heat, natural gas boilers are involved in all cases. This is probably due to the different profiles of heat and power demands of the load, presented in the heat and power balance subsection of chapter 3.

During summer months the heat demand is significantly reduced, while demands in electricity do not, resulting in the waste of the produced heat, also reducing the overall efficiency of the system.

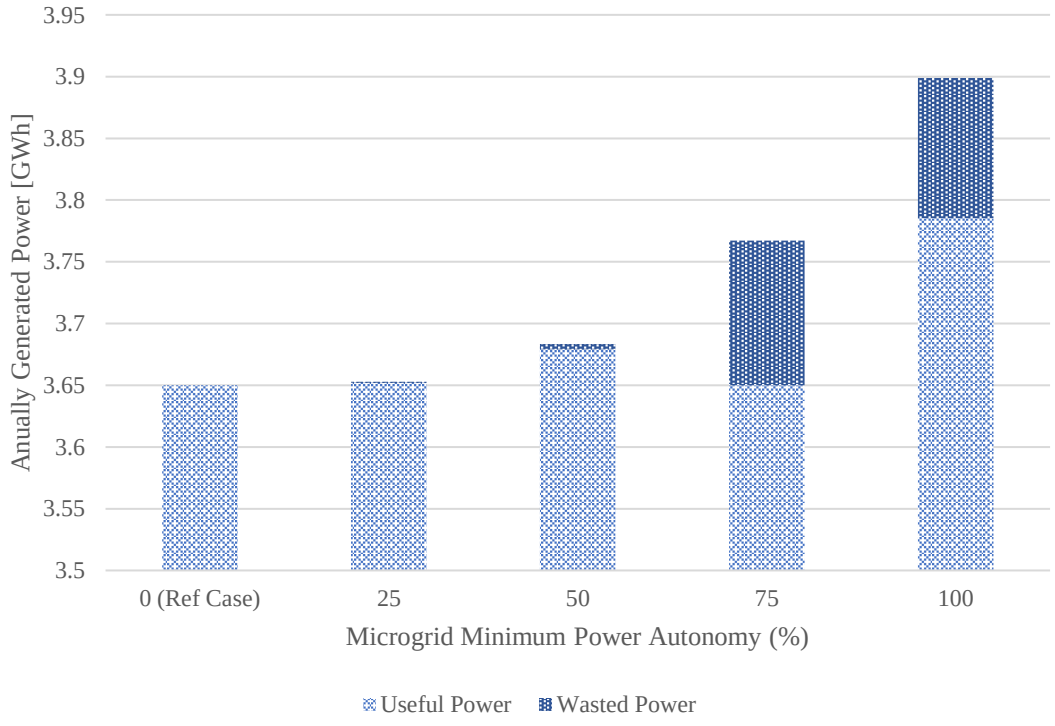

Figure 4.5: Total annually generated electricity, consumed and wasted, per autonomy case (Author, 2017)

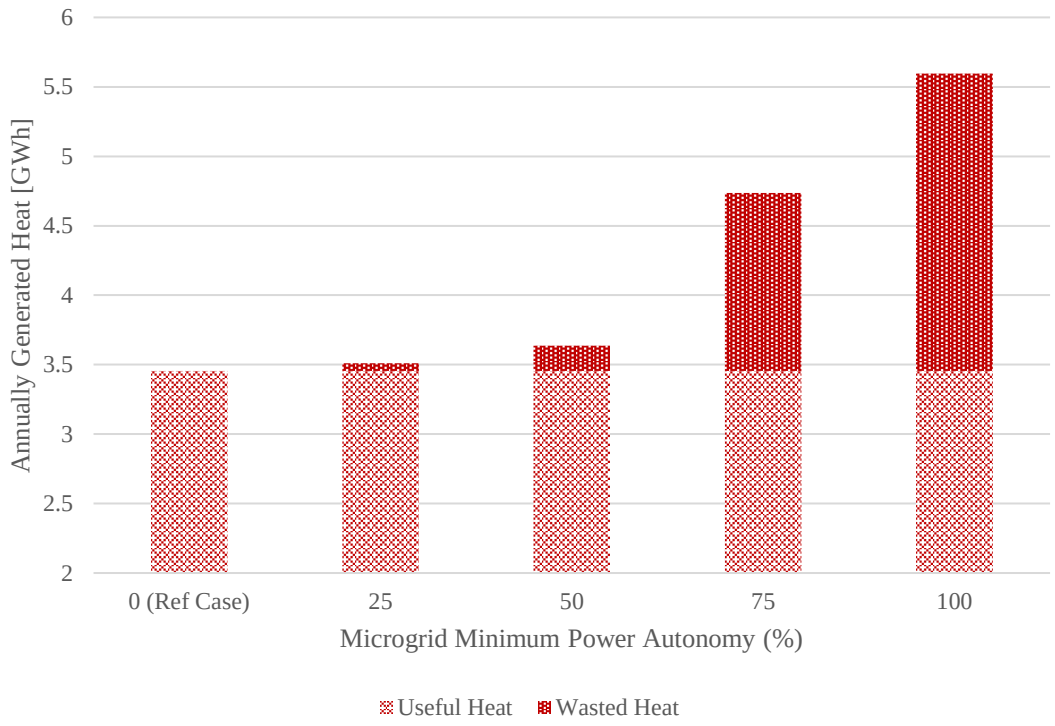

Figure 4.6: Total annually generated heat, consumed and wasted, per autonomy case (Author, 2017)

To recap, the minimum autonomy scenario produces a slightly less competitive solution for autonomy levels of up to 75 percent, while a full autonomy is an expensive option due to high installation costs of the wind turbines. The involvement of the microgrid's distributed resources to the final solution has the potential to reduce the carbon emissions by 10 to 35 percent. Nevertheless, the solutions of autonomies greater than 75 percent, result in great amounts of wasted power and heat, reducing the system's overall efficiency.

4.4 Carbon Emissions Reduction Scenario

The emissions reduction case study gives an insight to the optimal cost and the corresponding technology selection, for several rates of carbon dioxide emissions reduction. The generation of less carbon intensive power and heat is an international goal with new policies being constantly pledged by many countries worldwide. Polices that may enforce a reduction of the emissions produced from generation of electricity, can favor microgrids.

This case study focuses on the co-optimization of the main model of the reference case, so that the carbon dioxide that is released also gets reduced. This is achieved by introducing a new constraint to the program, which forces the final system to produce a smaller fraction of the emissions of the reference case.

In the reference case the carbon dioxide emissions originated from the electricity purchased from the macrogrid and from natural gas combustion in the gas-fired boiler. The annual carbon emissions produced in the reference case solution reached 2844 ton(CO_2)·y^{-1} in total.

The new model will still have the net present value of costs as an objective function, while this time it will also be subjected to the following constraint, which regulates the maximum carbon emissions produced.

$$E_{grid} + E_n + E_m \leq 2844 \cdot (1 - RedE)$$

Where, $RedE$ is the carbon emissions reduction fraction. There are four case studies that will be conducted for 25, 50, 75 and 100 percent reduction in the produced emissions. The optimization will minimize the net present value of costs, while also considering that the sum of the emissions produced must be kept below the value of interest.

The mathematical optimization program is an MILP which is solved in GAMS with the CPLEX method. The solution's design parameters are summarized in the following table.

Table 4.5: Summary of the variables' values after the optimization of the emissions reduction scenario, per case

Variables	**Units**	**Total Carbon Emissions Reduction (%)**				
		0 (Ref Case)	**25**	**50**	**75**	**100**
NPC	M$(@2017)	6.51	8.42	13.22	21.71	152.66
Capex	M$(@2017)	0.10	3.32	9.19	18.39	142.97
Opex	M$(@2017)	6.40	5.10	4.04	3.32	9.69
Σy		0	2	2	1	0
$P_{s,rated}$	kW	0	395	1139	2413	12620
$P_{w,rated}$	kW	0	0	340	881	19436
$Q_{j,rated}$	kW	0	45	271	763	1338
$Q_{n,rated}$	kW	1,340	912	861	1023	0
$L_{b,max}$	kWh	0	261	3314	8129	42751
E_m	ton$(CO_2)\cdot y^{-1}$	0	1088	837	204	0
E_n	ton$(CO_2)\cdot y^{-1}$	744	238	333	453	0
E_{grid}	ton$(CO_2)\cdot y^{-1}$	2,100	806	251	53	0

Figures 4.7 and 4.8 that follow, show the contribution of each technology to the total power and heat generation, respectively. From the power diagram, it is obvious that the solar PV technology is preferred for the production of electricity, especially at the 75 percent emissions reduction scenario.

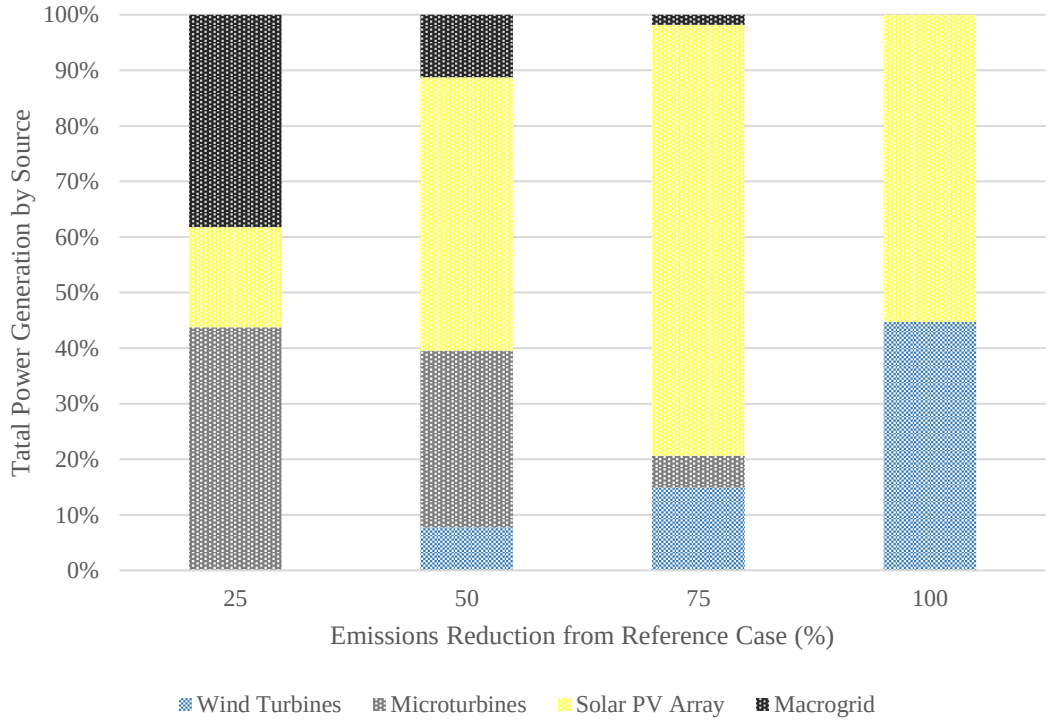

Figure 4.7: Contribution to power generation by source, for each emissions reduction scenario (Author, 2017)

While this goes against the fact that solar has a capital cost coefficient which is higher than that of wind (5,000 $\$\cdot kW^{-1}$ for solar vs 3,400 $\$\cdot kW^{-1}$ for wind).

The contribution to the net present value of costs from the solar photovoltaics is given by the following equation.

$$NPC_s = Capex_s + Opex_s = P_{s,rated} \cdot C_s \cdot \theta_s + P_{s,rated} \cdot O_s \cdot \varphi$$

A substitution to the parameters of the previous equation would give:

$$NPC_s = P_{s,rated} \cdot 5{,}000 \cdot 1 + P_{s,rated} \cdot 52 \cdot 11.7948 \cong P_{s,rated} \cdot 5{,}624$$

Likewise, the contribution to the net present value of costs from the wind turbines is given by:

$$NPC_w = P_{w,rated} \cdot C_w \cdot \theta_w + \sum_t P_w(t) \cdot O_w \cdot \varphi$$

The hourly power output of the wind turbines is proportional to their rated output multiplied by an availability hourly fraction, presented in equation 3.12.

$$P_w(t) = f_w(t) \cdot P_{w,rated}$$

Substituting the hourly output of eq3.12 to the net present value of wind turbines we receive the following expression.

$$NPC_w = P_{w,rated} \cdot C_w \cdot \theta_w + \sum_t f_w(t) \cdot P_{w,rated} \cdot O_w \cdot \varphi$$

The hourly fractional availability is calculated before the optimization. It is a parameter whose sum over a year's period can be estimated, and its value is about 1360. A substitution of this value, along with the values of the other parameters of the previous equation, will result in the following simple expression.

$$NPC_w = P_{w,rated} \cdot 3{,}400 \cdot 1 + P_{w,rated} \cdot 1360 \cdot 0.008 \cdot 11.7948 \cong P_{w,rated} \cdot 3{,}528$$

Despite that the total cost of wind turbines is lower than that of solar, the latter manages to meet almost 80 percent of the total power generation at the 75 percent emissions reduction scenario. Hence, solar may either be favored due to the higher power output that it probably achieves for the same capacity with a wind turbine, or due to the fact that peak hours in power demand mainly occur during daylight. As a result, power production and generation synchronizes to a degree, eliminating the need to purchase a battery bank of high capacity, which would further raise the net present value of costs.

Nevertheless, wind turbines also play a major role, especially at the 100 percent reduction scenario, meeting almost 45 percent of the total power generation.

Heat demand is primarily met from microturbines and natural gas boilers until the 75 percent reduction scenario. Electric boilers are selected after a 50 percent emissions reduction, and meet the whole demand in thermal energy at the zero emissions scenario, as expected.

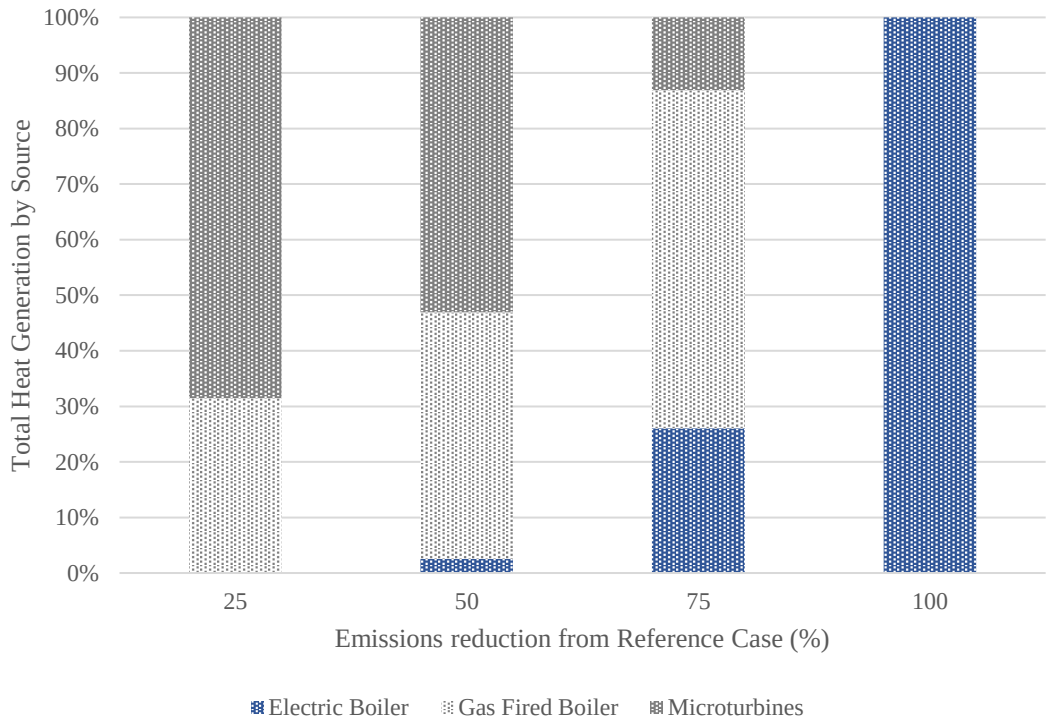

Figure 4.8: Contribution to total heat generation by source, for each emissions reduction case (Author, 2017)

The net present value of costs is presented for each case in figure 4.9. The costs per case rise in an almost exponential manner, reaching 153 million $ at the zero emissions scenario (100% emissions reduction). That is mainly due to the high installation costs of the distributed technology, as well as the need of very high capacities, due to the asynchronous power production and demand that solar and wind technology suffer from.

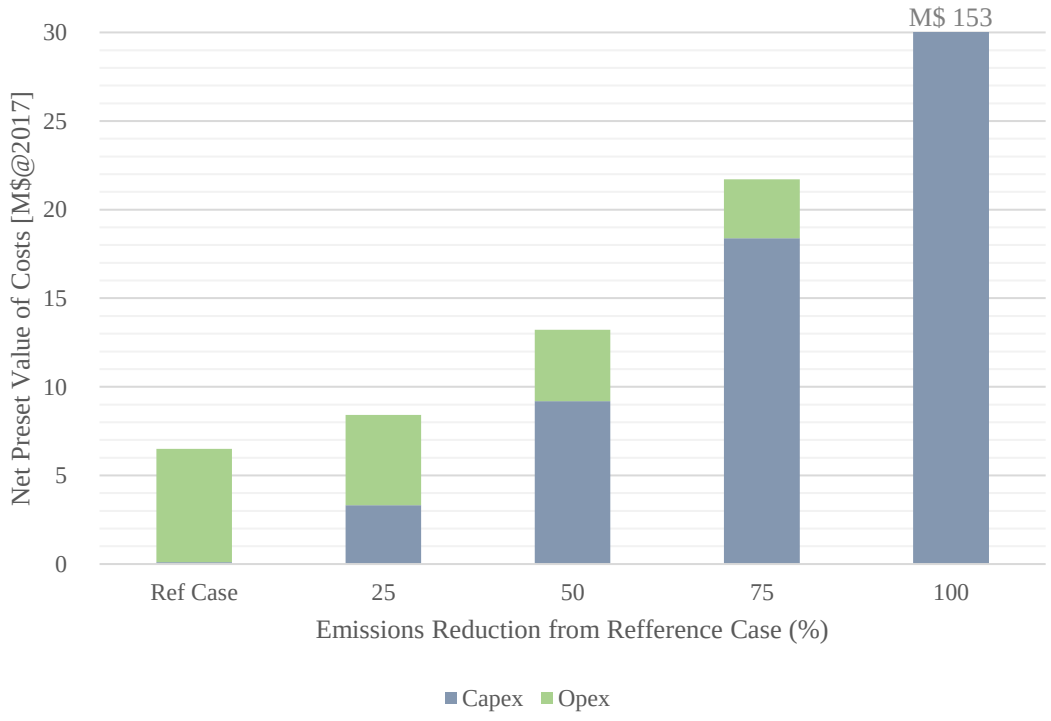

Figure 4.9: Net present value of costs for each emissions reduction case (Author, 2017)

A 25 percent emissions reduction, which is a goal needed to be reached by many countries, is about 30 percent more expensive than the reference case. A 50 percent reduction produces a solution which has almost the same (but less expensive) net present value as the 100 percent autonomy case, which only manages a 37 percent reduction in the produced carbon emissions.

Figures 4.10 and 4.11 show the useful and wasted heat and power generated throughout a year. Just like in the autonomy case, electricity that was consumed by the electrical boilers is considered as useful power.

While for low reduction fractions the wasted power is kept to low levels, the zero emissions scenario produces very high amounts of power which is wasted. This is, again, due to the asynchronous power generation by the wind turbines and solar photovoltaics, and the demand of the load.

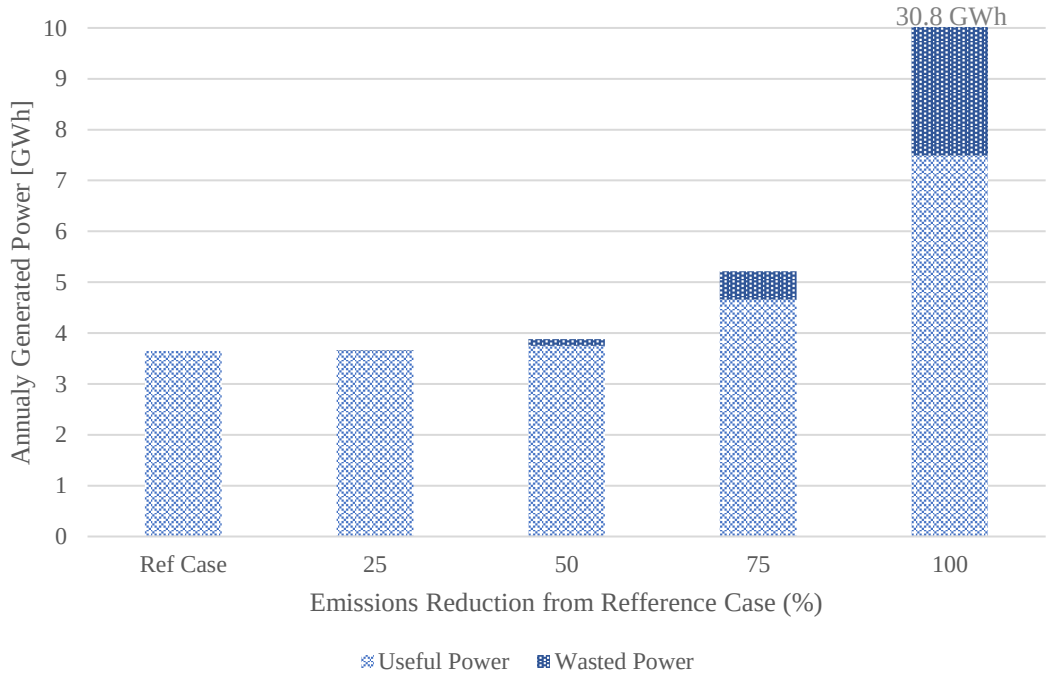

Figure 4.10: Total annually generated power, that is either consumed or wasted, per emissions reduction case (Auhtor,2017)

While dumped power increases as the emissions reduce, the opposite effect can be observed in the produced heat. Waste heat is maximized at low emission reductions, probably due to the microturbines that are operating at times of low demands in thermal and high demands in electrical energy.

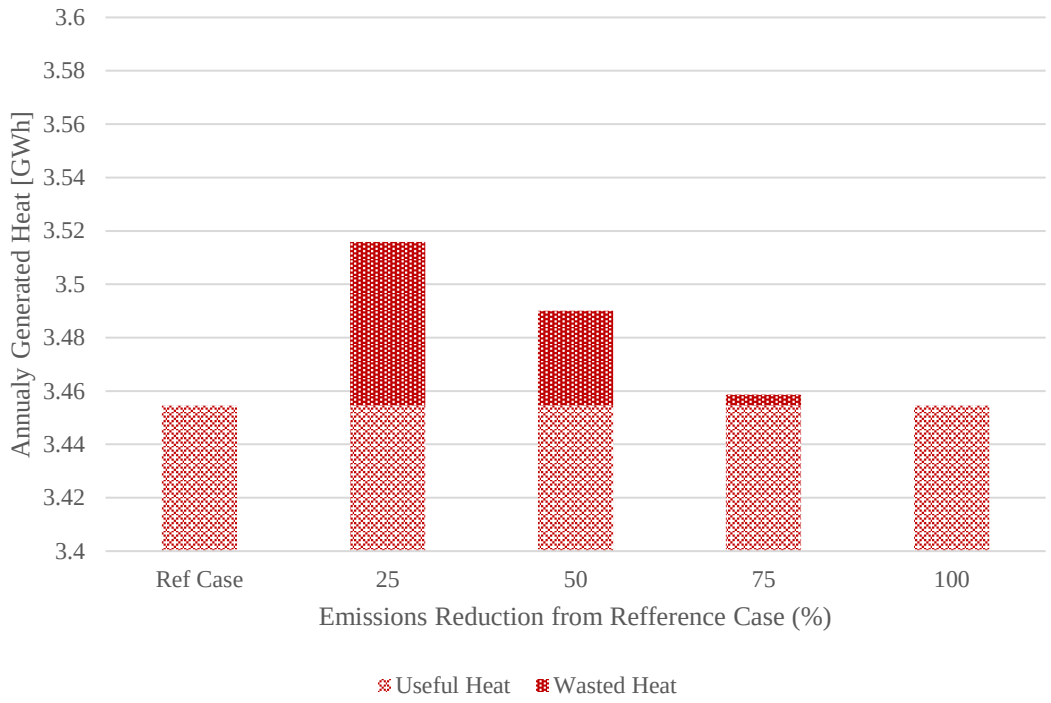

Figure 4.11: Total annually generated heat, that is either consumed or wasted, per emissions reduction case (Author, 2017)

It is obvious from this case study that a co-operation between the power generation units of the microgrid and the macrogrid, would give the optimal solution. In general, any utilization of the microgrid's distributed resources, should result in a significant reduction in the annual emissions that are produced. While the cost of a microgrid system is generally higher throughout a 20-year period, mainly due to equipment installation costs, it has many advantages that may lead to a future rapid growth of its market share.

Chapter 5

Conclusions

The optimization of the mixed integer linear program, presented in the previous chapters, was initially conducted, to evaluate the least expensive solution. The reference case considered no additional constraints, which may have forced power contribution from the microgrid's energy resources. The reference case solution resulted to a net present value of costs which raised at 6.51 M$ for a period of 20 years. This value mainly comprises of utility costs like natural gas and electricity purchase, since gas-fired boilers and macrogrid power were solely used to meet demands. Other distributed generation equipment was rejected due to high initial costs, which could not be mitigated throughout the 20-year lifespan of the system.

A minimum contribution to the load's power demand was forced in the minimum autonomy scenario, by inserting an additional constraint to the main program. The program was solved for a minimum autonomy of 25, 50, 75 and 100 percent. In all cases, microturbines are selected since their ability to cogenerate heat and power can mitigate to some degree the equipment purchase and maintenance costs. The introduction of one microturbine in the system, in the case of 25 percent minimum contribution to power, achieves a 9 percent emissions reduction and an overall efficiency increase, for an additional 30 k$ on the system's NPV, throughout its lifetime.

Nevertheless, the overdependence on microturbines for cogeneration may lead to significant power and heat losses, due to the asynchronous demands in heat and power and the additional maintenance costs that microturbines have upon each startup. Because of these factors, the solver chooses to keep the microturbines running even during off-peak hours of either power or heat, to reduce maintenance costs. That is, when there is a high demand on power and a low demand on heat, the thermal energy that is produced by these units is not recovered and vice versa; so the microturbines keep running, while the excess energy that is produced gets dumped.

Finally, a relative decrease to the total emissions produced by the microgrid and the macrogrid is being forced in the carbon emissions reduction scenario. The decrease is relative to the emissions acquired at the reference case, and is done for 25, 50, 75 and 100 percent reduction. The solution that occurs at 50 percent reduction, produces a smaller NPV than the full autonomy case which manages an emissions reduction by only 34 percent, and a significantly different unit selection, which implements all the available distributed resources of the microgrid.

In all cases solar PVs are highly favored, either due to the higher power output that it probably achieves for the same capacity with a wind turbine, or due to the fact that peak hours in power demand mainly occur during daylight. As a result, power production and generation synchronizes to a degree, eliminating the need to purchase a battery bank of high capacity, which would further raise the net present value of costs. The useful energy diagrams, show that power losses increase by implementing more renewable resources, since the weather-constrained power production may occur during off-peak hours.

It is obvious from all the scenarios that were considered, that the optimal technology selection may significantly differ for small changes in the selected constraints of the program. Hence the mathematical model must be carefully constructed, to obtain an optimal solution.

Chapter 6

Further Research Recommendations

One of the major problems faced throughout the conduction of this research, was the long calculation times that occurred during the optimization of the mathematical model. Despite that the model is a mixed integer linear program, the substantial number of single variables and equations, resulted in solution times that occasionally took over an hour to compute.

What is more, the assumption that the same pattern of demand in electricity and heat, as well as wind speed and insolation data, will be reproduced each year during the 20-year period, is an approximation that may lead to inaccurate results. That is, the values of these parameters are described by certain distributions of probability, due to uncertainty.

The solution process that was followed in this study, in which the collected data was assumed certain and repeatable, is called **deterministic optimization**. On the other hand, the solution of a mathematical program which also takes into account the probabilities of a parameter having a specific value, is called **chance-constrained** or **stochastic optimization**.

Stochastic optimization is a method currently followed mainly in the operations research field, but has many applications in engineering as well. Problems that contain one or all parameters whose values are chance constrained (e.g. temperature profiles, number of people inside a plane at each takeoff, etc.), should be treated as stochastic programs.

The general idea behind stochastic programming is the conversion of the chance-constrained parameters into deterministic, via a process which involves statistical analyses. The distribution of the values of the probabilistic parameter is being estimated, and future predictions can be calculated by the distribution's equations. After the program's conversion into deterministic, it can then be solved with common optimization techniques.

A treatment of the microgrid model as a stochastic program could potentially reduce the total number of variables, hence the computation time. Each parameter's collected data could undergo a statistical analysis to evaluate their distribution, for each hour of a day. That should enable the extraction of an expression, which can accurately describe the probability of that parameter to have a certain value at any time. The solutions that will be obtained from the stochastic optimization ought to be compared to the corresponding solutions that were obtained by this deterministic model.

References

Abdmouleh, Z., Gastli, A., Ben-Brahim, L., Haouari, M. and Al-Emadi, N. (2017). Review of optimization techniques applied for the integration of distributed generation from renewable energy sources. Renewable Energy, [online] 113, pp.266-280. Available at: https://www.sciencedirect.com/science/article/pii/S0960148117304822.

Andrews, J. and Jelley, N. (2013). Energy science. Oxford: Oxford University Press.

Anon, (2018). VAPOUR & COMBINED POWER CYCLE. [online] Available at: http://sounak4u.weebly.com/vapour--combined-power-cycle.html [Accessed 5 Dec. 2017].

Baj.or.jp. (2004). BAJ Website | Structure and Reaction Formula of Batteries. [online] Available at: http://www.baj.or.jp/e/knowledge/structure.html [Accessed 8 Dec. 2017].

brush.eu. (2018). Compressed Air Energy Storage (CAES) - Markets - Renewables - BRUSH. [online] Available at: http://www.brush.eu/en/31/BRUSH-Group/Markets/Renewables/Compressed-Air-Energy-Storage-CAES [Accessed 5 Jan. 2018].

Chen, H., Cong, T., Yang, W., Tan, C., Li, Y. and Ding, Y. (2009). Progress in electrical energy storage system: A critical review. Progress in Natural Science, 19(3), pp.291-312.

Department of the Environment and Energy. (2018). Department of the Environment and Energy. [online] Available at: http://www.environment.gov.au/climate-change/climate-science-data/climate-science/greenhouse-effect [Accessed 3 Jan. 2018].

Dervisoglu, R. (2012). Scheme of a proton-conducting fuel cell. [image] Available at: https://en.wikipedia.org/wiki/Fuel_cell#/media/File:Solid_oxide_fuel_cell_protonic.svg [Accessed 5 Jan. 2018].

Earthobservatory.nasa.gov. (2018). Global Warming : Feature Articles. [online] Available at: https://earthobservatory.nasa.gov/Features/GlobalWarming/ [Accessed 3 Jan. 2018].

ecourses.ou.edu. (2016). Thermodynamics eBook: Brayton Cycle. [online] Available at: http://www.ecourses.ou.edu/cgi-bin/ebook.cgi?topic=th&chap_sec=09.1&page=theory [Accessed 3 Jan. 2018].

Encyclopedia Britannica. (2017). Nuclear power. [online] Available at: https://www.britannica.com/technology/nuclear-power [Accessed 16 Dec. 2017].

energ-group.com. (2018). How CHP works | ENER-G Combined Power. [online] Available at: http://www.energ-group.com/combined-heat-and-power/cogeneration/how-it-works/ [Accessed 20 Dec. 2017].

Energy Storage Sense. (2017). Pumped Hydroelectric Storage (PHS). [online] Available at: http://energystoragesense.com/pumped-hydroelectric-storage-phs/ [Accessed 5 Jan. 2018].

Energymaxout.com. (2018). How do Batteries Work? [online] Available at: http://www.energymaxout.com/how-do-batteries-work/ [Accessed 4 Jan. 2018].

fepc.or.jp. (1999). The Challenge of High-level Radioactive Waste Disposal | FEPC. [online] Available at: http://www.fepc.or.jp/english/library/power_line/detail/04/ [Accessed 4 Jan. 2018].

ffden-2.phys.uaf.edu. (2018). Combined Power Cycles. [online] Available at: http://ffden-2.phys.uaf.edu/webproj/212_spring_2015/Andrew_Eklund/Combined%20Power%20Plants, %20Eklund/index.html [Accessed 6 Jan. 2018].

georgiapower.com. (2018). Coal Thermoelectric Plant Scherer, Georgia. [online] Available at: https://www.georgiapower.com/docs/about-us/1402870%20PLANT%20SCHERER%20INFO%20SHEET0108.pdf [Accessed 7 Jan. 2018].

gepower.com. (2017). Aeroderivative & Heavy-Duty Gas Turbines | GE Power. [online] Available at: https://www.gepower.com/gas/gas-turbines [Accessed 3 Jan. 2018].

indianbioenergy.com. (2015). WHAT IS BIODIESEL | INDIAN BIOENERGY. [online] Available at: http://indianbioenergy.com/www-indianbioenergy-com/bio-diesel/what-is-biodiesel/ [Accessed 4 Jan. 2018].

IPCC, 2014: Climate Change 2014: Synthesis Report. Contribution of Working Groups I, II and III to the Fifth Assessment Report of the Intergovernmental Panel on Climate Change [Core Writing Team, R.K. Pachauri and L.A. Meyer (eds.)]. IPCC, Geneva, Switzerland, 151 pp.

Knier, G. (2008). How do Photovoltaics Work? | Science Mission Directorate. [online] science.nasa.gov. Available at: https://science.nasa.gov/science-news/science-at-nasa/2002/solarcells [Accessed 9 Jan. 2018].

Kookos, I. (2009). Introduction to chemical plant design. (published in Greek) Athens, Greece: TZIOLAS PUBLICATIONS.

Kookos, I. and Koutinas, A. (2014). Processes and systems optimization with applications in MATLAB and GAMS. (published in Greek) Athens, Greece: TZIOLAS PUBLICATIONS.

Larminie, J. and Dicks, A. (2009). Fuel cell systems explained. 2nd ed. Chichester: Wiley.

Lasseter, R. (2007). Microgrids And Distributed Generation. Journal of Energy Engineering, [online] 133(3), pp.144-149. Available at: http://citeseerx.ist.psu.edu/viewdoc/download?doi=10.1.1.436.7654&rep=rep1&type=pdf.

Lasseter, R. and Piagi, P. (2004). Microgrid: a conceptual solution. Power Electronics Specialists Conference, 2004. PESC 04. 2004 IEEE 35th Annual. [online] Available at: http://ieeexplore.ieee.org/document/1354758/ [Accessed 7 Mar. 2017].

Lets Go Solar. (2018). Solar Power or Wind Power? | LetsGoSolar.com. [online] Available at: https://www.letsgosolar.com/consumer-education/solar-power-wind-power/ [Accessed 4 Jan. 2018].

Mashayekh, S., Stadler, M., Cardoso, G. and Heleno, M. (2017). A mixed integer linear programming approach for optimal DER portfolio, sizing, and placement in multi-energy microgrids. Applied Energy, [online] 187, pp.154-168. Available at: https://www.sciencedirect.com/science/article/pii/S0306261916316051#b0065.

McDonald, J., Wojszczyk, B., Flynn, B. and Voloh, I. (2012). Distribution Systems, Substations, and Integration of Distributed Generation. Electrical Transmission Systems and Smart Grids, pp.7-68.

Mechanical Engineering Community. (2017). How nuclear power plant works.jpg. [online] Available at: https://mechanical-engg.com/gallery/image/2563-how-nuclear-power-plant-worksjpg/ [Accessed 16 Jan. 2018].

Mehleri, E., Sarimveis, H., Markatos, N. and Papageorgiou, L. (2013). Optimal design and operation of distributed energy systems: Application to Greek residential sector. Renewable Energy, [online] 51, pp.331-342. Available at: https://www.sciencedirect.com/science/article/pii/S0960148112005757.

Meirong, H. Kurt, G. (2017). Open Cycle Gas Turbine: Advantages and Disadvantages. [online] ME Mechanical. Available at: https://me-mechanicalengineering.com/open-cycle-gas-turbine/ [Accessed 19 Jan. 2018].

nfcrc.uci.edu. (2017). NFCRC: Fuel Cells Explained: Fuel Cell Types. [online] Available at: http://www.nfcrc.uci.edu/3/FUEL_CELL_INFORMATION/FCexplained/FC_Types.aspx [Accessed 14 Jan. 2018].

NREL (2012). Life Cycle Greenhouse Gas Emissions from Solar Photovoltaics. Denver West Parkway: US National Renewable Energy Laboratory.

NREL (2017). U.S. Solar Photovoltaic System Cost Benchmark: Q1 2017. Denver West Parkway: US National Renewable Energy Laboratory.

Nuclear Power. (2017). Nuclear Fission - Fission Reaction. [online] Available at: http://www.nuclear-power.net/nuclear-power/fission/ [Accessed 10 Jan. 2018].

Nuclear-energy.net. (2017). Nuclear Fusion. [online] Available at: https://nuclear-energy.net/what-is-nuclear-energy/nuclear-fusion [Accessed 10 Jan. 2018].

OECD/IEA (2013). Resources to reserves 2013. Paris: Organisation for Economic Co-operation and Development & International Energy Agency. ISBN 978-92-64-08354-7

OECD/IEA (2015). World Energy Outlook 2015. [online] Paris: Organisation for Economic Co-operation and Development & International Energy Agency. Available at: https://www.iea.org/publications/freepublications/publication/WEO2015.pdf [Accessed 9 Nov. 2017].

Omu, A., Choudhary, R. and Boies, A. (2013). Distributed energy resource system optimisation using mixed integer linear programming. Energy Policy, 61, pp.249-266.

P3ppartners.com. (2015). What is CHP? | P3P Partners. [online] Available at: https://www.p3ppartners.com/chp/ [Accessed 6 Dec. 2017].

Parida, B., Iniyan, S. and Goic, R. (2011). A review of solar photovoltaic technologies. Renewable and Sustainable Energy Reviews, 15(3), pp.1625-1636.

Parra, D., Swierczynski, M., Stroe, D., Norman, S., Abdon, A., Worlitschek, J., O'Doherty, T., Rodrigues, L., Gillott, M., Zhang, X., Bauer, C. and Patel, M. (2017). An interdisciplinary review of energy storage for communities: Challenges and perspectives. Renewable and Sustainable Energy Reviews, 79, pp.730-749.

PNNL (2016). Electricity Distribution System Baseline Report. [online] WM Warwick: Pacific Northwest National Laboratory, pp.3-70. Available at: https://www.energy.gov/sites/prod/files/2017/01/f34/Electricity%20Distribution%20System%20Baseline%20Report.pdf [Accessed 12 Nov. 2017].

Power Technology. (2013). The 10 biggest hydroelectric power plants in the world - Power Technology. [online] Available at: http://www.power-technology.com/features/feature-the-10-biggest-hydroelectric-power-plants-in-the-world/ [Accessed 3 Jan. 2018].

power-thru.com. (2016). Flywheel UPS Technology | POWERTHRU | Clean Flywheel Energy Storage. [online] Available at: http://www.power-thru.com/carbon_fiber_flywheel_technology.html [Accessed 5 Jan. 2018].

protonex.com. (2017). Solid Oxide Fuel Cell Technology | Protonex. [online] Available at: https://webcache.googleusercontent.com/search?q=cache:7bigDlHh-84J:https://protonex.com/technology/solid-oxide-fuel-cell/+&cd=1&hl=el&ct=clnk&gl=gr [Accessed 11 Nov. 2017].

Rao, S. (2005). Engineering optimization. Norwich, NY: Knovel.

REN21 (2016). Renewables 2016 Global Status Report. Paris: REN21 Secretariat. ISBN 978-3-9818107-0-7

Sanaye, S. and Ardali, M. (2009). Estimating the power and number of microturbines in small-scale combined heat and power systems. Applied Energy, [online] 86(6), pp.895-903. Available at: http://www.sciencedirect.com/science/article/pii/S030626190800281X.

sinetech.co.za. (2018). Solar panels are not all the same. There are different kinds of solar panels. [online] Available at: http://www.sinetech.co.za/news-solar-panels-are-all-the-same.html [Accessed 4 Jan. 2018].

socratic.org. (2016). What is the photoelectric effect? | Socratic. [online] Available at: https://socratic.org/questions/what-is-the-photoelectric-effect-1 [Accessed 4 Jan. 2018].

SweetCrudeReports.com. (2018). UNIDO to provide $2.6bn for small hydro power plants in Nigeria - SweetCrudeReports. [online] SweetCrudeReports. Available at: http://sweetcrudereports.com/2015/09/30/unido-to-provide-2-6bn-for-small-hydro-power-plants-in-nigeria/ [Accessed 21 Jan. 2018].

thegmcrv.com. (2016). Electrical Part 2: Solar | The GMC RV. [online] Available at: http://www.thegmcrv.com/project/electrical-part-2-solar [Accessed 4 Jan. 2018].

Ton, D. and Smith, M. (2012). The U.S. Department of Energy's Microgrid Initiative. The Electricity Journal, [online] 25(8), pp.84-94. Available at: http://www.sciencedirect.com/science/article/pii/S1040619012002254.

US Department of Energy. (2017). Top 10 Things You Didn’t Know About Offshore Wind Energy. [online] Energy.gov Available at: https://energy.gov/eere/wind/articles/top-10-things-you-didn-t-know-about-offshore-wind-energy [Accessed 7 Jan. 2018].

US Department of Energy. (2018). Electricity Generation | Department of Energy. [online] Energy.gov Available at: https://energy.gov/eere/geothermal/electricity-generation [Accessed 13 Jan. 2018].

US EIA (2017). Hydropower - Energy Explained, Your Guide To Understanding Energy - Energy Information Administration. [online] Eia.gov. Available at: https://www.eia.gov/energyexplained/index.cfm?page=hydropower_home [Accessed 17 Jan. 2018].

US EPA. (2017). Centralized Generation of Electricity and its Impacts on the Environment | US EPA. [online] Available at: https://www.epa.gov/energy/centralized-generation-electricity-and-its-impacts-environment [Accessed 11 Nov. 2017].

US EPA. (2018). Global Greenhouse Gas Emissions Data | US EPA. [online] Available at: https://www.epa.gov/ghgemissions/global-greenhouse-gas-emissions-data [Accessed 3 Jan. 2018].

US EPA. (2018). What is Acid Rain? | US EPA. [online] Available at: https://www.epa.gov/acidrain/what-acid-rain [Accessed 22 Jan. 2018].

w3.usa.siemens.com. (2017). Microgrids Solutions - Smart Grid Solutions - Siemens. [online] Available at: http://w3.usa.siemens.com/smartgrid/us/en/microgrid/pages/microgrids.aspx [Accessed 24 Dec. 2017].

Weatherspark.com. (2018). Average Weather in Sarnia, Canada, Year Round - Weather Spark. [online] Available at: https://weatherspark.com/y/17373/Average-Weather-in-Sarnia-Canada-Year-Round#Sections-Temperature [Accessed 2 Jan. 2018].

World Energy Council (2016). World Energy Resources 2016. London: World Energy Council. ISBN: 978 0 946121 62 5

World Nuclear Association. (2017). Nuclear Fusion : WNA - World Nuclear Association. [online] World-nuclear.org Available at: http://www.world-nuclear.org/information-library/current-and-future-generation/nuclear-fusion-power.aspx [Accessed 26 Jan. 2018].

Zachar, M., Trifkovic, M. and Daoutidis, P. (2015). Policy effects on microgrid economics, technology selection, and environmental impact. Computers & Chemical Engineering, 81, pp.364-375.

Appendix A

Scripts Compiled In Matlab

Table A.1: Linearization of cost coefficients calculation

```
clear all
clc

syms CCref xref a x b xL xU err
assume(CCref>0);assume(xref>0);assume(a>0);
assume(x>0);assume(b>0);assume(xL>0);assume(xU>0);
assume(err<5);assume(err>-5);

eq1=int((CCref*(x/xref)^a-b*x)^2,x,xL,xU)
eq1=diff(eq1,b);

beta=solve(eq1==0,b)

C_s=double(subs(beta,[xref,CCref,a,xL,xU],[300, 1620000, 0.94, 0, 2000]))
C_w=double(subs(beta,[xref,CCref,a,xL,xU],[300, 1380000, 0.80, 0, 2000]))
C_j=double(subs(beta,[xref,CCref,a,xL,xU],[180, 21600, 0.60, 0, 1500]))
C_n=double(subs(beta,[xref,CCref,a,xL,xU],[180, 21600, 0.60, 0, 1500]))
C_b=double(subs(beta,[xref,CCref,a,xL,xU],[150, 45000, 0.95, 0, 5000]))
```

Table A.2: Calculation of NPV factors

```
clear all
clc

d=0.083; %discount rate
i=0.025; %inflation rate

y = linspace(1,20,20);

I=(d-i)/(1+i);

phi_m2=((1+I)^20-1)/(I*(1+I)^20) %PVIFA

theta=(1+d).^-(y-1); %PVIF
theta_b=theta(1)+theta(6)+theta(11)+theta(16)
theta_j=theta(1)+theta(17)
theta_n=theta_j
```

Table A.3: Calculation of wind turbine's rated power fractional availability

```
clear all
clc

vr=12; % Rated wind speed [m/s]
vci=3; % Cut in speed [m/s]
vco=25; % Cut out speed [m/s]
h=30; % Site's altitude [m]
href=10; % Altitude at the site of reference [m]
a=1/7;

v=xlsread('Original_CCEdata','A2:A8761');

fw=zeros(length(v),1);

for i=1:length(v)

if (v(i)<vci) || (v(i)>vco)
    fw(i,1)=0;
elseif (vci<=v(i))&&(v(i)<=vr)
    fw(i,1)=(v(i)^3-vci^3)/(vr^3-vci^3);
else
    fw(i,1)=1;
end

end

scatter(linspace(1,8760,8760),fw,'.')
```

Appendix B

Scripts Compiled In GAMS

Table B.1.1: Reference case main script (part 1/5)

```
sets t  time interval (one hour) /t1*t8760/

     mm maximum number of microturbines considered /m1, m2, m3/

     eq equipment considered in the model

  /  m  "Microturbines"
     w  "Wind turbines"
     s  "Solar PVs"
     j  "Electric boilers"
     n  "Natural gas boilers"
     b  "Battery bank"  /;

*~~~~~~~~~~~~~~~~~~~~~~~~~~~ Excel Data Extraction ~~~~~~~~~~~~~~~~~~~~~~~~~~~~~

set  sd statistical data of parameters /fw, H, Pl, Ql/;

*Where: fw = Availability fraction of Rated Power Output of wind turbines
*       H  = Hourly solar radiation
*       Pl = Power consumed by the Load
*       Ql = Heat consumed by the Load

* Conversion of Excel file to GDX file
$CALL GDXXRW.EXE GAMS_DATA_1.xlsx par=dataset rng=Sheet1!A1:E8761

*Iporting DATA from GDX to compilation script
parameter dataset(t,sd);
$GDXIN GAMS_DATA_1.gdx
$LOAD dataset
$GDXIN
*~~~~~~~~~~~~~~~~~~~~~~~~~~~~~~~~~~~~~~~~~~~~~~~~~~~~~~~~~~~~~~~~~~~~~~~~~~~~~~~

parameters

C(eq)            capital cost coefficient of the equipment

              /   m = 594000
                  w = 3400
                  s = 5000
                  j = 60
                  n = 60
                  b = 132      /
```

Table B.1.2: Reference case main script (part 2/5)

```
O(eq)             maintenance cost coefficient of the equipment

                /   m = 0.02
                    w = 0.008
                    s = 52
                    j = 0.0075
                    n = 0.0075
                    b = 0.00143  /;


scalars

Agrid             purchase cost of power from the macrogrid [$ per kWh]   /0.108/
Ang               purchase cost of natural gas [$ per kWh]                /0.0302/
gamma             heat-to-power ratio of microturbines [-]                /1.5/
Hr                reference solar radiation of PVs [kW per m2]            /1/
nm                electrical efficiency of microturbines [-]              /0.27/
nbm               charging efficiency of battery bank [-]                 /0.9/
nbp               discharging efficiency of battery bank [-]              /0.95/
nj                power conversion efficiency of the electric boiler [-]  /0.9/
nn                natural gas conversion efficiency of the NG boiler [-]  /0.85/
Ostartup          microturbine additional cost per startup [$ per start]  /10/
Pmr               rated power output for each microturbine [kW]           /165/
Hng               assumed heating value for natural gas [kWh per m3]      /9.83/
theta_n           NPV factor of capital cost of NG boiler                 /1.2792/
theta_j           NPV factor of capital cost of electric boiler           /1.2792/
theta_b           NPV factor of capital cost of battery bank              /2.4241/
phi_ng            NPV factor of annual purchase cost of natural gas       /11.7948/
phi_grid          NPV factor of annual purchase cost of power from grid   /11.7948/
phi_maint         NPV factor of maintenance cost of all the equipment     /11.7948/
Fng               natural gas CO2 emissions coefficient [tonCO2 per kWh]
/0.000183/
Fgrid             macrogrid CO2 emissions coefficient [tonCO2 per kWh]
/0.000575/;



binary variables

x(t,mm)           micriturbine mm is on
y(mm)             microturbine mm is installed
z(t,mm)           microturbine mm is started up;


positive variables

Capex             capital expenditures [USD]
Opex              operational expenditures [USD]
Pwr               rated power of windturbines [kW]
Psr               rated power of solar PVs [kW]
Qjr               rated heat of electric boiler [kW]
Qnr               rated heat of natural gas boiler [kW]
Lbmax             maximum energy storage of battery bank [kW]
Pm(t,mm)          microturbine hourly power output [kWh]
Pw(t)             windturbine power output [kWh]
Qn(t)             natural gas boiler hourly heat output [kWh]
Qj(t)             electric boiler hourly heat output [kWh]
Pbplus(t)         battery bank hourly discharge [kWh]
```

Table B.1.3: Reference case main script (part 3/5)

```
Gm(t,mm)          natural gas hourly consumption by the MTs [m3]
Gn(t)             natural gas hourly consumtion by the NGB [m3]
Pgrid(t)          hourly power purchased from the grid [kWh]
Ps(t)             hourly power produced by solar PVs [kWh]
Pbminus(t)        battery bank hourly charge [kWh]
Pj(t)             hourly electric boiler power consumption [kWh]
Pd(t)             power dumped each hour [kWh]
Qm(t,mm)          hourly heat produced by the MTs [kWh]
Qd(t)             dump heat load during an hour [kWh]
Lb(t)             hourly energy storage level [kWh]
En                gas fired boiler emissions [ton(CO2)]
Em                microturbine emissions [ton(CO2)]
Egrid             macrogrid emissions [ton(CO2)];

variable NPC      net present value of costs [USD];


equations

eq1               sum of the capital costs
eq2               sum of the annual operational costs
eq3(t)            electric power balance
eq4(t)            heat balance
eq5a(t,mm)        lower bound from MTs efficiency constraint
eq5b(t,mm)        upper bound from MTs efficiency constraint
eq6(t,mm)         useful heat generated from MTs
eq7(t,mm)         microtubines fuel consumption
eq8(t,mm)         number of activated MTs limitation by the number intalled
eq9(t,mm)         track of startups of microturbines
eq10(t)           solar PVs power balance
eq11(t)           wind turbine power balance
*eq12a(t)         lower bound of EB hourly consumption constraint
eq12b(t)          upper bound of EB hourly consumption constraint
*eq13a(t)         lower bound of NGB hourly consumption constraint
eq13b(t)          upper bound of NGB hourly consumption constraint
eq14(t)           heat to power conversion of EB
eq15(t)           natural gas conversion of NGB
eq16(t)           battery bank power balance
eq17a(t)          lower bound in battery bank storage level constraint
eq17b(t)          upper bound in battery bank storage level constraint
mtCO2             microturbine CO2 emissions
ngbCO2            gas fired boiler CO2 emissions
gridCO2           macrogrid CO2 emissions

obj               sum of capital and operational expenditures;


*~~~~~~~~~~~~~~~~ Annual Operational and Capital expenses ~~~~~~~~~~~~~~~~~~~~~

eq1..             Capex =e= sum(mm,y(mm))*C('m')
                          +Pwr*C('w')
                          +Psr*C('s')
                          +Qjr*C('j')*theta_j
                          +Qnr*C('n')*theta_n
                          +Lbmax*C('b')*theta_b;
```

Table B.1.4: Reference case main script (part 4/5)

```
eq2..            Opex  =e= Psr*O('s')*phi_maint+sum(t,
                           sum(mm,(Pm(t,mm)*O('m')+z(t,mm)*Ostartup))*phi_maint
                           +Pw(t)*O('w')*phi_maint
                           +Qn(t)*O('n')*phi_maint
                           +Qj(t)*O('j')*phi_maint
                           +Pbplus(t)*O('b')*phi_maint
                           +(sum(mm,Gm(t,mm))+Gn(t))*Ang*phi_ng
                           +Pgrid(t)*Agrid*phi_grid );

*~~~~~~~~~~~~~~~~~~~~~~~~~~ Power and Heat Balance ~~~~~~~~~~~~~~~~~~~~~~~~~~~~

eq3(t)..         sum(mm,Pm(t,mm))+Ps(t)+Pw(t)+Pbplus(t)+Pgrid(t) =e=
                 dataset(t,'Pl')+Pbminus(t)+Pj(t)+Pd(t);

eq4(t)..         sum(mm,Qm(t,mm))+Qj(t)+Qn(t) =e= dataset(t,'Ql')+Qd(t);

*~~~~~~~~~~~~~~~~~~~~~~~~~~~~ Equipment Design ~~~~~~~~~~~~~~~~~~~~~~~~~~~~~~~~

*Microturbines

eq5a(t,mm)..    0.5*x(t,mm)*Pmr =l= Pm(t,mm);

eq5b(t,mm)..    Pm(t,mm) =l= x(t,mm)*Pmr;

eq6(t,mm)..     Qm(t,mm) =e= Pm(t,mm)*gamma;

eq7(t,mm)..     Gm(t,mm) =e= Pm(t,mm)/nm;

eq8(t,mm)..     x(t,mm) =l= y(mm);

eq9(t,mm)$(ord(t) le card(t)-1)..
                z(t+1,mm) =g= x(t+1,mm)-x(t,mm);

*Solar PV Array

eq10(t)..        Ps(t) =e= Psr*dataset(t,'H')/Hr;

*Wind Turbines

eq11(t)..        Pw(t) =e= dataset(t,'fw')*Pwr;

*Boilers

*eq12a(t)..       0 =l= Qj(t);

eq12b(t)..       Qj(t) =l= Qjr;

*eq13a(t)..       0 =l= Qn(t);

eq13b(t)..       Qn(t) =l= Qnr;

eq14(t)..        Pj(t) =e= Qj(t)/nj;

eq15(t)..        Gn(t) =e= Qn(t)/nn;

*Battery Bank
```

Table B.1.5: Reference case main script (part 5/5)

```
eq16(t)..         Lb(t) =e= Lb(t-1)+Pbminus(t)*nbm-Pbplus(t)/nbp;

eq17a(t)..        0.2*Lbmax =l= Lb(t);

eq17b(t)..        Lb(t) =l= Lbmax;

*~~~~~~~~~~~~~~~~~~~~~~~~~~~~~~~ CO2 Emissions ~~~~~~~~~~~~~~~~~~~~~~~~~~~~~~~~

mtCO2..           Em =e= sum(t,sum(mm,Gm(t,mm)))*Fng;

ngbCO2..          En =e= sum(t,Gn(t))*Fng;

gridCO2..         Egrid =e= sum(t,Pgrid(t))*Fgrid;

*~~~~~~~~~~~~~~~~~~~~~~~~~~~~~ Objective Function ~~~~~~~~~~~~~~~~~~~~~~~~~~~~~

obj..             NPC =e= Opex + Capex;


model    Microgrid       /ALL/;

options  MIP   = CPLEX
         optcr = 0.01 ;

Microgrid.iterlim=1000000;

solve Microgrid using MIP minimizing NPC



*~~~~~~~~~~~~~ Unload to GDX file (occurs during execution phase) ~~~~~~~~~~~~~~~

execute_unload "Ref_Case.gdx"    Pgrid.L Qn.L Qj.L Pw.L Ps.L Pm.L Qm.L Lb.L
                                 Capex.L Opex.L NPC.L y.L Psr.L Pwr.L Lbmax.L
                                 Qjr.L Qnr.L Em.L En.L Egrid.L;
```

Table B.2: Autonomy case additions to the main script

```
scalars

Auton             fraction of autonomy of the microgrid                    /0.25/;

*solve for Autonomy fraction of 0.25, 0.50, 0.75, 1.00

equations

autonomy          autonomy imposition to the microgrid    ;

autonomy..        sum(t,Pgrid(t)) =l= (1-Auton)*sum(t,dataset(t,'Pl')+Pj(t));
```

Table B.3: Emissions reduction case additions to the main script

```
scalars

Ref_E            emissions in reference case [tonCO2 per year]           /2843/
Red_E            emissions reduction fraction from ref case [-]          /0.25/;

*solve for reduction fraction of 0.25, 0.50, 0.75, 1.00

equations

maxCO2           maximum emissions constraint;

maxCO2..         Egrid + Em + En =l= Ref_E*(1-Red_E);
```